Proceedings and workbook of the

Electroporation-based Technologies and Treatments

International SCIENTIFIC WORKSHOP and POSTGRADUATE COURSE

Ljubljana, Slovenia
November 13-19, 2022

ISBN 978-961-243-442-7

Proceedings is available in PDF format at ***2022.ebtt.org/proceedings***

Electroporation-based Technologies and Treatments 2022

November 13-19, 2022
Ljubljana, Slovenia

Proceedings and workbook of the

Electroporation-based Technologies and Treatments

International SCIENTIFIC WORKSHOP and POSTGRADUATE COURSE

Edited by:
Peter Kramar
Damijan Miklavčič

Organised by:
University of Ljubljana
Faculty of Electrical Engineering

Institute of Oncology, Ljubljana

Supported by:

Bioelectrochemical Society (BES)

International Society for Electroporation-Based Technologies and Treatments (ISEBTT)

Bia
Elea
Galvanize
IGEA
Intuitive
Iskra Medical
Iskra PIO
Jafral
Labtim
Meditech
Medtronic
mPOR
Mikro+Polo
Omega
Pulse Biosciences

www.ebtt.org

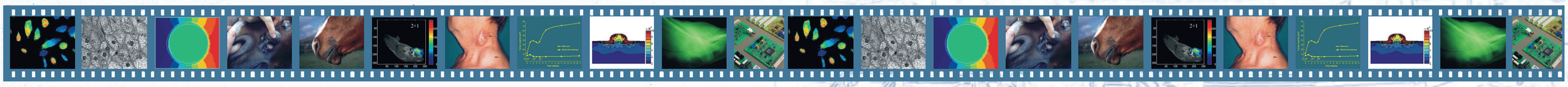

Univerza *v Ljubljani*

bia TRUSTED LAB PARTNER

elea

Galvanize

ICEA® CLINICAL BIOPHYSICS

INTUITIVE

IskraMedical

p:o Clean visions.

JAFRAL passion for biosolutions

Labtim

MEDITECH Empowered with Tecan.®

Medtronic

mikro+polo® vaš partner za laboratorij

omega

Pulse Biosciences

ISEBTT International Society for Electroporation-Based Technologies and Treatments

B E S The Bioelectrochemical Society

9 - 13 June 2024
Portorož | Slovenia

embec 2024

9th European
Medical and Biological
Engineering Conference

embec2024.org

Come, share and enjoy!

We could not make it in 2020...so we booked 2024 to make it right!

International Federation for Medical and Biological Engineering IFMBE

European Alliance for EAMBES Medical and Biological Engineering & Science

SLOVENIAN SOCIETY FOR MEDICAL AND BIOLOGICAL ENGINEERING
Faculty of Electrical Engineering, Tržaška 25, 1000 Ljubljana, Slovenia
tel.: +386 1 4768 783, homepage: www.sdmbts.si, e-mail: info@sdmbts.si

University *of Ljubljana* Faculty *of Electrical Engineering*

November 13-19, 2022
Ljubljana, Slovenia

Proceedings and workbook of the

Electroporation-Based Technologies and Treatments

International SCIENTIFIC WORKSHOP and POSTGRADUATE COURSE

Edited by:

Peter Kramar
Damijan Miklavčič

Organised by:

University of Ljubljana
Faculty of Electrical Engineering

Institute of Oncology, Ljubljana

Organising committee:

Chair:
Peter Kramar
Members:
Matej Kranjc, Helena Cindrič,
Aleksandra Cvetkoska, Duša Hodžič

Supported by:

Bioelectrochemical Society
(BES)

International Society for
Electroporation-Based
Technologies and Treatments
(ISEBTT)

Bia
Elea
Galvanize
IGEA
Intuitive
Iskra Medical
Iskra PIO
Jafral

Labtim
Meditech
Medtronic
mPOR
Mikro+Polo
Omega
Pulse Biosciences

www.ebtt.org

CIP - Kataložni zapis o publikaciji
Narodna in univerzitetna knjižnica, Ljubljana

602.621(082)
577.352.4(082)

ELECTROPORATION-based Technologies and Treatments (delavnica) (2022 ; Ljubljana)
Proceedings and workbook of the Electroporation-based Technologies and Treatments : international scientific workshop and postgraduate course : [Ljubljana, Slovenia, November 13-19, 2022] / edited by Peter Kramar, Damijan Miklavčič ; organised by University of Ljubljana, Faculty of Electrical Engineering [and] Institute of Oncology, Ljubljana. - 1. izd. - Ljubljana : Založba FE, 2022

ISBN 978-961-243-442-7
COBISS.SI-ID 127714563

Založnik: Založba FE, Ljubljana
Izdajatelj: UL Fakuleta za elektrotehniko, Ljubljana
Urednik: prof. dr. Sašo Tomažič

Natisnil: Birografika Bori d.o.o.
Naklada: 80 izvodov
1. izdaja

Welcome note

Dear Colleagues, dear Students,

The idea of organizing the Workshop and Postgraduate Course on Electroporation-Based Technologies and Treatments (EBTT) at the University of Ljubljana had been developing for several years. After preliminary discussions, the Workshop and Course was organised for the first time in 2003. In 2022 the Course is organised for the 16th time! In these nineteen years, the Course has been attended by 960 participants coming from 43 different countries. And this year again we can say with great pleasure: "with participation of many of the world leading experts in the field". The goals and aims of the Workshop and Course however remain unchanged: to provide the participants with sufficient theoretical background and practical knowledge to allow them to use electroporation effectively in their working environments.

It is a great pleasure to welcome you to the EBTT and in particular to the practical lab work taking place at the University of Ljubljana, Faculty of Electrical Engineering organised as an integral part of the Interdisciplinary doctoral programme Biomedicine. From the very beginning we were aiming to prepare lab work for participants, which would complement the lectures. As preparing lab work takes more time than preparing and organizing lectures, we introduced lab work at the second workshop in 2005. Lab work covers different aspects of research: biological experiments taking place in the cell culture labs, microbiological lab, lab for tissue and planar lipid bilayer; numerical and molecular dynamics modelling, e-learning using computer classrooms, pulse generator development and electrical measurements using electronic laboratory workshop and magnetic resonance electrical impedance tomography.

Following the experience gained in 2020 when due to pandemic we organised the course entirely on-line, we decided to continue organising the course as a hybrid, to enable participation also to those who are still facing difficulties in traveling. The team here in Ljubljana will thus provide on-site hands-on labworks as well as live webinars of the lab works so that you will be able to benefit most even if not actually being in the lab.

The biological experiments were pre-recorded and will be organised in the Infrastructural Centre "Cellular Electrical Engineering", part of the Network of Research and Infrastructural Centres of University of Ljubljana in the Laboratory of Biocybernetics. Lab works would not be possible without extensive involvement and commitment of numerous members of the Laboratory of Biocybernetics and Igor Serša from Jožef Stefan Institute for what I would like to thank them all cordially.

It also needs to be emphasized that all written contributions collected in the proceedings have been reviewed and then thoroughly edited by Peter Kramar. We thank all authors and reviewers. Also, I would like to express our sincere thanks to the faculty members and invited lecturers for their lectures delivered at the course. Finally, I would like to thank our sponsors who are making our EBTT possible:

Bia (Slovenia), Elea (Germany), Galvanize (USA), IGEA (Italy), Intuitive (USA), Iskra Medical (Slovenia), Iskra PIO (Slovenia), Jafral (Slovenia), Labtim (Slovenia), Meditech (Slovenia), Medtronic (USA), mPOR (Slovenia), Mikro+Polo (Slovenia), Pulse Bioscience (USA), Bioelectrochemical Society and ISEBTT International Society for Electroporation-Based Technologies and Treatments.

I sincerely hope you will enjoy the experience, benefit from being with us and enlarge your professional network.

Sincerely Yours,

Damijan Miklavčič

INVITED LECTURERS

The Biophysics of Cell Membrane Electroporation

Lea Rems; *University of Ljubljana, Faculty of Electrical Engineering, Tržaska 25, SI-1000 Ljubljana, SLOVENIA*

INTRODUCTION

The plasma membrane of a mammalian cell is a complex organization of lipids and proteins that separates the cell interior from the outside environment and transduces messages between the environment and the internal cellular apparatus. The membrane lipid bilayer is composed of hundreds of different types of lipids, asymmetrically distributed between the two bilayer leaflets and organized in domains, which are enriched (or depleted) with specific lipids like cholesterol. The lipid bilayer hosts numerous types of membrane proteins which tightly regulate transmembrane traffic and participate in cell signalling. The membrane also provides attachments for the underlying actin cortex, which dictates the membrane's mechanical properties, and acts as a dynamic modulator of the cell shape. When we electroporate cells, all membrane components (lipids, membrane proteins, and the actin cortex) are affected [1]. Since membrane organization and integrity are essential for the life and proper function of a cell, it is important to understand how, why and under which conditions these individual membrane components become affected. This lecture will focus on the known biophysical effects of electroporative pulses on the plasma membrane organization, using insights from computational and experimental studies on model membrane systems.

METHODS

Model membrane systems are indispensable because they enable a systematic bottom-up approach to study the biophysics of electroporation. The results presented in the lecture will be based on the following methods. Molecular dynamics (MD) is a computer simulation for analysing the physical movements of atoms and molecules. The output of MD is a trajectory, which is determined by solving the classical equations of motion for a system of interacting particles. MD offers spatiotemporal resolution superior to any experimental method. However, due to its computational demand, we can mainly use MD to study small systems with dimensions on the order of 10-100 nm and temporal scales on the order of 1-10 μs, depending on whether we use all-atom or coarse-grained representation of the molecular system. To study electroporation on the scale of single cells and cell clusters, we need to design a set of ordinary and partial differential equations that describe the physical behavior of the system. The equations can be solved with different numerical methods, such as finite elements, transport lattices, or similar. When studying electroporation experimentally, giant unilamellar vesicles (GUVs) have become very popular, since they resemble the cell size and can be easily visualized with optical microscopy. GUVs can be prepared with various types of lipids and lipid mixtures. Emerging techniques enable preparation of GUVs with embedded membrane proteins or actin cortex.

RESULTS AND DISCUSSION

The most accepted models, that describe electroporation on the whole-cell level, consider that pores can form only in the lipid domains of the plasma membrane and that all pores exhibit more or less the same kinetic behaviour. However, accumulating evidence from experiments and simulations on model systems speaks against these assumptions [2,3]. Poration kinetics of pores in pure lipid bilayers has been shown to depend on the type of lipids and their phase state; since the lipids in the plasma membrane organize in domains, there must exist locations which are more and less likely to porate. Indeed, coarse-grained MD simulations of membranes mimicking the realistic plasma membrane composition show that pores preferentially form in domain characterized by specific features such as high content of polyunsaturated lipids. Moreover, our research suggests that pores can nucleate also within some membrane proteins causing protein denaturation and lipid rearrangement. Such lipid/protein complex pores can be more stable than pure lipid pores and are more likely to explain the persistent increase in plasma membrane permeability following exposure to electric pulses. Studies on GUVs with encapsulated actin network have further shown that pore formation, expansion and resealing is affected by the actin network. Finally, electroporation has also been found to be associated with oxidative damage of polyunsaturated lipids. As lipids are oxidized, their tails become less hydrophobic and consequently more permeable to ions and molecules. Further research is, however, needed to connect these new findings into a coherent picture which will allow to understand what can or cannot happen in the plasma membrane depending on the parameters of the applied pulses and other experimental conditions.

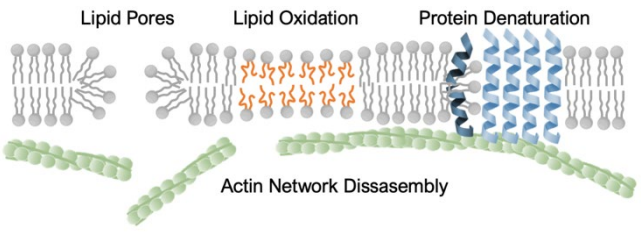

Figure 1: Molecular mechanisms of electroporation.

REFERENCES

[1] T. Kotnik, L. Rems, M. Tarek, D. Miklavčič, *Annu. Rev. Biophys.*, vol. 48, pp. 63-91, 2019.

[2] L. Rems, M. Kasimova, I. Testa, L. Delemotte, *Biophys. J.*, vol. 119, pp. 90-105, 2020.

[3] D. Perrier, A. Vahid, V. Kathavi, L. Stam, L. Rems, Y. Mulla, A. Muralidharan, G.H. Koenderink, M.T. Kreutzer, P.E. Boukany, Sci. Rep., vol. 9, pp. 8151, 2019.

Nanosecond imaging of cell membrane voltage using strobe photography and streak camera microscopy

Joel N. Bixler[1] *Bioeffects Division, Air Force Research Laboratory, San Antonio, TX, United States*

INTRODUCTION

Direct observation of rapid membrane potential changes is critical to fully understanding the biophysics resulting from pulsed electric field exposure. This can be a challenging endeavour, particularly when the applied electric field is only present for tens to hundreds of nanoseconds. Traditional microscopy methods are limited to frame rates with millisecond limitations, preventing capture of dynamics during pulse exposure.

Recently, we have developed two complementary methods capable of resolving membrane voltage response during the application of nanosecond pulsed electric fields. The first, termed steak camera microscopy (SCM), can provide single shot acquisition of the full time dynamics of membrane charging for a single spatial axis of information. Complementary to this is strobe photography, a technique that utilizes multiple short duration flashes of light to capture a snapshot of the dynamics at a single point in time. Resolving the full time sequence of an event requires multiple exposures of both the light flash and the pulsed electric field.

Methods

Strobe photography is a powerful tool that enables one to acquire images with both high spatial and temporal resolution relative to any other ultrafast imaging technique. Here, the exposure time of a given frame is not controlled by the microscope's image sensor, but instead by the duration of the light pulse used to illuminate the field of view. The use of laser sources with nanosecond pulse widths can then provide strobe images that capture dynamics with nanosecond time resolution. Sequentially varying the time into an event at which the laser pulse arrives allows a user to record the full time dynamics, so long as the event is highly repeatable. This limits the overall utility of strobe photography for highly porating electric fields. A respresentative schematic for a strobe photography system is shown in Fig 1.

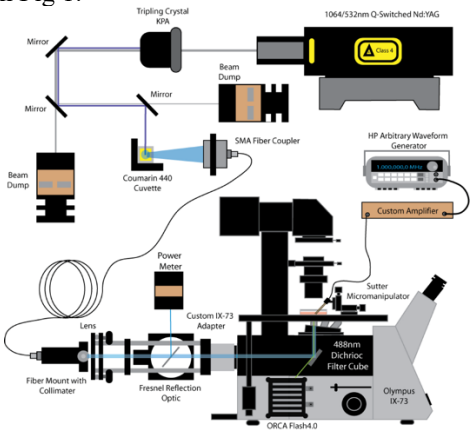

Figure 1: The genearl schematic of a strobe photography system. Full details can be found in [1].

SCM is a unique tool that enables one to record the full membrane charging dynamics in response to a pulsed electric field exposure [2], but with several unique limitations. First, this type of imaging can only record from a single spatial axis of information due to the limiting entrance slit needed for streak camera operation. Streak cameras operate much like spectrometers in that an entrance slit is used to limit the information being sampled, and the width of that slit directly impacts the time resolution (spectral resolution in the case of a spectrometer). Second, as each row of pixels only contains fluorescence signal from a very short time window (typically single to tens of nanoseconds) a high quantum efficiency dye is needed in combination with a high-power excitation source. This limits the application of SCM to cell types which respond more favourably to high loading concentrations, and those that are less phototoxic. Sample images from SCM are shown Fig. 2 showing membrane dynamics for CHO cells during exposure to a 40 kHZ and 80 kHz sinewave.

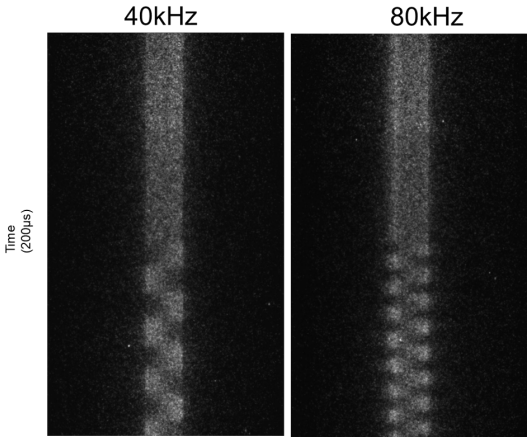

Figure 2: Example SCM images for 40 kHz and 80 kHz sinewaves

Conclusions

SCM and strobe photography are powerful tools that can be used to visualize membrane charging dynamics under a variety of electrostimulation parameters.

REFERENCES

[1] A. S. Kiester, B. L. Ibey, Z. N. Coker, A. G. Pakhomov, and J. N. Bixler, "Strobe photography mapping of cell membrane potential with nanosecond resolution," *Bioelectrochemistry*, p. 107929, Aug. 2021,

[2] H. T. Beier, C. C. Roth, J. N. Bixler, A. v. Sedelnikova, and B. L. Ibey, "Visualization of Dynamic Sub-microsecond Changes in Membrane Potential," *Biophys J*, vol. 116, no. 1, pp. 120–126, Jan. 2019.

Plasma membrane Repair Mechanisms

Jesper Nylandsted; *Danish Cancer Society Research Center, Membrane Integrity, Strandboulevarden 49, DK-2100 Copenhagen, Denmark / University of Southern Denmark, Department of Molecular Medicine, J.B. Winsløws Vej 21-25Odense C - DK-5000, DENMARK*

ABSTRACT

The plasma membrane of eukaryotic cells defines the essential boundary to the extracellular environment and, thus injuries to the cell membrane pose a lethal threat to cells. Cells cope by activating their plasma membrane repair system, which includes mechanisms to reseal and remove damaged membrane. Inadequate repair responses can tip the balance between physiology and pathology, highlighting the significance of plasma membrane integrity. For example, an over-activated repair response can promote cancer invasion, while the inability to efficiently repair membrane can drive neurodegeneration and muscular dystrophies [1]. However, the underlying molecular and biophysical mechanisms used to repair membrane lesions during physiological and pathological conditions are not well characterized. The family of annexins are Ca2+-triggered proteins involved in various steps of the plasma membrane repair response. Our recent results, based on interdisciplinary research synergy across molecular cell biology, experimental membrane physics, and computational simulations show that annexins have additional biophysical functions in the repair response besides enabling membrane fusion. Our data suggest that annexins possess different membrane-shaping properties, allowing for a tailored response that involves rapid bending, constriction, and fusion of membrane edges for resealing [2]. Moreover, some annexins have high affinity for highly curved membranes that appear at free edges near rupture sites, a property that might accelerate their recruitment for rapid repair. To this end, cancer cells are more dependent on efficient plasma membrane repair to counteract stress-induced membrane injuries, which opens novel avenues to target cancer cells through their repair system [3]. Here, novel aspects of plasma membrane repair and regeneration [4] will be presented.

REFERENCES

[1] Dias C, Nylandsted J. Plasma membrane integrity in health and disease: significance and therapeutic potential. *Cell Discovery*. 2021; 19;7(1):4.

[2] Boye TL, Maeda K, Pezeshkian W, Lauritzen SP, Hager SC, Gerke V, Simonsen AC,and Nylandsted J. Annexin A4 and A6 induce membrane curvature and constriction during cell membrane repair. *Nature Communications*. 2017; 8(1):1623.

[3] Jaiswal JK, Lauritzen SP, Scheffer L, Sakaguchi M, Bunkenborg J, Simon SM, Kallunki T, Jäättelä M, Nylandsted J. S100A11 is required for efficient plasma membrane repair and survival of invasive cancer cells. *Nature Communications*. 2014; 8;5:3795.

[3] Sønder SL, Häger SC, Heitmann ASB, Frankel LB, Dias C, Simonsen AC, Nylandsted J. Restructuring of the plasma membrane upon damage by LC3-associated macropinocytosis. *Science Advances*. 2021; 7(27):eabg1969.

Prophylactic and Therapeutic Applications of Gene Electrotransfer

Richard Heller[1], Jody Synowiec[1], Samantha Mannarino[1], Julie Singh[1], Mark Jaroszeski[1] and Guilan Shi[1]; [1]*Department of Medical Engineering, University of South Florida, Tampa, Florida, 33612, USA*

INTRODUCTION

Gene-based medicine has the potential to be used in multiple applications for the prevention or treatment of disease. Significant progress is being made including several therapies gaining regulatory approvals. However, there are still areas that need to be improved including to efficacy and toxicity. A key hurdle that still needs to be overcome is delivery. Non-viral approaches still lag behind viral delivery approaches, but significant progress is being made. Physical delivery methods have shown increased utility. Gene electrotransfer (GET) has made the most progress. The key to protocol development is to find parameters to achieve reproducible expression with minimal to no adverse effects.

PROPHYLACTIC APPLICATIONS

The development of nucleic acid vaccines has seen tremendous growth particularly in vaccines developed for SARS-CoV2. This type of vaccine approach is an attractive alternative to standard vaccines, due to potential for decreased toxicity, quick modifications to address pathogen mutation and relatively quick manufacture. The key issue, as with many nucleic acid-based approaches has been effective delivery. However, GET has been demonstrated to be an effective tool to enhance delivery and increase immune response [1-2].

We have established that the addition of moderate heat (43ºC) in combination with GET can enhance delivery. We used this concept to deliver a DNA vaccine against Hepatitis B Virus (HBSAg). Guinea pigs were injected intradermally with a plasmid encoding HBSAg followed by GET with or without heat [3]. After a prime/boost vaccination, αHBSAg serum titers indicated a 230-fold increase in antibodies when delivered with moderate heat compared to injection only and 20-fold over the delivery with GET without heat (Figure 1).

THERAPEUTIC APPLICATIONS

We previously demonstrated that treatment with plasmid IL-12 delivered with GET alone resulted in prolonged disease-free survival and induced long term immune memory protecting against challenge in a mouse melanoma model [4-5]. To further test the potential of this approach, we utilized a metastatic model consisting of subcutaneous (subq) B16.F10 tumor and B16.F10 cells expressing luciferase injected via the intraperitoneal route. Treatment with pIL-12 GET while successful in reducing or eliminating the subcutaneous tumor was only successful in about 50% of the mice in reducing or eliminating the peritoneal spread. When combining a subq injection of anti-PD-1 and pIL-12 GET to the subq tumor results were enhanced.

Another therapeutic application being explored is protein replacement therapy. One concept being explored is to deliver a plasmid encoding Factor IX to the skin utilizing GET. This was tested again using moderate heat to augment delivery to the skin. Increased levels of Factor IX were obtained and lasted for up to 3 months [6].

CONCLUSIONS

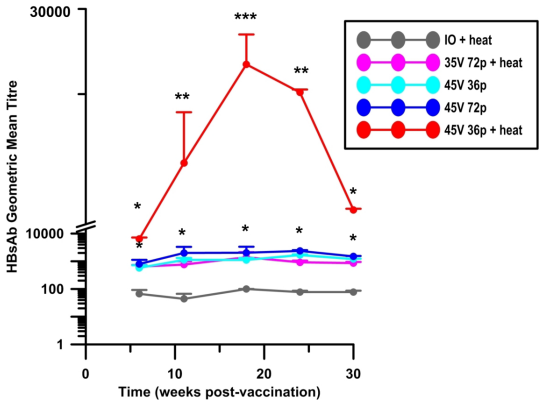

Figure 1. HBsAb production induced by moderate heat-assisted GET after a prime-boost DNA vaccination protocol against HBV. Prime and boost were separated by two weeks.

GET is a powerful tool that can be used to efficiently deliver plasmid DNA for a variety of applications. Dependent on the therapeutic or prophylactic target a specific tissue target and transgene can be utilized. Developing a specific delivery protocol is essential to achieving the desired clinical outcome. In addition to delivering of DNA vaccines to the skin this approach could also be utilized to deliver a plasmid encoding Human Factor IX as a protein replacement therapy for treating Haemophilia B. In addition to immunotherapy for melanoma other tumor types can also be treated with this approach including breast and pancreatic cancer. Translation of GET has been moving forward and has now utilized in over 130 clinical trials.

REFERENCES

[1] NY Sardesai, DB Weiner, "Electroporation delivery of DNA vaccines; prospects for success" Curr Opin Immuno, 23(3) pp421-429, 2011.

[2] A Donate, D Coppola, Y Crua, R Heller, "Evaluation of a novel non-penetrating electrode for use in DNA vaccination" Plos One, 6(4) pp e19181, 2011.

[3] Edelblute, CM, Mangiamele, C and Heller, R. Moderate heat-assisted gene electrotransfer for cutaneous delivery of a DNA vaccine against Hepatitis B virus. Human Gene Therapy, 32(21-22):1360-1369.

[4] ML Lucas, R Heller, "IL-12 gene therapy using an electrically mediated nonviral approach reduces metastatic growth of melanoma" DNA Cell Biol, 22(12 pp 755-763, 2003.

[5] G Shi, C Edelblute, S Arpag, C Lundberg, R Heller, "IL-12 gene electrotransfer triggers a change in immune response within mouse tumors" Cancers, 10(12) pp 498, 2018.

[1] [6] Edelblute, CM, Mangiamele, C and Heller, R. Moderate heat-assisted gene electrotransfer for Factor IX protein replacement therapy in the skin. Pharmaceutics, 13(11):908, 2021.

Pulsed Electric Field technology (PEF) in food processing for improving food quality, safety and competitiveness

Javier Raso, *Food Technology, Faculty of Veterinary, University of Zaragoza, C/ Miguel Servet, 177 50013 Zaragoza, SPAIN*

INTRODUCTION

Most of the raw foodstuffs need to be processed to be made suitable for consumption. Food processing techniques used in the food industry involve many different operations such as cleaning, separating, size reduction, thermal processing, drying etc. These operations increase food availability, ensure food safety, increase food diversity, change the flavour and texture of foods etc. Although many benefits derive from food processing this industrial activity has also some drawbacks. Some of the operations used in the food industry for processing affect the sensorial and nutritional properties of foods. On the other hand, generally, methods and techniques used for food processing require high energy consumption and as a result of the processing of raw materials, a lot of waste is generated. These last two issues have a great economic and environmental impact because the food industry represents the main industrial activity of the European Union.

Foodstuffs processed for the food industry come from animals and plants that have a cellular structure. Electroporation of these cells by pulsed electric fields (PEF) can change the structural integrity of animal or plant tissues being this effect very relevant to the food industry to facilitate the transformation of raw material in foods or to improve process efficiency. On the other hand, modifying the permeability of the cytoplasmic membrane by PEF improves mass transfer operations aiming to extract a given intracellular compound located in the cell (Figure 1). Finally, the capability of PEF for inactivating microorganisms at temperatures below those used in thermal processing is very attractive for the food industry that is interested in reducing the negative effects of heat treatments in foods.

The feasibility of PEF for improving food processing operations has been demonstrated in laboratory and pilot plant studies since the beginning of the 1990s. However, the lack of reliable industrial equipment limited the commercial exploitation of PEF in the food industry. The development in the last years of pulse power systems responding to the food industry requirements has allowed the successful transfer of the technology for industrial applications. Currently, different industrial scale PEF units for different applications are manufactured for different companies and more than 200 of these units have been installed in the food industry all around the world.

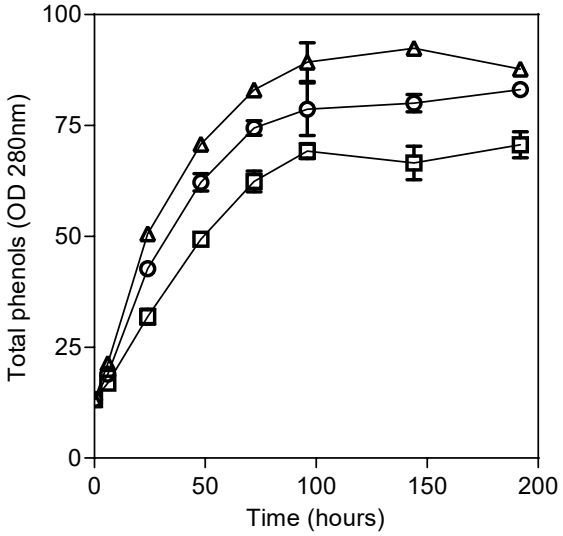

Figure 1: Comparison of the extraction of polyphenols from untreated grapes (□) and grapes treated by PEF at 5 kV/cm (○) and 10 kV/cm (Δ) during vinifcation of Tempranillo grapes.

In this lecture, it will be presented and discussed how PEF may improve the competitiveness of several industrial sectors (winemaking, olive oil, etc) by improving process efficiency and making their activities more energy-efficient and sustainable

REFERENCES

[1] J. Raso, V. Heinz, I. Álvarez, S. Toepfl. P*ulsed Electric Fields Technology for the Food Industry: Fundamentals and Applications (second edition). Switzerland: Springer Cham,* 2022

Treatment of Epilepsy with Temporal Interference Stimulation and Focal Ablations using Electroporation

Adam Williamson[1]; [1] *Aix-Marseille University, Jardin du Pharo, 58 Boulevard Charles Livon, 13007 Marseille, FRANCE*

During presurgical evaluation, patients suffering from focal drug-resistant epilepsy often require invasive recordings using stereo-electroencephalography (SEEG), involving the implantation of numerous electrodes in different brain regions for the electrophysiological monitoring of seizure onset and the subsequent localization of an epileptogenic zone (EZ) [1], [2]. Electrical stimulation from the intracranial electrodes is often necessary to help define an EZ, with electrophysiological discharges and seizures triggered by different frequencies of stimulation[3], [4]. In general, pathological discharges from the EZ are characterized by several biomarkers, primarily the generation of high-frequency oscillations in the beta/gamma range, classically referred to as rapid-discharges[5]–[7]. Although currently performed with invasive SEEG, less-invasive methods capable of evoking such discharges and seizures during the localization of EZ tissue would be highly interesting as positive surgical outcomes are well-correlated with the removal of tissue regions which generate such high-frequency oscillations[8]–[11].

To address this, we utilize the method of temporal interference (TI) stimulation, a focal stimulation method that has the ability to stimulate deep brain structures with envelopes of interference at points located at a significant distance from the surface electrode[12]. This can be achieved by the use of two high frequencies (>1 KHz) which are known to not have an impact on the neurons[13]. The two frequencies have to have an offset which will be the frequency of the DBS stimulation. We use this to identify seizure foci, evoke epileptiform discharges, and show neuromodulatory effects of TI to suppress epileptogenic biomarker.

Although effective, TI does not yet have the ability to permanently stop seizures. For this only surgery remains. In epilepsy, the most frequent surgical procedure for patients suffering from drug-resistant focal-onset epilepsy is resective surgery[14]. In the most common type of drug-resistant epilepsy, mesial temporal lobe epilepsy (MTLE), while associated with high-rates of seizure freedom surgical resection can often impact neurocognitive function. For drug-resistant MTLE, focal thermal ablation is a less-invasive method being explored for surgical treatment to achieve high-degrees of seizure freedom while maintaining memory and other cognitive functions associated with the basal and lateral temporal areas[15], [16] . Although, radio-frequency (RF) ablation and laser interstitial thermal therapy (LITT, aka laser ablation) are the methods with the most attention, achieving reasonable seizure-free rates with less negative impact on neurocognitive function[17], there remain technical questions about these two methods of thermal ablation, primarily thermal injury to surrounding tissues, edema due to hemorrhage [18] and poor directionality.

Consequences of surgery can vary strongly depending on the brain region targeted for removal, as surgical morbidity and collateral damage can lead to significant complications, particularly when bleeding and swelling are located near delicate functional cortical regions. Although focal thermal ablations are well-explored in epilepsy as a minimally invasive approach, hemorrhage and edema can be a consequence as the blood-brain barrier is still disrupted. Non-thermal irreversible electroporation (NTIRE), common in many other medical tissue ablations outside the brain, is a relatively unexplored method for the ablation of neural tissue, and has never been reported as a means for ablation of brain tissue in the context of epilepsy. Here, we present a detailed visualization of non-thermal ablation of neural tissue in mice and report that NTIRE successfully ablates epileptic foci in mice, resulting in seizure-freedom, while causing significantly less hemorrhage and edema compared to conventional thermal ablation. The NTIRE approach to ablation preserves the blood-brain barrier while pathological circuits in the same region are destroyed. Additionally, we see the reinnervation of fibers into ablated brain regions from neighboring areas as early as day 3 after ablation. Our evidence demonstrates that NTIRE could be utilized as a precise tool for the ablation of surgically challenging epileptogenic zones in patients where the risk of complications and hemorrhage is high, allowing not only reduced tissue damage but potentially accelerated recovery as vessels and extracellular matrix remain intact at the point of ablation.

REFERENCES

[1] L. Koessler *et al.*, “Source localization of ictal epileptic activity investigated by high resolution EEG and validated by SEEG,” *NeuroImage*, vol. 51, no. 2, pp. 642–653, Jun. 2010, doi: 10.1016/j.neuroimage.2010.02.067.

[2] F. Bartolomei, P. Chauvel, and F. Wendling, “Epileptogenicity of brain structures in human temporal lobe epilepsy: a quantified study from intracerebral EEG,” *Brain J. Neurol.*, vol. 131, no. Pt 7, pp. 1818–1830, Jul. 2008, doi: 10.1093/brain/awn111.

[3] C. Munari *et al.*, “Intracerebral Low Frequency Electrical Stimulation: a New Tool for the Definition of the ‘Epileptogenic Area’?,” in *Advances in Stereotactic and Functional Neurosurgery 10*, Vienna, 1993, pp. 181–185. doi: 10.1007/978-3-7091-9297-9_42.

[4] M. Guye, "The role of corticothalamic coupling in human temporal lobe epilepsy," *Brain*, vol. 129, no. 7, pp. 1917–1928, Jul. 2006, doi: 10.1093/brain/awl151.

[5] P. J. Allen, D. R. Fish, and S. J. M. Smith, "Very high-frequency rhythmic activity during SEEG suppression in frontal lobe epilepsy," *Electroencephalogr. Clin. Neurophysiol.*, vol. 82, no. 2, pp. 155–159, Feb. 1992, doi: 10.1016/0013-4694(92)90160-J.

[6] F. Bartolomei, F. Wendling, J.-J. Bellanger, J. Régis, and P. Chauvel, "Neural networks involving the medial temporal structures in temporal lobe epilepsy," *Clin. Neurophysiol.*, vol. 112, no. 9, pp. 1746–1760, Sep. 2001, doi: 10.1016/S1388-2457(01)00591-0.

[7] F. Wendling, F. Bartolomei, J. J. Bellanger, and P. Chauvel, "Identification de réseaux épileptogènes par modélisation et analyse non linéaire des signaux SEEG," *Neurophysiol. Clin. Neurophysiol.*, vol. 31, no. 3, pp. 139–151, Jun. 2001, doi: 10.1016/S0987-7053(01)00255-6.

[8] G. Alarcon, C. D. Binnie, R. D. C. Elwes, and C. E. Polkey, "Power spectrum and intracranial EEG patterns at seizure onset in partial epilepsy," *Electroencephalogr. Clin. Neurophysiol.*, vol. 94, no. 5, pp. 326–337, May 1995, doi: 10.1016/0013-4694(94)00286-T.

[9] S. Lagarde *et al.*, "Seizure-onset patterns in focal cortical dysplasia and neurodevelopmental tumors: Relationship with surgical prognosis and neuropathologic subtypes," *Epilepsia*, vol. 57, no. 9, pp. 1426–1435, 2016, doi: 10.1111/epi.13464.

[10] B. Frauscher *et al.*, "High-frequency oscillations: The state of clinical research," *Epilepsia*, vol. 58, no. 8, pp. 1316–1329, 2017, doi: 10.1111/epi.13829.

[11] C. Cuello Oderiz *et al.*, "Association of Cortical Stimulation–Induced Seizure With Surgical Outcome in Patients With Focal Drug-Resistant Epilepsy," *JAMA Neurol.*, vol. 76, no. 9, pp. 1070–1078, Sep. 2019, doi: 10.1001/jamaneurol.2019.1464.

[12] N. Grossman *et al.*, "Noninvasive Deep Brain Stimulation via Temporally Interfering Electric Fields," *Cell*, vol. 169, no. 6, Art. no. 6, Jun. 2017, doi: 10.1016/j.cell.2017.05.024.

[13] B. Hutcheon and Y. Yarom, "Resonance, oscillation and the intrinsic frequency preferences of neurons," *Trends Neurosci.*, vol. 23, no. 5, pp. 216–222, May 2000, doi: 10.1016/S0166-2236(00)01547-2.

[14] S. Wiebe, W. T. Blume, J. P. Girvin, M. Eliasziw, and Effectiveness and Efficiency of Surgery for Temporal Lobe Epilepsy Study Group, "A randomized, controlled trial of surgery for temporal-lobe epilepsy," *N. Engl. J. Med.*, vol. 345, no. 5, Art. no. 5, Aug. 2001, doi: 10.1056/NEJM200108023450501.

[15] Y. B. Bezchlibnyk, J. T. Willie, and R. E. Gross, "A neurosurgeon`s view: Laser interstitial thermal therapy of mesial temporal lobe structures," *Epilepsy Res.*, vol. 142, pp. 135–139, May 2018, doi: 10.1016/j.eplepsyres.2017.10.015.

[16] R. E. Gross *et al.*, "Stereotactic laser amygdalohippocampotomy for mesial temporal lobe epilepsy: SLAH Outcomes for MTLE," *Ann. Neurol.*, vol. 83, no. 3, Art. no. 3, Mar. 2018, doi: 10.1002/ana.25180.

[17] R. E. Gross, B. Mahmoudi, and J. P. Riley, "Less is more: novel less-invasive surgical techniques for mesial temporal lobe epilepsy that minimize cognitive impairment," *Curr. Opin. Neurol.*, vol. 28, no. 2, Art. no. 2, Apr. 2015, doi: 10.1097/WCO.0000000000000176.

[18] M. J. Howenstein and K. T. Sato, "Complications of radiofrequency ablation of hepatic, pulmonary, and renal neoplasms," *Semin. Interv. Radiol.*, vol. 27, no. 3, Art. no. 3, Sep. 2010, doi: 10.1055/s-0030-1261787.

Pulsed Field Ablation (PFA): current knowledge and future challenges

Tomás García-Sánchez, *Department of Information and Communication Technologies, Universitat Pompeu Fabra, Carrer Roc Boronat 138, Barcelona, SPAIN.*

INTRODUCTION

In the last 20 years, atrial fibrillation (AF) has become one of the most important public health problems (predicted to affect 17.9 million patients in Europe by 2060)[1] and is a significant cause of increasing health care costs in western countries. Over the past 15 years, remarkable advances have revolutionized the management of cardiac arrhythmias. In this regard, ablation – the selective destruction of areas of cardiac tissue – has been established as a therapeutic option in patients not responding to antiarrhythmogenic medication.

The current standard ablation technologies are based on thermal methods; either by heating the target tissue with radiofrequency (RF), or alternatively, by using extreme cold to destroy tissue (cryoablation). Despite the successful results of these ablation technologies, there are still a non-negligible number of cases where recurrent disease cannot be correctly managed, or some complications occur. The possible complications include thromboembolism, damage to the phrenic nerve, vascular stenosis, severe oesophageal injury leading to atrio-oesophageal fistula or in rarer cases cardiac perforation and stroke.

In the last years, the use of irreversible electroporation (IRE) as a non-thermal method for ablation of cardiac arrhythmias, also known as Pulsed Field Ablation (PFA), has rapidly moved from preclinical studies to clinical application in recent years. The potential of IRE to create myocardial lesions without two of the most troubling complications associated with thermal injury (pulmonary vein stenosis and serious oesophageal damage) has placed electroporation as the promise in the future of cardiac ablation.

CURRENT KNOWLEDGE

Since the publication of the first human cases in 2018[2] a considerable number of papers have demonstrated in preclinical or clinical studies the ability of PFA to create cardiac lesions while preserving surrounding cardiac tissues such as the esophagus or the phrenic nerve. After the approval of the first commercial PFA system at the beginning of 2021 in Europe, more than 5000 patients have been already treated with this technology. A recent publication with relatively large dataset (more than 1600 patients) demonstrated no instances of esophageal injury, permanent phrenic nerve paralysis or vein stenosis [3]. This confirms one, if not the most, important advantage of PFA with respect to thermal ablation technologies: its safety.

The first long-term results of arrhythmia recurrence in a small group of patients seem to show similar recurrence rates comparted to RF ablation [4]. However, more data is needed in larger groups of patients to provide a definitive answer about whether PFA will have better long term efficacy results than the other ablation modalities. Furthermore, all the previous observations come from the usage of the same commercial system. We should wait to have results from different PFA systems to extract strong conclusions about PFA long term efficacy. Fortunately, these data will be available sooner than later. In August 2022, a second system received CE mark and all the main multinational companies in the field are developing PFA technology with multiple ongoing clinical trials around the world.

FUTURE CHALLENGES

Despite the great initial success of the technology, there are still many unknowns that must be addressed and understood. Unlike the case of cancer treatment, the development of the PFA technology has been mainly driven by companies with a clear focus on rapidly making it available in the clinical setting. This makes that studies of basic science and mechanisms around PFA are still scarce.

One of the statements about the technology that has been poorly demonstrated is tissue specificity. Although long term preservation of non-cardiac cells around the area of ablation application is observed, whether this comes from a real selective effect of electroporation or other factors such as tissue regeneration, electric field exposure level, etc., has not been demonstrated.

Another important challenge for the future of PFA relates to the waveforms used to deliver the electric field to tissue. Because the companies are keeping this information confidential, mechanistic or comparison studies can not be correctly performed. Companies should understand the importance of reporting the waveform used to increase the quality scientific knowledge about PFA.

Many of the mechanisms that drive lesion formation and its impact on safety and efficacy remain unclear. Also, some collateral effects observed during PFA application such as coronary spasms or silent cerebral lesions (SCL) deserve special attention. Although the technology development status is quite advanced there are still some technological challenges. For instance, in the treatment of ventricular arrhythmias to safely increase lesion depth, or the development of real time indicators that would enable the titration of the delivered dose by the operator.

REFERENCES

[1] C. A. Morillo, A. Banerjee, P. Perel, D. Wood, and X. Jouven, “Atrial fibrillation: The current epidemic,” *J. Geriatr. Cardiol.*, vol. 14, pp. 195–203, 2017.

[2] V. Y. Reddy *et al.*, “Ablation of Atrial Fibrillation With Pulsed Electric Fields: An Ultra-Rapid, Tissue-Selective Modality for Cardiac Ablation,” *JACC Clin. Electrophysiol.*, vol. 4, no. 8, pp. 987–995, 2018.

[3] E. Ekanem *et al.*, “Multi-national survey on the methods, efficacy, and safety on the post-approval clinical use of pulsed field ablation (MANIFEST-PF).,” *Europace*, vol. 24, no. 8, pp. 1256–1266, Sep. 2022.

[4] V. Y. Reddy *et al.*, “Pulsed Field Ablation of Paroxysmal Atrial Fibrillation: 1-Year Outcomes of IMPULSE, PEFCAT, and PEFCAT II,” *JACC Clin. Electrophysiol.*, vol. 7, no. 5, pp. 614–627, 2021.

The Role of DNA Electrophoresis in Gene Electrotransfer

Shaurya Sachdev; *Faculty of Electrical Engineering, University of Ljubljana, Trzaska 25, SI-1000 Ljubljana, SLOVENIA*

INTRODUCTION

Gene electrotransfer (GET) is a technique that employs pulsed electric fields to deliver DNA and other nucleic acids to cells. However, pulsed electric fields not only permeabilize the cell membrane (electroporation), but also push DNA molecule towards the cathode (electrophoresis). It is well accepted that electrophoresis is critical to GET. For instance, *in vivo*, where DNA mobility is restricted, a high-voltage pulse for electroporation is generally followed by a long-duration, low-voltage pulse to enhance DNA electrophoresis, thereby also enhancing GET efficiency [1]. Even *in vitro*, long duration pulses (µs to ms) with a strong electrophoretic component resulted in a higher GET efficiency compared to ultra-short duration pulses (ns) lacking a strong electrophoretic component [2]. Understanding the role of DNA electrophoresis is thus crucial to understanding GET. In this lecture, I will elaborate the role DNA electrophoresis plays during GET across various length scales (Figure 1). These include – (1) the short-nanoscopic length scale of DNA moving across the cell membrane, (2) the microscopic length scale of DNA coming close to the cell membrane and establishing a DNA-membrane contact, and (3) the macroscopic length scale of DNA migrating in the tissue due to electrophoresis.

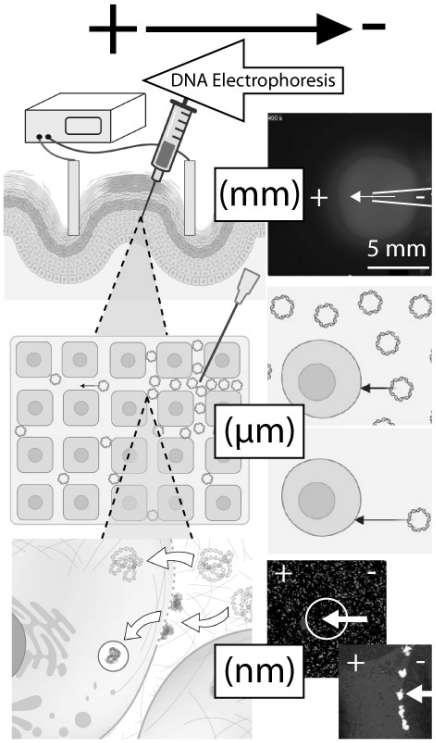

Figure 1: DNA electrophoresis across various length scales during GET.

TRANSPORT ACROSS THE CELL MEMBRANE

It is believed that DNA is translocated across the cell membrane by active process of endocytosis which takes place after pulse electric field termination, implying a negligible role of electrophoresis in DNA transport across the cell membrane. However, depending on the size of the DNA, two modes of DNA transport are observed: DNA aggregate formation followed by endocytosis for large DNA molecules (>1000 bp), and direct translocation of DNA into the cytoplasm without DNA aggregation for small DNA molecules (<100 bp) [3]. It is for smaller DNA molecules that DNA transport across the cell membrane is driven by electrophoresis [4].

CONTACT WITH THE CELL MEMBRANE

Although endocytosis of DNA aggregates might be independent of electrophoresis, accumulation of DNA in aggregates at the cell membrane is driven by electrophoresis [5]. Based on calculations of electrophoretic drift during pulsed electric field and diffusional migration of DNA, a *Peclet* (*Pe*) number is defined which quantifies the role of electrophoresis in bringing the DNA molecule in contact with the cell membrane [2]. The *Pe* helps to identify the contribution of electrophoresis in DNA-membrane contact for a wide variety of pulsing conditions – ns pulses, High-frequency bipolar pulses, µs pulses, and ms pulses.

MACROSCOPIC ELECTROPHORESIS IN TISSUES

Electrophoresis by short duration (µs to ms), high intensity (kV/cm) PEF results in DNA migration of < $O(1)$ µm *in vivo* [6]. However, long-duration, low-intensity electric currents can be employed to achieve DNA migration over macroscopic distances of $O(1)$ mm. Electrophoresis by these long-duration, low-intensity currents allows greater control over macroscopic distribution of DNA in tissues compared to pressure-based injection of DNA using syringes.

ACKNOWLEDGEMENTS

Horizon 2020 Widening Fellowship (No.: 101038051).

REFERENCES

[1] Satkauskas, S. *et al*., *Molecular Therapy*, vol. 5(2), pp. 133-140, 2002.
[2] Potočnik, T., Sachdev, S., *et al.*, D., *Applied Sciences*, vol. 12(16), pp. 8237, 2022.
[3] Sachdev, S. *et al.*, *BBA-Biomembranes*, vol. 1862(2), pp.183089, 2020.
[4] Sachdev, S. *et al.*, *Soft Matter*, vol. 15(45), pp. 9187-9194, 2019.
[5] Escoffre, J.M., *et al.*, *BBA-Biomembranes*, vol. 1808(6), pp.1538-1543, 2011.
[6] Henshaw, J.W. *et al.*, *Bioelectrochemistry*, vol. 71(2), pp.233-242. 2007.
[7] Plaschke, C.C et al Calcium electroporation for recurrent head and neck cancer: A clinical phase I study. Laryngoscope Investig. *Otolaryngol*. 2019, 4, 49–56.

SHORT PRESENTATIONS

Real-time analysis of electroporation phenomenon of individual cells

Anne Calvel[1,2], Katia Grenier[1], David Dubuc[1], Marie-Pierre Rols[2]; *[1] Laboratory for Analysis and Architecture of Systems (LAAS-CNRS), 7. Av. du Colonel Roche, F-31031 Toulouse, FRANCE [2] Institute of Pharmacology and Structural Biology (IPBS), 205 rte de Narbonne, 31077 Toulouse cedex 4, FRANCE (CNRS UMR 5089)*

INTRODUCTION

Electroporation (EP) is a promising approach for solid tumour treatment when combined with drug delivery, with high success rates (60-70% of complete remission) [1]. Leading single cell studies could provide a better understanding and mastery of EP at larger scales. Microdevices are adapted to perform such *in vitro* and *in situ* studies, while requiring low voltages.

MATERIALS AND METHODS

We perform *in situ* studies with a microdevice originally designed to analyse single cells by microwave dielectric spectroscopy [2]. It consists of three different parts: (a) a microfluidic channel (b) a metallic coplanar waveguide composed of a central signal conductor, between two ground planes, which contains a 10 μm gap in the middle and (c) a cell trap placed in the center of the microfluidic channel. The trap is located above the gap that constitutes the microwave sensing zone. The microfluidic channel, made of photoresist, is transparent, allowing to observe the trapped cell. Monitoring of cellular behaviour during EP using fluorescent biomarkers is also possible. A solution containing thousands of cells (PC3-GFP) is added to the fluidic inlet of the microdevice. Thanks to a continuous flow maintained by a syringe pump, the flow passes through the microfluid channel. A cell can be captured by a mechanical trap specifically designed to catch and maintain a single cell during the study. Once a cell is trapped, electrical pulses are delivered in a buffer solution. A generator (AFG3022C Tektronix) applies pulses through tungsten electrodes positioned on both sides of the coplanar signal lines. We study the effect of different voltages (from 3V to 10V) in order to determine the permeabilization threshold. The impact of the pulses on the individual cell is visualized with two different fluorescent biomarkers: (a) calcein AM to assess membrane integrity and cell viability and (b) propidium iodide to quantify permeabilization. A real-time monitoring of the fluorophores' intensity is carried out.

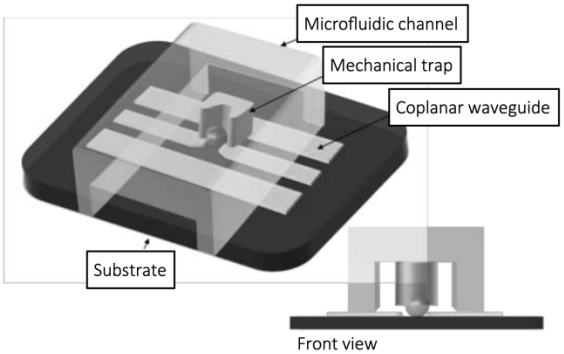

Figure 1: Schematics of the microdevice used for single cell EP and analysis [3].

RESULTS

8 pulses of 5 ms and 100 μs width at a frequency of 1 Hz are applied to different single cells. For pulses of 5 ms width, we observe that low electric field intensities (under 4.5 V) do not lead to permeabilization and maintain cell integrity. High field intensities (above 4.5 V) lead to membrane permeabilization as shown by the uptake of propidium iodide. These results are consistent with previous studies that have been realised for bulk EP [4].

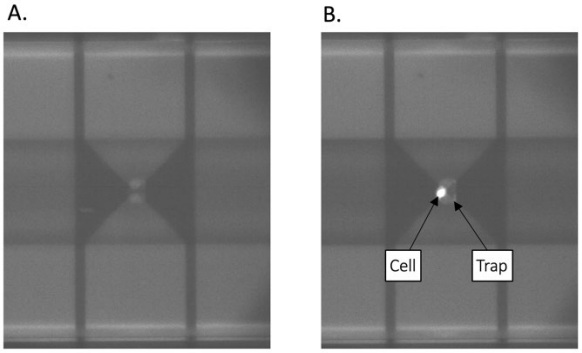

Figure 2: Image taken under fluorescence microscopy (m-cherry filter) of a single PC3-GFP cell trapped. A. After adding propidium iodide and before performing EP. B. After performing EP (8 pulses of 100 μs duration, 10 V magnitude, 1 Hz frequency).

CONCLUSIONS

We demonstrated that the microdevice previously developed enables *in situ* EP and real time analyses. The studies carried out allow to determine EP thresholds for different types of electrical pulses.

REFERENCES

[1] Gehl, J. *et al.*, "Updated standard operating procedures for electrochemotherapy of cutaneous tumours and skin metastases," *Acta Oncologica*, vol. 57, no. 7, pp. 874–882, 2018.

[2] Chen, T. *et al.*, "Microwave biosensor dedicated to the dielectric spectroscopy of a single alive biological cell in its culture medium," *IEEE International Microwave Symposium*, Seattle, USA, 2013.

[3] Tamra, A. *et al.*, "Single cell microwave biosensor for monitoring cellular response to electrochemotherapy," *IEEE Trans. On BioMedical Engineering,* 2022.

[1] [4] Pucihar, G. *et al.*, "Electropermeabilization of dense cell suspensions," *Eur Biophys J*, 36, 173–185, 2007.

Microsystem for culture, monitoring and electroporation of spheroids: application to electrochemotherapy

Pauline Bregigeon[1], Théo Le Berre[1], Julien Marchalot[1], Laure Franqueville[1], Christian Vollaire[1], Charlotte Rivière[2,3,4], Marie Frénéa-Robin[1]; *[1] Univ Lyon, Ecole Centrale de Lyon, INSA Lyon, Université Claude Bernard Lyon 1, CNRS, Ampère, UMR5005, 69130 Ecully, France [2] Institut Lumière Matière, Claude Bernard Lyon 1 Université, CNRS, F-69622, Villeurbanne, France [3] Institut Universitaire de France (IUF), France [4] Institut Convergence PLAsCAN, Centre de Cancérologie de Lyon, INSERM U1052-CNRS UMR5286, Université de Lyon, Université Claude Bernard Lyon 1, Centre Léon Bérard, Lyon, France*

INTRODUCTION

As the interest for treatment based on electroporation (EPN) is growing, the need for reliable tumour models to study the effect of pulsed electric fields on cells is increasing. Spheroids have been identified as a good tumour model [1] to try to have a better understanding of EPN mechanisms on in vivo tissues, as they are able to reproduce cell-cell interaction. In the literature, the proposed approaches usually consist in first fabricating the spheroids using hanging drop methods or ultra-low attachment plates, and then introducing them in an electroporation cuvette connected to a pulse generator or using hand-held electrodes [1]. It involves several handling steps, which can potentially damage spheroids and induce a lack of reproducibility of the results. To address this challenge, we designed a microfluidic platform enabling culture and electroporation of a large number of spheroids sharing similar characteristics without requiring any manipulation (Figure 1a) [2]. Here, we demonstrate the application of the device to the delivery of a classic ECT molecule, bleomycin, in HT29 colorectal cancer cell spheroids using sine wave bursts [3].

METHODS

To produce the spheroids, a 2% agarose hydrogel is moulded and grafted on an amine-functionalized ITO-coated glass slide, used as an electrode for EPN. HT29 colorectal cancer cells are then seeded in the microwells to form spheroids of reproducible size and location (Figure 1b). A silicone seal is placed around the hydrogel to form a microfluidic chamber (Figure 1c), which is closed with another ITO coated glass slide, and mounted inside a sealing device ensuring water tightness and electrical contact. EPN Hepes buffer supplemented with the anticancer drug bleomycin (20 µg/mL), is then injected inside the microfluidic chamber, to change the medium inside the chamber from culture to EPN buffer. EPN is performed by applying 2 sine bursts (300 Vpp, 10 kHz, 5 ms) of previously determined parameters (data not shown). Spheroid growth is monitored with ImageJ measurement of spheroid area on microscope images.

RESULTS

EPN parameters used here led to a reversible EPN as similar growth evolutions can be seen for non-treated spheroids and spheroids only submitted to EPN (Figure 1d). As expected, growth of spheroids in contact with bleomycin only is not affected. Moreover, ECT is efficient as growth is inhibited for spheroids treated with EPN in presence of bleomycin.

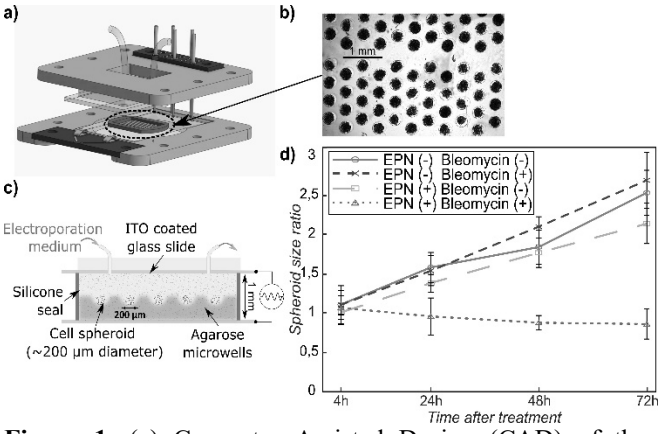

Figure 1: (a) Computer Assisted Design (CAD) of the microsystem. (b) 2.5X bright field image of spheroids in the agarose microwells. (c) Schematic drawing of the microfluidic chamber (side view). (d) HT29 cell spheroid surface ratio evolution after experiment with (+) and/or without (−) EPN and/or bleomycin.

CONCLUSION

These results highlight the functionality of our device as an in vitro platform to test and monitor anti-cancer drug uptake in spheroids by EPN. After this first application, we are working on the complexification of the tumour model, by producing co-culture spheroids with both cancerous cells and fibroblasts. We also intend to optimize the electrode design to allow in situ bio-impedance monitoring of spheroid growth.

REFERENCES

[1] J. Hoarau-Véchot, et al., "Halfway between 2D and Animal Models: Are 3D Cultures the Ideal Tool to Study Cancer-Microenvironment Interactions?" *Int. J. Mol. Sci.*, vol. 19, 2018.

[2] P. Bregigeon, et al., "Integrated platform for culture, observation, and parallelized electroporation of spheroids," *Lab on a Chip*, vol. 22, pp. 2489–2501, 2022.

[3] T. García-Sánchez, et al., "Sine wave electro-permeabilization reveals the frequency-dependent response of the biological membranes," *BBA-Biomembranes*, vol. 1860, 2018.

Molecular dye transportation through GUVs bilayer under Pulse electric field exposure.

Rupesh Kumar, Rochish Thaokar, *Indian Institute of Technology Bombay, Mumbai, INDIA*

INTRODUCTION

The Giant Unilamellar Vesicles (GUVs) are micrometer-sized vesicles made up of lipid bilayers. The micrometer's size and formation with lipid bilayers make GUVs the right choice as a bio mimic cell. We aim to study the GUVs lipids bilayer permeability under pulsed electric field exposure. For that, we prepared the GUVs filled with FITC-dextran dye (mw 40,000) to know the extent of permeability by measuring the dye leakage in epi-fluorescence microscopy. The loss in fluorescence intensity from inside of GUVs correlated with the dye leakage.

RESULTS

It was found that lipid bilayer membrane forms hydrophilic micrometers size pores under single pulse treatment (0-3kV, 1ms Pulse duration), but the pore closing time was minimal. (in milliseconds). The significantly less closing time of pores makes a membrane permeable for a short time, and significant intensity loss was not observed inside GUVs. We hypothesized that to make the membrane permeable for a long duration, multiple pulses were applied, and a considerable reduction in the intensity would be observed. The multiple pulses either increase the size of the pores, which are still not closed or create a newer pore. However, in multiple pulses, we see that membrane permeability cannot be increased for a long time because, after the first pulse, pores created in the bilayer will increase the conductance of the membrane and reduce the effect of subsequent pulses. If the pulses were applied with a long-time-interval gap, then we saw that membrane was permeable only for (20-40ms) after an application of each pulse, and the significant size of the GUVs reduced. However, this maintains a permeability for 20-40ms with each pulse, not to increase the permeability for a second or more extended time.

CONCLUSION

It is better to change the bilayer properties instead of applying multiple pulses to increase membrane permeability.

REFERENCES

[1] Rafael B. Lira, Rumiana Dimova, Karin A. Riske, Giant Unilamellar Vesicles Formed by Hybrid Films of Agarose and Lipids Display Altered Mechanical Properties, Biophysical Journal, Volume 107, Issue 7,2014.

[2] Perrier, D. L., Vahid, A., Kathavi, V., Stam, L., Rems, L., Mulla, Y., ... & Boukany, P. E. (2019). Response of an actin network in vesicles under electric pulses. Scientific reports, 9(1), 1-11.

[3] Riske, K. A., Knorr, R. L., & Dimova, R. (2009). Bursting of charged multicomponent vesicles subjected to electric pulses. Soft Matter, 5(10), 1983-1986.

Reactive Oxygen Species Electrochemistry on Stainless Steel Electrodes in Physiological Conditions

Eva Miglbauer[1], Jiri Ehlich[2], Eric Daniel Glowacki [1,2]; *[1] Laboratory of Organic Electronics, Linköping University, Bredgatan 33, SE-60 174 Norrköping, SWEDEN [2] Central European Institute of Technology, Brno University of Technology, Purkyňova 123, CZ-621 00 Brno, CZECH REPUBLIC*

INTRODUCTION

Stainless steel is a popular metallic biocompatible material used for biomedical applications such as dental implants, stents or stimulation electrodes.

Recently, the relation of stainless steel and reactive oxygen species in the context with high voltage pulses is discussed.[1–3]

However, there is a lack of proper electrochemical characterization of stainless steel in physiological environment, which is not only addressing the metal release of Fe and Cr ions when anodically polarized, but also H_2O_2 generation when catholically polarized and the consecutive formation of radicals when the released metal ions react with H_2O_2 in a Fenton like way.

With this publication we address this gap and provide the readers with the electrochemical characterization of 316L stainless steel in physiological environment and present our findings about metal ion release and ROS formation.

METHODS

The applied methods include electrochemical characterization methods as cyclic voltammetry, chronoamperometry as well as H_2O_2 quantification with an amperometric, H_2O_2 specific sensor.

Additionally, spectrophotometric assays are applied for the quantification of released metal ions and fluorescence based assays are used to show radical formation.

RESULTS

Our results show that stainless steel is capable of generating H_2O_2 at a potential window of -0.4V - -0.9 V vs Ag/AgCl in phosphate buffered saline (PBS). At more negative potentials hydrogen evolution is the dominant reaction. When positively polarized, stainless steel releases first chromium ions and then iron ions at a minimum potential of 1.6 V vs Ag/AgCl.

Moreover, we use fluorescence-based assays to qualitatively show the formation of hydroxyl radicals.

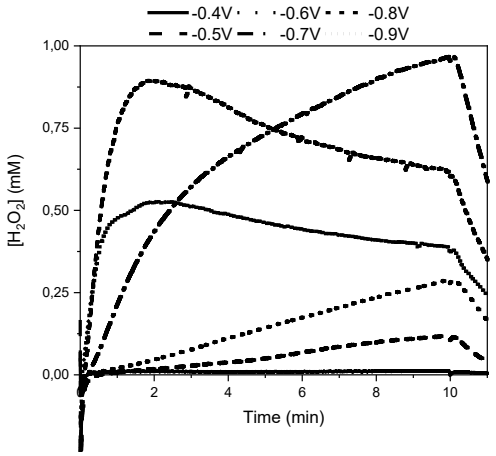

Figure 1: Electrochemically generated H_2O_2 at a 316L stainless steel electrode at different potentials in phosphate buffered saline quantified with an amperometric sensor specific to H_2O_2.

CONCLUSION

We show that stainless steel itself can generate ROS not only with high but also with low voltage pulses, which can be a potential application for anti-tumour treatment.

REFERENCES

[1] Tomov, T. and Tsoneva, I. Are the stainless steel electrodes inert? Bioelectrochemistry Bioenerg. 51, 207–209, 2000

[2] Ruzgys, P., Novickij, V., Novickij, J. and Šatkauskas, S. Influence of the electrode material on ROS generation and electroporation efficiency in low and high frequency nanosecond pulse range. *Bioelectrochemistry* **127**, 87–93, 2019

[3] Saulis, G., Rodaitė-Riševičienė, R. and Saulė, R. Cytotoxicity of a Cell Culture Medium Treated with a High-Voltage Pulse Using Stainless Steel Electrodes and the Role of Iron Ions. *Membranes (Basel).* **12**, 2022

Tumor location methodology by means of neural networks and multi-electrode structures.

Pablo Briz Zamorano, *Department of electrical engineering and communications. I3A. University of Zaragoza. C/María de Luna,1, 50018, Zaragoza. SPAIN.*

INTRODUCTION

Electroporation based procedures for tumor ablation have many advantages over other methods such as surgical ablation or thermal therapies. One of the current challenges is the focus of the treatment on the tumor tissue. In this work, an approach to locate tumors, by means of multi-electrode electroporation system and neural networks, is proposed, thus allowing to focus the treatment, and minimizing unnecessary healthy tissue damage.

METHODS

This section presents the data acquisition system and the data processing performed.

At first, a high-performance multi-output generator was used to generate and apply the desired voltage waveform to the electrodes [1]. It has 18 differential outputs, that work in conjunction with the multi-electrode structure in Fig. 1.

This system can deliver electroporation treatments and also measure the impedance in different parts of the tissue.

In this work, 81 impedance measurements are taken with different cell configurations. The higher conductivity of tumor tissue over healthy tissue is exploited to find the tumor tissue between electrodes [2].

Data processing is based on a matrix of 18 independent neural networks each one with 81 inputs and a single output. In first place, tissue between electrodes is depicted in two planes of 3-by-3 voxels (Fig. 1b), and each neural network outputs a true or false statement if there is or not at least 2 % of tumor tissue in the voxel they are associated with.

This architecture of neural networks allows to keep them simple, with a single layered feedforward network architecture of just 10 neurons, which are faster and more robust to train than a bigger and more complex architecture [3]. They have been trained with simulation data, obtained from a model developed with the software Comsol® Multiphysics.

EXPERIMENTAL EVALUATION AND RESULTS

An experimental evaluation procedure was developed using phantom gels of known conductivity [4]. Samples with a base conductivity near 0.1 S/m, like the potato tissue, with inserts of gel with 2 to 5 times more conductivity were used to simulate tumor tissue of different sizes and locations. In Fig. 2 one of the evaluation cases is shown. Though all tested cases were successful, further experimentation is required.

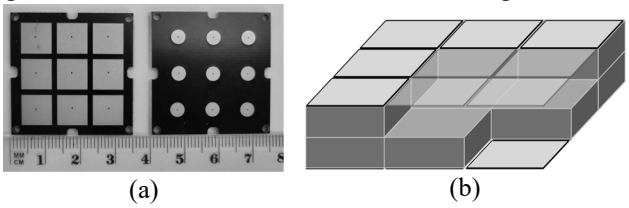

(a) (b)

Figure. 1. (a) Multi-electrode structure. (b) Tissue between electrodes depicted in voxels.

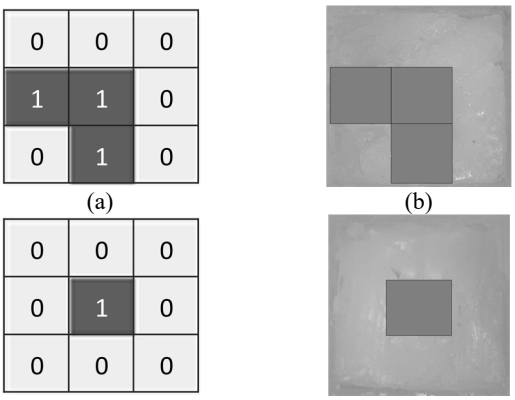

(a) (b)

(c) (d)

Figure. 2. (a) and (c) represent the top and bottom estimated areas that contain tumor tissue of a gel sample. (b) is the top face and (d) the bottom one of that sample. The more conductive gel, emulating tumor tissue, is highlighted.

CONCLUSIONS

The exposed method can locate tumor tissue between the electroporation electrodes without the need of external measurement systems, which is much more convenient and time saving. Once the tumor tissue location is known between electrodes, this system is able to focus the treatment, improving efficacy and minimizing unnecessary healthy tissue affection.

ACKNOWLEDGEMENTS

Work produced with the support of the MICINN-ISCII project, IIS-210_PI21/00440, and by the DGA under the PhD grant 2021-2025.

REFERENCES

[1]López-Alonso, B., Sarnago, H., Lucía, O And Burdío, J.M., Multiple-Output Generator for Omnidirectional Electroporation and Real-Time Process Monitoring, 2021 IEEE Applied Power Electronics Conference and Exposition (APEC), 2021, pp. 1388-1392

[2] Miklavcic, D., Pavselj, N., and Hart, F. Electric Properties of Tissues, 2006, Wiley Encyclopedia of Biomedical Engineering, isbn 9780471740360.

[3]Rymarczyk, T.; Kłosowski, G.; Kozłowski, E. A Non-Destructive System Based on Electrical Tomography and Machine Learning to Analyze the Moisture of Buildings. Sensors 2018, 18, 2285.

[4] Campana, L. et Al. Effect of Tissue Inhomogeneity in Soft Tissue Sarcomas: From Real Cases to Numerical and Experimental Models. Technology in Cancer Research & Treatment, 2018.

Electroporation mediated protein elution from CHO and 4T1 cells

Salvijus Vykertas[1], Baltramiejus Jakštys[1], Saulius Šatkauskas[1]; [1] *Biophysical research group, Vytautas Magnus University, Vileikos 8, Kaunas, LT – 44404, LITHUANIA*

INTRODUCTION

The impact of irreversible electroporation (IRE) based treatments considering the anticancer efficacy is complex, interconnected with cancerous cell death, release of DAMPs and propagation of immune response [1]. Moreover, poor coverage of the whole tumour usually leads to low anticancer response in the patient and the remaining viable cancerous cells tend to increase malignancy and metastatic burden after unsuccessful treatment [2]. In our group's previous work, we shown that intracellular molecules present in EP derived supernatant (SN) is responsible for cell viability elevation after EP are larger than 30 kDa [3]. While, electroporation in ATP enriched EP media gave no significant change in cell viability. Suggesting, that the key player DAMPs that elevate cell viability in tumour microenvironment are proteins. Thus, more thorough understanding of EP mediated protein elution is needed and its role in IRE induced microenvironment.

MATERIALS AND METHODS

Experiments were carried out using Chinese Hamster Ovary (CHO-K1, European Collection of Authenticated Cell Cultures 85050302) and Mammary gland stage IV cancer cells (4T1, ATCC, USA) cells.

Prepared cells were electroporated with BTX T820 electroporator. 1, 5 or 9 HV pulses were delivered (0.6–4.8 kV/cm, 100 μs,1 Hz). Total protein leakage from the cells after electroporation were determined using BCA assay (Thermo scientific, USA) and specific by SDS-Page electrophoresis.

RESULTS AND SICUSSION

Our goal is to evaluate of protein elution mediated by electroporation from both CHO (Figure 1. A) and 4T1 (Figure 1. B) cell lines and measured the amounts of proteins in the EP SN after application from 1, 5 and 9 HV pulses which intensity varied from 0.6 to 4.8 kV/cm.

Results revealed, that indeed, proteins get eluted in a manner that is dependent on pulse parameters and cell line. 1, 5 and 9 HV pulses eluted total protein amount corelated with pulse intensity of which 5 and 9 HV pulses showed identical trends and 1 HV pulse differed by lower protein elution in almost all of the tested intensities apart of the lowest and highest pulses. In both cell types we observed that protein elution mediated by EP has a threshold which is dependent on cell type. Based on our results it seems that CHO cells are more resilient to EP mediated protein elution than 4T1 cells as CHO cells significant protein elution was achieved from 1.8 kV/cm compared to 4T1 0.6 kV/cm threshold. Also, worth mentioning is that this cell type dependent EP mediated protein elution threshold is also a differentiation point for 5, 9 HV pulses and 1 HV pulse trends.

Regarding electroporation mediated total protein elution we showed that within 1, 5 and 9 HV groups eluted protein amount plateaued in both CHO and 4T1 cells when ~ 60% of total cell protein was eluted. Although, for 4T1 cell line to reach this value required lower intensity pulses (CHO cell line plateaued at 3 kV/cm for 5, 9 HV and 4T1 cell line plateaued at 2.4 kV/cm for 5, 9 HV). Interestingly at high intensities (4.2 – 4.8 kV/cm) 1 HV pulse in both cell lines reached the same protein elution as 5 and 9 HV.

Subsequently, we performed SDS-PAGE analysis of the EP SN in order to see the size fractions of eluted proteins. Surprisingly, our results showed that in all electroporated samples large peptides are relatively abundant and can't be distinguished from control or after electroporation in qualitative manner.

Thus, our data suggest that EP mediated protein elution from cells are manipulated alike in a way that's qualitatively independent from number and field intensity of the pulses, if pulse length is kept constant (in our case - 100 μs)

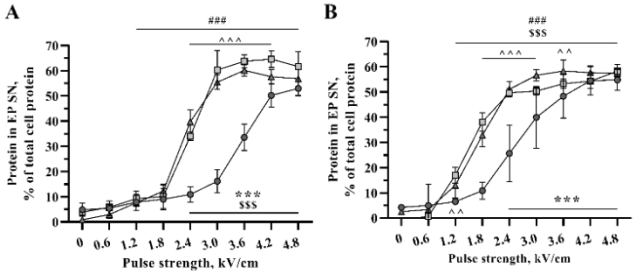

Figure 1: CHO (A) and 4T1 (B) cells' total cell protein in EP media. 1 (circle), 5 (square) or 9 (triangle) HV pulses with varying intensities. n ≥ 4.

CONCLUSIONS

Our results show, that cells types differ by susceptibility to electroporation mediated protein elution up to a threshold point after which if cells are exposed to 5 and 9 HV pulses protein elusion becomes significant but is limited, independent of cell type, to ~ 60% of total cell protein and is qualitatively independent from number and field intensity of the pulses, if pulse length is kept constant.

REFERENCES

[1] Scheffer, H. J. et al. Irreversible electroporation of locally advanced pancreatic cancer transiently alleviates immune suppression and creates a window for antitumor T cell activation. OncoImmunology 8, 1652532 (2019).

[2] Golberg, A., Bruinsma, B. G., Jaramillo, M., Yarmush, M. L. & Uygun, B. E. Rat liver regeneration following ablation with irreversible electroporation. PeerJ 4, (2016).

[3] Jakstys, B., Jakutaviciute, M., Uzdavinyte, D., Satkauskiene, I. & Satkauskas, S. Correlation between the loss of intracellular molecules and cell viability after cell electroporation. Bioelectrochemistry 135, 107550 (2020).

Autophagy is involved in lipid droplet formation and cancer cell survival in starved HeLa cervical cancer cells

Maida Jusović[1,2], Mauro Danielli[1], Špela Koren[1,2], Tjaša Leban[1], Toni Petan[1]
[1]Jožef Stefan Institute, Department of Molecular and Biomedical Sciences, Jamova 39, SI-1000 Ljubljana, SLOVENIA [2]Jožef Stefan International Postgraduate School, Jamova 39, SI-1000 Ljubljana, SLOVENIA

INTRODUCTION

Cells store fat in the form of triacyglycerols and cholesterol esters within organelles called lipid droplets [1]. Lipid droplets are increasingly being recognized as important participants in cellular stress responses. In cancer cells, lipid droplet formation is triggered by a variety of stresses, such as nutrient deficiency/excess, hypoxia, or elevated oxidative stress [2]. All eukaryotic cells employ autophagy, literally translated from the Greek rootes of the word as "self-eating," as a major cellular recycling system and stress response mechanism. Recent research points to a complex relationship between lipid droplets and autophagy, whereby autophagy may either contribute to lipid droplet formation or promote their degradation. In this study, we aim to uncover the importance of autophagy for lipid droplet metabolism in cancer cells. In addition, we want to understand how autophagy affects lipid droplet metabolism as well as cancer cells' resistance to nutrient stress.

MATERIALS AND METHODS

HeLa cervical cancer cells were routinely cultured in DMEM media and supplemented with 10% FBS. Depending on the desired severity of nutrient stress during experiments, cells were cultivated either in media lacking serum and amino acids (severe nutrient stress; HBSS complemented with 0.02% FAF-BSA), or solely in serum-deprived media (mild nutrient stress; DMEM complemented with 0.02% FAF-BSA).

Autophagy was pharmacologically inhibited by bafilomycin-A1 (Baf-A1), or by genetic depletion of essential autophagic genes, and lipid droplet dynamics and cell death were followed over time. Lipid droplet dynamics and cell death were measured by flow cytometry, whereas autophagic flux was followed by western blot analysis of LC3, a widely used autophagic marker, and visualized by live-cell confocal fluorescence microscopy imaging using autophagosome- and lipid droplet-specific dyes and protein markers.

RESULTS

In this study, we found that lipid droplets are dynamically formed in HeLa cervical cancer cells depending on the severity and length of nutrient stress. Furthermore, we found that autophagic flux is elevated in starved HeLa cancer cells and that blocking autophagy leads to inhibition of lipid droplet formation and an increase in cell death.

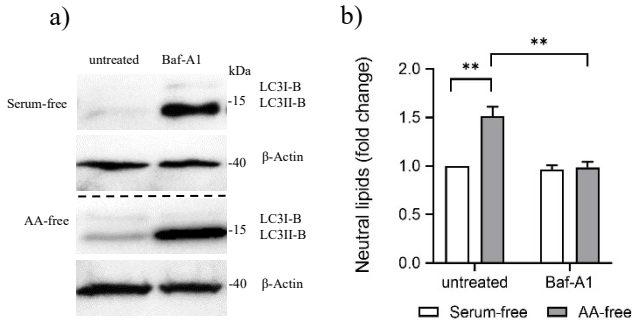

Figure 1: a) Amino acid (AA)-induced autophagy results in higher autophagic flux compared to mild nutrient stress; b) Autophagy-driven lipid droplet formation in starved HeLa cervical cancer cells.

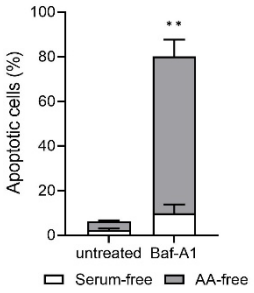

Figure 2: Autophagy promotes cancer cell survival during severe nutrient stress.

CONCLUSIONS

Overall, our results demonstrate that autophagy contributes to lipid droplet formation during severe nutrient stress and that lipid droplets and autophagy may cooperate to promote the resilience of HeLa cancer cells to stress.

REFERENCES

[1] T. Petan, E. Jarc, and M. Jusović, "Lipid droplets in cancer: Guardians of fat in a stressful world," *Molecules*, vol. 23, pp. 11–15, 2018.

[2] A. S. Rambold, S. Cohen, and J. Lippincott-Schwartz, "Fatty acid trafficking in starved cells: regulation by lipid droplet lipolysis, autophagy, and mitochondrial fusion dynamics.," *Dev Cell*, vol. 32, pp. 678–692, 2015.

Cytosolic RNA sensors activation in murine melanoma B16F10 cells using plasmid DNA encoding Interleukin- 12 gene electrotransfer

Ajda Medved[1, 2], Tanja Jesenko[1,2], Gregor Sersa[1, 3], Maša Bošnjak[1], Maja Cemazar[1, 4]; *[1] Institute of Oncology Ljubljana, Zaloska cesta 2, SI-1000 Ljubljana, SLOVENIA [2] University of Ljubljana, Faculty of Medicine, Vrazov trg 2, SI-1000 Ljubljana, Slovenia [3] University of Ljubljana, Faculty of Health sciences, Zdravstvena pot 5, SI-1000 Ljubljana, SLOVENIA [4] University of Primorska, Faculty of Health Sciences, Polje 42, SI-6310 Izola, SLOVENIA*

INTRODUCTION

In cancer gene therapy, exogenous nucleic acids, like plasmid DNA or RNA are introduced into target cells to produce the therapeutic protein of interest, however, those exogenous nucleic acids are recognized by cells as pathogen invasion, detected by binding and activating endosomal and cytosolic nucleic acid-specific pattern recognition receptors (PRRs). Retinoic acid-inducible gene-I-like receptors (RLRs) are part of PRRs family responsible for detecting and binding RNA molecules. Activation of RLRs cause specific immune response, which can lead to antitumor effects [1, 2]. One of the novel cancer gene therapies is gene electrotransfer (GET) of plasmid DNA encoding interleukin-12 (pmIL-12) [3]. Besides the sensing of plasmid DNA by DNA specific PRRs, transcribed IL-12 mRNA can additionally activate the RNA specific RLRs, which could contribute to the overall induced immune response.

METHODS

For GET into melanoma (B16-F10) cells, plasmid DNA encoding therapeutic - murine IL-12 (1 mg/ml, pmIL-12), control- non-coding backbone plasmid DNA (1 mg/ml, pScramble), and plasmid encoding green fluorescent protein (pEGFP, BD Biosciences Clontech, Palo Alto, California) were used. Parallel electrodes with 2-mm gap and clinically used pulse protocol for electrochemotherapy were used for GET: 8x 1300 V/cm pulses of 100-microsecond duration at the frequency of 5 Hz were applied with CLINIPORATOR® (IGEA S.P.A., Carpi, Italy). Cell viability was determined 3 days after treatment, using PrestoBlue™ Cell Viability Reagent (Thermo Fischer Scientific, Thermo Fisher Scientific, Waltham, MA USA) assay, transfection efficiency was determined 2 days after electrotransfer of pEGFP, using fluorescence microscopy and expression of three RLRs: retinoic acid-inducible gene I (RIG-I), melanoma differentiation-associated protein 5 (MDA5) and laboratory of genetics and physiology 2 (LGP2), was determined using qRT-PCR, 2 days after treatment.

RESULTS

The employment of clinically used electroporation protocol led to 24 % of transfected cells. Cell viability was significantly reduced after therapeutic and control plasmid GET, leading to four times lower cell viability compared to a control group. pmIL-12 GET also caused significant upregulation of one of three evaluated RLRs, RIG-I sensor (Fig. 1).

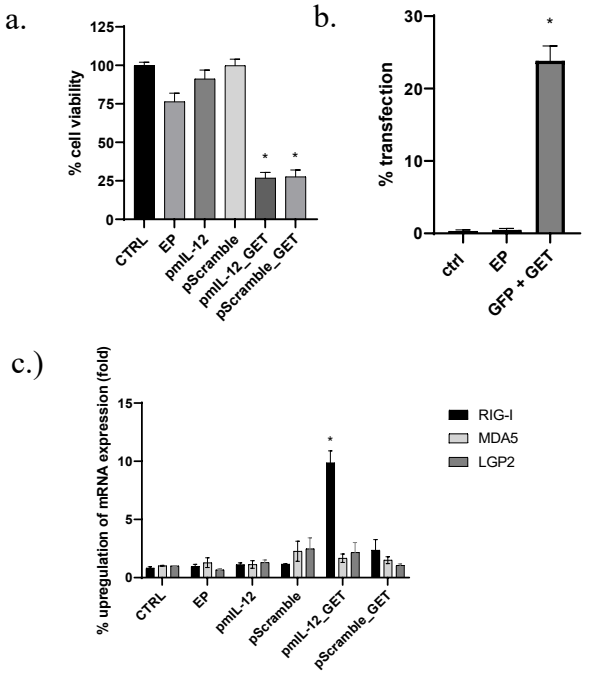

Figure 1: a.) Cell viability of B16-F10 cells after GET. *p ≤ 0.001, compared to every other group without *. b.) transfection efficiency after GET. c.) RIG-I, MDA5 and LGP2 mRNA levels after GET normalized to control group. *p ≤ 0.05, compared to every other group (EP-electric pulses).

CONCLUSION

Taken together, GET of both plasmids resulted in similar reduction of cell viability. However, GET of therapeutic plasmid led to upregulation of cytosolic RNA sensor RIG-I, which was not observed after GET of control plasmid indicating on possible sensing of transcribed mRNA for IL-12.

REFERENCES

[1] D. Goubau, S. Deddouche, C. Reis e Sousa, "Cytosolic sensing of viruses" *Immunity*, vol.38, pp.855-869, 2013.

[2] J. Rehwinkel, M.U. Gack, "RIG-I-like receptors: their regulation and roles in RNA sensing" *Nature Reviews Immunology*, vol.20, pp.537–551, 2020.

[3] M. Cemazar, T. Jarm, G. Sersa. "Cancer electrogene therapy with interleukin-12." *Current gene therapy* vol. 10, pp. 300-311, 2010.

[4.] Kos, S. et al. "Non-Clinical In Vitro Evaluation of Antibiotic Resistance Gene-Free Plasmids Encoding Human or Murine IL-12 Intended for First-in-Human Clinical Study." *Pharmaceutics* vol. 13, 2021.

Gene electrotransfer using commercial porous inserts

Tina Cimperman, Anja Blažič, Tjaša Potočnik, Schaurya Sadchev, Lea Rems; [1] *University of Ljubljana, Faculty of Electrical Engineering, Trzaska 25, SI-1000 Ljubljana, SLOVENIA*

INTRODUCTION

Delivery of genetic material into cells using electroporation, known as Gene Electrotransfer (GET), is crucial for gene therapy and gene editing. The disadvantage of conventional GET is the highly permeabilized cell membrane, which can cause severe cell damage often leading to cell death. By localizing electric field over a small membrane area using nanoporous materials it is possible to improve GET efficiency while providing greater cell survival and better control over gene expression [1], [2]. The disadvantages of such nanofabricated devices are that they are not widely available and require expertise in nanofabrication and access to cleanroom.

Recently, [2], [3] a system based on polydimethylsiloxane holder with a commercially available polycarbonate membrane containing pores with a diameter of 0.1-0.2 μm and commonly used for water filtration was suggested, which resulted in successfully delivered nucleic acids, proteins and ribonucleoproteins to cells attached to the polycarbonate membrane. Authors achieved highly efficient transfection (up to 80%) without a significant effect on cell survival (<5% dead cells) [2]. Their study inspired us to test whether similar success could be achieved with porous membranes embedded in commercial cell culture inserts, which are mainly used for studying drug transport across cell monolayers, cell invasion and migration.

METHODS AND MATERIALS

In the Comsol Multiphysics 6.0, we made two numerical models. We first modelled electroporation of a cell on a small part of a porous membrane. We then created model of the complete experimental system, consisting of an insert with a porous membrane, a conductive medium and wire electrodes.

Based on the numerical results, we optimized the final experimental system and selected the pulse parameters for GET. We then performed GET experiments on Chinese hamster ovary cells using plasmid DNA pEGFP-N1 with two different plasmid concentrations, 100 μg/μl and 500 μg/μl. The fraction of transfected cells was determined using the Attune NxT flow cytometer at 24 h post GET. In parallel we also performed MTS viability test at 24 h post GET, whereby the sample absorbance was determined with spectrophotometer Infinite M200 (Tecan). Detailes are presented in [4].

RESULTS

Cells grown on the porous membrane of the insert were exposed either to one 10 ms pulse of 10 V, 20 V or 40 V or to several pulses (4, 8 or 12) of 20 V.

With one applied pulse, the proportion of transfected cells was highest at 20 V and reached 12%. As the number of pulses increased, the proportion of transfected cells reached over 30% (Figure 1a). Cell survival after GET was above 90% in all experiments (Figure 1b). By increasing the plasmid concentration to 500 μg/μl, 44% transfection was achieved with 4 applied pulses of 20 V.

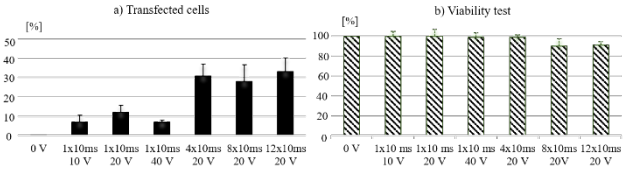

Figure 3. a) Percentage of transfected and b) viable cells.

CONCLUSION

The transfection efficiency obtained in our study is comparable to that obtained with classical electroporation (~40% transfection) [5], however with better cell viability. Another advantage of porous inserts is the use of low-voltage pulses, which precludes the need of expensive high-voltage electroporators. Porous membranes are also commercially accessible, and no special equipment or premises are needed to set up an experimental system.

Nevertheless, the obtained transfection efficiency is lower than in the study of Cao et al. (~80% transfection). However, a direct comparison of our results with those of Cao et al.[2] is not possible, as the latter performed experiments on other cell lines and porous membrane, which also have greater porosity and are made of polycarbonate.

AKNOWLEDGENEMTS

This work was supported by European Commission (MSCA-IF 893077 and MSCA-WF 101038051) and Slovenian Research Agency (J2-2503 and P2-0249).

REFERENCES

[1] P. E. Boukany *et al.*, “Nanochannel electroporation delivers precise amounts of biomolecules into living cells,” *Nat. Nanotechnol.*, vol. 6, no. 11, pp. 747–754, Nov. 2011, doi: 10.1038/nnano.2011.164.

[2] Y. Cao *et al.*, “Nontoxic nanopore electroporation for effective intracellular delivery of biological macromolecules,” *Proc. Natl. Acad. Sci.*, vol. 116, no. 16, pp. 7899–7904, Apr. 2019, doi: 10.1073/pnas.1818553116.

[3] P. Mukherjee, S. S. P. Nathamgari, J. A. Kessler, and H. D. Espinosa, “Combined Numerical and Experimental Investigation of Localized Electroporation-Based Cell Transfection and Sampling,” *ACS Nano*, vol. 12, no. 12, pp. 12118–12128, Dec. 2018, doi: 10.1021/acsnano.8b05473.

[4] T. Vindiš, A. Blažič, D. Khayyat, T. Potočnik, S. Sachdev, and L. Rems, “Gene Electrotransfer into Mammalian Cells Using Commercial Cell Culture Inserts with Porous Substrate,” *Pharmaceutics*, vol. 14, no. 9, Art. no. 9, Sep. 2022, doi: 10.3390/pharmaceutics14091959.

[5] T. Potočnik, D. Miklavčič, and A. Maček Lebar, “Gene transfer by electroporation with high frequency bipolar pulses in vitro,” *Bioelectrochemistry*, vol. 140, p. 107803, Aug. 2021, doi: 10.1016/j.bioelechem.2021.107803.

Towards pharmacological treatment screening of cardiomyocyte cells using Si nanowire field-effect transistors

Natalia Naumova[1], Ihor Zadorozhnyi[2], Hanna Hlukhova[2], Yurii Kutovyi[2], Volodymyr Handziuk[2], Andreas Offenhaeusser[2], Svetlana Vitusevich[2] *[1] CNRS UMR 9018 - METSY, Institut Gustave-Roussy, 114 rue Edouard Vaillant, 94805 Villejuif, FRANCE, [2] Bioelectronics (ICS-8), Forschungszentrum Juelich, 52425 Juelich, GERMANY*

INTRODUCTION

Silicon nanowires (Si NWs) are the most promising candidates for recording biological signals due to improved interfacing properties with cells and the possibility of high-speed transduction of biochemical signals into detectable electrical responses. The recording of extracellular action potentials (APs) from cardiac cells is important for fundamental studies of AP propagation features reflecting cell activity and the influence of pharmacological substances on the signal. We applied a novel approach of using fabricated Si NW field-effect transistors (FETs) in combination with fluorescent marker techniques to evaluate the functional activity of cardiac cells. Extracellular AP signal recording from HL-1 cardiomyocytes was demonstrated. This method was supplemented by studies of the pharmacological effects of stimulations using noradrenaline (NorA) as a modulator of functional activity on a cellular and subcellular levels, which were also tested using fluorescent marker techniques. The role of calcium alteration and membrane potential were revealed using Fluo-4 AM and tetramethylrhodamine, methyl ester, perchlorate (TMRM) fluorescent dyes. In addition, chemical treatment with sodium dodecyl sulfate (SDS) solutions was tested. The results obtained demonstrate positive prospects for AP monitoring in different treatments for studies related to a wide range of myocardial diseases using lab-on-chip technology.

RESULTS AND DISCUSSION

In this work, we combine in vitro monitoring of cardiomyocyte cell culture APs activity using Si NW FETs with fluorescence microscopy to develop a bio-platform that enables us to reveal the effect of pharmacologically active agents on the living cell community by tracking the cell calcium content, mitochondrial membrane potential, and cellular electrical spiking activity. We demonstrate the high-quality material and electrical properties of fabricated Si NW FET structures (Figure 1).

/

Figure 1: (a) Schematic cell-nanowire interface with the measurement configuration for cardiomyocyte electrical activity monitoring using NW FET biosensor. (b) Nanowire chip with a grid layout containing 32 measurement channels. (c) Chip encapsulated within a glass ring and PDMS as a reservoir for the medium and cell culture.

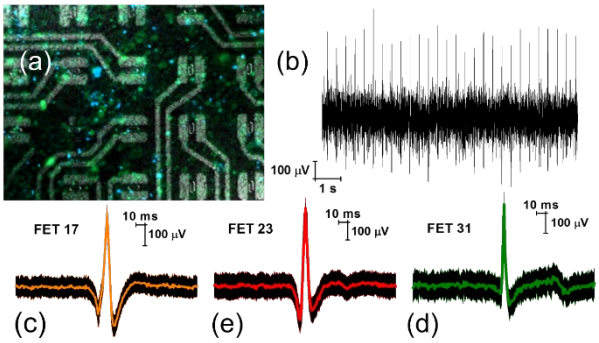

Figure 2: (a) Live/dead staining of HL-1 cardiac cells on Si NW chips using green fluorescent calcein AM dye and blue fluorescent DAPI dye; (b) Typical recorded timetrace with action potential activity; (c),(d),(e) Extracted action potential shapes for FETs 17, 31, 23. The colored lines show averaged values for action potentials found in the timetrace, while the black background shows the standard deviation.

We show that transistors operate without leakage current in culture media due to multi-stage fabrication process optimization. We apply the novel approach of using Si NW structures as a bio-platform in combination with fluorescence microscopy techniques to monitor the effects of pharmacologically active agents such as NorA on the cells' functional activity (Figure 2). The results of studies on the pharmacological treatment and electrical activity of HL-1 cells demonstrate that Si NW FETs can be used to investigate and select biologically active solutions to tune and control cardiac activity from the viewpoint of different physiological and pathological conditions of cardiac activity.

REFERENCES

[1] Vitusevich, S., Zadorozhnyi, I., 2017. Semicond. Sci. Technol. 32, 1–21 043002.
[2] Maybeck, V., Edgington, R., Bongrain, A., Welch, J.O., Scorsone, E., Bergonzo, P.,Jackman, R.B., Offenhäusser, A., 2014. Adv. Healthc. Mater. 3, 283–289.
[1] [3] Jansen, M., 2014. Schluesseltechnologien/Key Technologies.Band 82, vol. 82. Forschungszentrum Juelich, Juelich, 9783893369447pp. 181.

Enhanced Cell Killing Effects of Combination of Nanosecond Electric Pulses and Microsecond Electric Pulses

Wencheng Peng, Yaqi Yue, Shoulong Dong, Chenguo Yao; *School of Electrical Engineering, Chongqing University, Shapingba District, Shazheng Street 174, 400044 Chongqing, CHINA*

INTRODUCTION

With the rapid development of irreversible electroporation (IRE) induced by microsecond electric pulses (μsEP), there are more and more practical applications in the biomedical fields [1]. The tumor ablation by IRE is a promising technique, but there still exist some problems to be solved. Due to the limitation of the voltage amplitude and the distribution of μsEP, conventional IRE is more suitable for the tumor treatment within the size of 3 cm [2]. In order to enlarge the ablation regions, we proposed a combination of nsEP and μsEP. Studies have shown that μsEP mainly acted on cell membrane, causing IRE of cell membrane, while high-voltage nsEP can act on not only cell membrane, but also intracellular organelles such as the nucleus due to the high frequency component [3]. To further study the cell killing effects of combined pulses, cell experiments were performed, including cytotoxicity test and monolayer cell ablation. The results showed that combined pulses had better cell killing effect on tumor cells and could produce larger ablation zone with the smaller energy.

METHODS

Murine hepatoma cell line Hepa 1-6 was treated by electric pulses. 2 mm-gap cuvette was used to delivery different numbers of three pulse sequences. Pulse parameters are given in Table 1. For monolayer cell ablation, the electric pulses were delivered through two stainless steel needle electrodes placed normal to the 2-D cell layer. Detailed methods can be found in the reference [4].

Table 1: Experimental pulse parameters (EP- electric pulses).

Pulse sequence	Voltage/ Distance (kV/cm)	Pulse width	Pulse interval	Pulse number
nsEP	10	500 ns	/	10, 20, 30, 60, 80
μsEP	1.5	100 μs	/	10, 20, 30, 60, 80
ns+μsEP	/	/	10 μs	5, 10, 20, 30, 40

RESULTS AND FIGURES

The cell viability treated by electric pulses is shown in Figure 1, the killing efficiency of tumor cells is correlated with the number of pulses. The results shows that the combined pulses could induce stronger cell killing effects than independent nanosecond pulses or independent microsecond pulses.

To illustrate visually the advantages of combined pulses over nanosecond pulses and microsecond pulses, the ablation experiment of monolayer cells was performed with three kinds of pulses. Figure 2 shows staining results of cells after 24 h. As we can see, the ablation area of combined pulses is significantly larger than that for nanosecond pulses and microsecond pulses

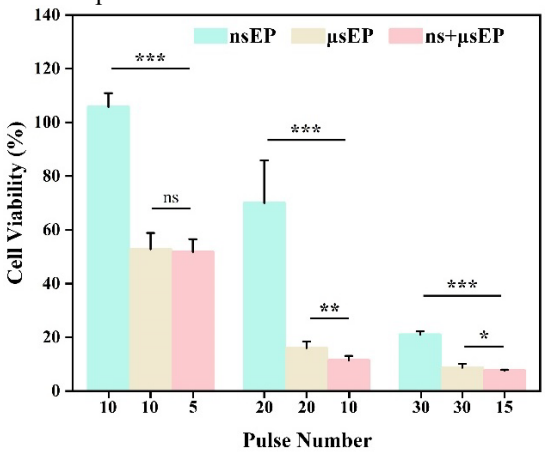

Figure 1: Cell viability with different pulse parameters.

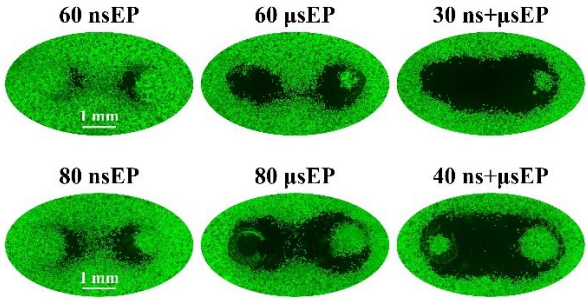

Figure 2: Ablation area with different pulse parameters.

CONCLUSIONS

According to the cell killing assay and the ablation experiment of monolayer cells, compared with the microsecond pulse, the combined nsEP and μsEP have advantages in tumor ablation and can achieve a stronger therapeutic effect with the smaller energy.

REFERENCES

[1] B. Rubinsky, *Irreversible electroporation*. Heidelberg: Verlag, 2010.

[2] M.T. Silk *et al.*, "Percutaneous ablation of peribiliary tumors with irreversible electroporation," *J. Vasc. Interv. Radiol.*, vol. 25, pp. 112-118, 2014.

[3] C. Yao, *et al.*, "Nanosecond pulses targeting intracellular ablation increase destruction of tumor cells with irregular morphology," *Bioelectrochemistry*, vol. 132, pp. 1-11, 2020.

[1] [4] H. Liu *et al.*, "Application of bioimpedance spectroscopy to characterize chemoresistant tumor cell selectivity of nanosecond pulse stimulation," *Bioelectrochemistry*, vol. 135, pp. 1-7, 2020.

New high frequency electroporation protocols for human and veterinary medecine applications

Alexia de Caro[1], Jean-Baptiste Leroy[2], Muriel Golzio[1], Marie-Pierre Rols[1]; *[1] Institute of Pharmacology and Structural Biology (IPBS), 205 rte de Narbonne, 31077 Toulouse cedex 4, FRANCE (CNRS UMR 5089); [2] Leroy Biotech, 7 Bd du Libre Échange, 31650 Saint-Orens-de-Gameville, FRANCE.*

INTRODUCTION

Electroporation (EP) is a physical method allowing the permeabilization of cells and therefore massive penetration of molecules. For more than 30 years, electroporation is gaining momentum in the treatment of skin cancers. By increasing the cytotoxic effect of anti-tumor drugs (bleomycin, cisplatin), electrochemotherapy (ECT) has already proven its effectiveness on tumors in human medicine [1] but also in veterinary practice [2]. However, this treatment requires loco-regional or even general anesthesia, as electrical pulses can be painful and cause muscle contractions [1]. Several publications proved that application of high frequency pulses (5,000 Hz) resulted in much less discomfort to the patient compared to 1 Hz protocol used in clinical practice [3]. In order to maintain the effectiveness of the treatment and reduce the pain associated with muscles contractions, we are developing new protocols using a high-frequency generator, and new multipolar electrodes.

MATERIALS AND METHODS

HCT-116 cells, a colon cancer cells line are harvested in supplemented DMEM medium, centrifuged 5 minutes at 300 g and diluted in a low conductivity phosphate buffer. After incubation with cisplatin (0.01 mg/mL), bleomycin (30 nM) or calcium gluconate (3 mM), the cells are pulsed according to two electrical protocols: ECT (8 pulses of 100 µs, 1 kV/cm, 1Hz) and High Frequency HF-ECT using specific electrodes (figure 1): 33 or 36 periods of 8 pulses of 3 µs, 1.14 kV/cm or 1.43 kV/cm. Cell viability was determined by clonogenic assay incubating 300 cells in culture medium in wells (35 mm diameter) in 37 °c. After ten days, the cells are fixed 5 minutes to 70% ethanol and colored with 0.1% crystal violet in the pulsation buffer. The colonies formed are counted manually, and converted to percentage.

Figure 1: HF-ECT multipolar electrodes. These electrodes operate with rotating field and are activated in electrodes pairs. One period consists of a cycle of 8 pulses.

RESULTS AND DISCUSSION

Our results indicate that the two electrical protocols studied do not cause significant cell mortality: 20 to 30% of cells were affected by electroporation alone compared to non-pulsed control. Control experiments were also conducted by coupling HCT-116 with three different anti-cancer drugs. In absence of electric field cisplatin and calcium have no effect on cell viability while bleomycin affect 50% of cells. However, as observed on figure 2, electroporation significantly increases the cytotoxicity of all three drugs. The ECT protocol in combination with antitumor molecules causes 90% of cell mortality. Regarding the HF-ECT protocols (36 periods of 3 µs at 1.14 kV/cm applied with cisplatin and bleomycin; 33 periods of 3 µs at 1.43 kV/cm applied with calcium gluconate), appear more lethal: 1 to 5% cell viability has been quantified.

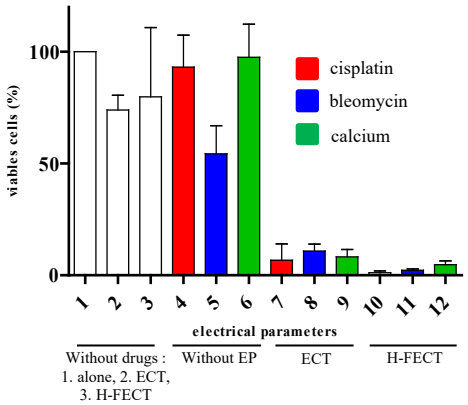

Figure 2: Effect of ECT and H-FECT protocols on cell viability. Cell viability percentages are determined in function of drugs used: cisplatine (red), bleomycin (blue), calcium (green). n = 4

Comparing the two electrical pulse protocols, we observe no significant difference between them, indicating that they have the same efficiency on suspended cells with three drugs tested.

CONCLUSION

HF-ECT protocols are efficent to permeabilize HCT-116 cells allowing internalization of drugs and therefore amplify their mortality. These protocols are promising for clinical applications.

REFERENCES

[1] Mir, L.M., et al. « Standard operating procedures of the electrochemotherapy ». *EJC Supplements*, vol. 4, pp.14-25, 2006

[2] Rols, M.P., et al. « Electrochemotherapy of horses. A preliminary clinical report ». *Bioelectrochemistry*, pp.101-105, 2001.

[2] [3] Županic, A., et al. « Increasing the repetition frequency of electric pulse delivery reduces unpleasant sensations that occur in electrochemotherapy ». *NEOPLASMA*, vol. 3, pp. 246- 250, 2007.

Evidence of the Bystander Effect After Calcium Electroporation, Bleomycin Electrotransfer and Irreversible Electroporation

Neringa Barauskaite[1], Paulius Ruzgys[1], Saulius Satkauskas[1]; [1] *Biophysical Research Group, Faculty of Natural Sciences, Vytautas Magnus University, Vileikos str.8, Kaunas, LT-44404, LITHUANIA*

INTRODUCTION

Electroporation is one of the techniques used for local cancer therapy in a form of electrochemotherapy and electroablation. When electric fields are applied to cells the process electroporation on affected membranes are trigged. Depending on the cumulated transmembrane potential pores can be transient (Reversible electroporation) or permanent (Irreversible electroporation). Transient pores are used for anticancer drug delivery (typically Bleomycin) [1] to target cell (electrochemotherapy) and permanent electropores for irreversibly destructing cell homeostasis (electroablation) [2]. Radiotherapy, as a different local cancer treatment approach, share certain similarities with aforementioned electroporation-based cancer therapies.

It is well established that cells, exposed to radiation, do release signalling molecules that have an impact on neighbouring cells. The name given to this phenomenon is "bystander effect" [3]. In the field of radiotherapy, the phenomenon is well known. However, only few studies have been published showing the bystander effect after electroporation-based anticancer therapies [4,5]. The purpose of this study is to assess the bystander effect affect to the viability of neighbouring cells after treatment with irreversible electroporation, electrotransfer of the anticancer drug Bleomycin, and $CaCl_2$ electroporation.

MATERIALS AND METHODS

4T1 (mouse breast cancer) cells were used in the experiments. A single electrical pulse with an amplitude of 1400 V/cm and a duration of 100 µs was used to electrotransfer $CaCl_2$ and the anticancer drug BLM. A single electrical pulse with an amplitude of 2800 V/cm and a length of 100 µs was used to accomplish irreversible electroporation.

Following electroporation, the cells were cultured in a 24-well plate with 0.2 ml of RPMI growth media for 48 hours. The medium is collected after incubation and spun twice in a centrifuge. A Finally, the "bystander effect" was created by adding the collected media to untreated cells. By applying a cell colony formation assay to estimate cell viability, the effectiveness of the "bystander effect" was determined.

RESULTS AND DISCUSSION

Throughout this study, the cells were described as directly affected, indirectly affected ("bystander effect") and unaffected [5]. In this research, we have analysed the influence of the "bystander effect" for directly untreated cells. During these experiments, cells were grown in a medium collected from cells that were treated using bleomycin electrotransfer or irreversible electroporation.

The results showed that after the bleomycin electrotransfer and 48 hours of incubation, the "bystander effect" had a strong negative impact on cell viability, resulting in elimination of all cells. Also, the similar results were achieved with irreversible electroporation and calcium electroporation.

Additionally, we found that various combinations of calcium electroporation, irreversible electroporation, and bleomycin electrotransfer result in different strength of the bystander effect. The bystander effect did not arise when the media were diluted. The amount of cell viability was significantly reduced when two separate bystander effects were combined, such as adding half of the media from cells after irreversible electroporation and half of the media from cells after bleomycin electrotransfer. Additionally, by combining calcium electroporation and bleomycin electrotransfer, we can achieve similar outcomes.

CONCLUSIONS

The results showed the viability decrease of the neighbouring (directly unaffected) 4T1 cells after the electrotransfer of the anticancer drug bleomycin, calcium electroporation or irreversible electroporation.

REFERENCES

[1] U. Probst, I. Fuhrmann, L. Beyer and P. Wiggermann. "Electrochemotherapy as a new modality in interventional oncology: A review". *Technol. Cancer Res. Treat*, vol 17, 2018.

[2] J. Zhao, X. Wen, L. Tian, T. Li, C. Xu and X. Wen. Melancon, M.P.; Gupta, S.; Shen, B.; Peng, W.; et al. "Irreversible electroporation reverses resistance to immune checkpoint blockade in pancreatic cancer". *Nat. Commun*. vol. 10, pp. 1–14, 2019.

[3] N. Jalal, S. Haq, N. Anwar, S. Nazeer and U. Saeed. "Radiation induced bystander effect and DNA damage". *J. Cancer Res. Ther.*, vol. 10, pp. 819–833, 2014.

[4] E. Pirc, C. Federici, M. Bošnjak, B. Perić, M. Reberšek, M., L. Pecchia, L, N. Glumac, M. Čemažar, M. Snoj, G. Serša. "Early Cost-effectiveness Analysis of Electrochemotherapy as a Prospect Treatment Modality for Skin Melanoma". *Clin. Ther.,* vol. 42, pp. 1535–1548, 2020.

[3] [5] P. Ruzgys, N. Barauskaite, V. Novickij, J. Novickij, S. Satkauskas. "The Evidence of the Bystander Effect after Bleomycin Electrotransfer and Irreversible Electroporation". *Molecules.* vol. 26,19 6001, 2021.

Toll-like receptors 2 and 4 differentially regulate the self-renewal and differentiation of spinal cord neural precursor cells

Marina Sánchez-Petidier[1*,2,3], Consuelo Guerri[2], Victoria Moreno[3], Franck Andre[1], Lluis M. Mir[1]; [1] *Institut Gustave Roussy, CNRS, Metabolic and Systemic Aspects of the Oncogenesis (METSY), Université Paris-Saclay, 114 Rue Edouard Vaillant 94805 Villejuif, FRANCE* [2] *Prince Felipe Research Center, Neural and Tissue Regeneration Laboratory, Carrer d'Eduardo Primo Yúfera, 3, 46012 Valencia, SPAIN* [3] *Prince Felipe Research Center, Cellular and Molecular Pathology of Alcohol Laboratory, Carrer d'Eduardo Primo Yúfera, 3, 46012 Valencia, SPAIN.* [*] *current address*

INTRODUCTION

Toll-like receptors (TLRs) represent critical effectors in the host defence response against various pathogens; however, their known function during development has also highlighted a potential role in cell fate determination and neural differentiation. While several studies have shown that TLRs in hippocampal precursors are able to modulate the cell differentiation and proliferation [1], the role of these receptor in Neural progenitor cells (NPC) from spinal cord remains incompletely described.

METHODS

TLR2, TLR4 knock-out and the WT mice were employed for spinal cord tissue analysis and NPCs isolation at early post-natal stage. Neural stem cell marker (SOX2, FOXJ1) served to identify the stem cell population in the tissue by immunofluorescence. NPC-derived from spinals cords were analysed in growth and spontaneous differentiations conditions to study the effect of both TLRs in self-renewal and neuronal and glial contribution after differentiation process.

RESULTS

Our results showed that the deletion of TLR2 or TLR4 significantly reduced the number of SOX2-the earliest transcription factors expressed in neural stem cells- positive NPCs in the neonatal mouse spinal cord. We found that this reduction appears in the nuclear SOX2 expression, corresponding to migrating and non-dividing cells primarily located to the grey matter.

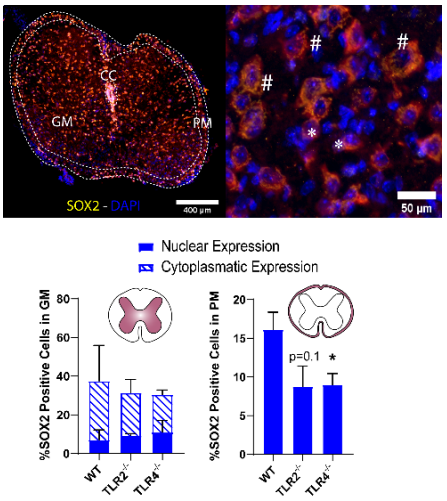

Figure 1: SOX2 expression in spinal cord. GM: grey matter; CC: central canal; PM: perimeter.

In vitro-expanded NPCs derived from mouse neonatal spinal cords, we discovered that deletion of TLR2 displayed enhanced self-renewal, increased proliferation and apoptosis, and delayed neural differentiation showing an increased in the Doublecortin marker producing a high number of neurons with immature morphology while the absence of TLR4 promoted the neural differentiation without affecting proliferation, producing long projecting neurons. TLR4 knock-out NPCs showed significantly higher expression of Neurogenin1, that would be involved in the activation of this neurogenic program by a ligand and microenvironment-independent mechanism. Interestingly, the absence of each TLR2 or TLR4, in NPCs impeded oligodendrocyte precursor cell maturation to a similar degree suggesting a critical role for TLR2 and TLR4 in oligodendrocyte maturation [2].

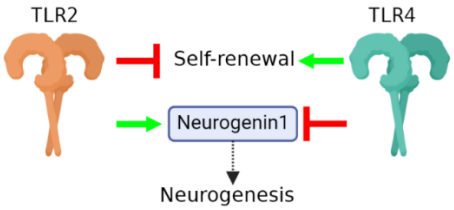

Figure 2: Summary results from *in vitro* experiments.

CONCLUSIONS

We found a ligand and microenvironment-independent program that regulates neural precursor cells population maintenance and the neural differentiation at the neonatal stages involving TLR2 and TLR4 depending-signalling and the constitutive expression of Neurogenin1. Thus, TLR signalling regulation could represent a promising avenue to increase cellular plasticity and promote neural differentiation in the spinal cord.

REFERENCES

[1] Rolls A, Shechter R, London A, Ziv Y, Ronen A, Levy R, *et al*. "Toll-like receptors modulate adult hippocampal neurogenesis" *Nat Cell Biol*. 2007 Sep;9(9):1081–8.

[2] Sanchez-Petidier, M., Guerri, C. & Moreno-Manzano, V. "Toll-like receptors 2 and 4 differentially regulate the self-renewal and differentiation of spinal cord neural precursor cells". Stem Cell Res Ther. 2022 Mar;13, 117.

Use of electroporation to influence the process of cell differentiation by modulating calcium oscillations in mesenchymal stem cells and induced neural stem cell

Romain Fernandes[1], Leslie Vallet[1], Marina Sanchez-Petidier[1], Natalia Naumova[1], Eloise Quantin[1], Franck Andre[1], Lluis M. Mir[1]; [1] *Université Paris-Saclay, Institut Gustave Roussy, CNRS, Metabolic and systemic aspects of oncogenesis (METSY), 94805, Villejuif, FRANCE*

INTRODUCTION

Stem cells are undifferentiated cells with two main properties. These cells have the ability to self-renew as well as the ability to differentiate [1]. Different types of stem cells with distinct differentiating abilities exist in the body.

For instance, Mesenchymal Stem Cells (MSCs) are multipotent cells with different advantages in the context of regenerative therapies. First, the sources for isolating MSCs are varied: bone marrow, adipose tissue, breast milk, dental pulp, umbilical cord. They can differentiate into various cell types (chondrocytes, myocytes, osteocytes, etc.)[2]. In addition, they can have an influence on other cells in their environment within the body. For instance, they are able to rescue metabolically stressed cells thanks to their ability to transfer mitochondria [3]. They have as well immuno-modulatory functions, which make them very interesting in an inflammatory context [4]. Other stem cells have been generated *in vitro* for the purpose of research. For instance, induced Neural Stem Cells (iNSCs) are multipotent stem cells derived from induced Pluripotent Stem Cells (iPSC) [5]. These iNSCs can differentiate into neurons, glial cells, oligodendrocytes and astrocytes [6-9]. Therefore, they are an interesting model to study neurogenesis.

The Ca^{2+} ion is present in all cell types. It is an essential element of life, which explains its very fine regulation within the cells and the body, and therefore the importance of its study. Ca^{2+} oscillations are variations of free calcium concentration in cells which can take the form of "spikes". Specific Ca^{2+} oscillatory schemes are interpreted by downstream intracellular effectors, which then activate different cellular processes. This signal transduction can occur by frequency modulation (FM) or amplitude modulation (AM), very similar to a radio signal [10]. Both types of stem cells mentioned above display Ca^{2+} oscillations. Very interestingly, Ca^{2+} oscillations patterns change in the context of differentiation processes.

AIM OF WORK

The monitoring of these oscillations along differentiation of both cell types (MSCs and iNSCs) is currently carried out. Indeed, our first objective is to determine the kinetics of the Ca^{2+} oscillatory patterns during the differentiation of iNSCs and MSCs. Subsequently we aim to imitate these natural oscillations, with the use of an electrical tool. Then we will assess whether we can use it to guide these cells toward differentiation. This electrical tool involves the use of Pulsed Electric Fields (PEFs) of microsecond duration and allows to add oscillations similar to the natural ones in shape and amplitude or to abolish them [11].

REFERENCES

[1] Kolios G. Moodley Y.: Introduction to Stem Cells and Regenerative Medicine; Respiration. 2013;85(1):3-10

[2] Dominici M, Le Blanc K, Mueller I, Slaper-Cortenbach I, Marini F, Krause D, Deans R, Keating A, Prockop Dj, Horwitz E.: Minimal criteria for defining multipotent mesenchymal stromal cells. The International Society for Cellular Therapy position statement. Cytotherapy. 2006;8(4):315-7

[3] Paliwal S, Chaudhuri R, Agrawal A, Mohanty S.: Regenerative abilities of mesenchymal stem cells through mitochondrial transfer. J Biomed Sci 2018 Mar 30;25(1):31

[4] Praveen Kumar L, Sangeetha Kandoi, Ranjita Misra, Vijayalakshmi S, Rajagopal K, Rama Shanker Verma.: The mesenchymal stem cell secretome: a new paradigm towards cell-free therapeutic mode in regenerative medicine. Cytokine Growth Factor Rev. 2019 Apr;46:1-9.

[5] Marcel M. Daadi (ed.).: Neural Stem Cells: Methods and Protocols, Methods in Molecular Biology, vol. 1919, Chapter 1

[6] Zhao C., Teng E.M., Summers R.G., Ming G.L., Gage F.H.: Distinct morphological stages of dentate granule neuron maturation in the adult mouse hippocampus. J. Neurosci. 2006; 26: pp. 3-11.

[7] Ming G.L., Song H.: Adult neurogenesis in the mammalian brain: significant answers and significant questions. Neuron 2011; 70: pp. 687-702.

[8] Xing Y.L., Röth P.T., Stratton J.A., Chuang B.H., Danne J., Ellis S.L., Ng S.W., Kilpatrick T.J., Merson T.D.: Adult neural precursor cells from the subventricular zone contribute significantly to oligodendrocyte regen- eration and remyelination. J. Neurosci. 2014; 34: pp. 14128-14146.

[9] Araque A., Carmignoto G., Haydon P.G., Oliet S.H., Robitaille R. : Vol- terra A.: Gliotransmitters travel in time and space. Neuron 2014; 81: pp. 728-739.

[10] Smedler E, Uhlén P.: Frequency decoding of calcium oscillations Biochim Biophys Acta. 2014 Mar;1840(3): 964-9.

[11] Hanna Hanna, Franck M Andre, Lluis M Mir.: Electrical control of calcium oscillations in mesenchymal stem cells using microsecond pulsed electric fields Stem Cell Res Ther. 2017 Apr 20;8(1):91

LABORATORY SAFETY

Laboratory safety S1

Duša Hodžić
University of Ljubljana, Faculty of Electrical Engineering

BIOSAFETY

There are four biosafety levels (BSLs) for working with live organisms; each BSL consists of combinations of laboratory practices and techniques, safety equipment and laboratory facilities. Each combination is specifically appropriate for the operations performed, the suspected routes of transmission of the organisms and the laboratory function or activity.

Biosafety Level 1 represents a basic level of containment. It is suitable for work involving well-characterized agents not known to cause disease in healthy adult humans. The potential hazard to laboratory personnel and the environment is minimal.

Biosafety Level 2 is suitable for work involving agents that can cause human disease and have a moderate potential hazard to personnel and the environment. Precautions must be taken for handling and disposing of contaminated material, especially needles and sharp instruments. The laboratory must have limited access.

Biosafety Level 3 is used in laboratories where work is done with pathogens, indigenous or exotic agents which may cause serious or potentially lethal disease as a result of exposure by the inhalation route. Such microorganism can present a serious hazard to workers and a risk of spreading to the community, but there is usually effective prophylaxis or treatment available. BSL 3 requires special facilities with self-closing double doors and sealed windows, decontamination of clothing before laundering and controlled access.

Biosafety level 4 is required for work with pathogens which pose a high individual risk of aerosol-transmitted laboratory infections and life-threatening disease, for which there is no effective prophylaxis or treatment available. Such organisms present a serious hazard to workers and may present a high risk of spreading to the community. The BSL 4 facility is generally a separate building with specialized ventilation and waste management systems to prevent release of live pathogens to the environment.

GENERAL SAFETY RULES FOR WORKING IN THE LABORATORY

The following basic safety rules should be observed at all times in the laboratory:

1. Wash your hands with liquid soap and dry them with paper towels upon entering and prior to leaving the laboratory.
2. Wear laboratory coat and gloves. Tie back loose hair.
3. Do not carry your personal belongings in the laboratory; place them in specified locations – never on bench tops.
4. Do not smoke, eat, drink, apply cosmetics or insert contact lenses in a laboratory.
5. Keep doors and windows closed during the laboratory session to prevent contamination from air currents.
6. Contaminated spots on clothes or body can be sprayed with disinfectant and washed with water. Contaminated material should be put into special containers.
7. If you had any contact with hazardous chemicals while wearing your gloves, change the gloves before you touch other laboratory equipment, do not touch your face or your clothes with contaminated gloves.
8. Do not allow water or any water-based solution to come into contact with electrical cords or conductors. Make sure your hands are dry when you handle electrical equipment.

9. Report all accidents immediately to the instructor.

RULES FOR HANDLING CHEMICALS

Almost all chemicals can be harmful in some way and prolonged exposure may cause long-term effects as yet unknown. Preparation of hazardous chemicals must be conducted under the fume hood.

When handling chemicals the following rules must be strictly met:

1. **Always read labels before handling any chemical**. Learn hazard warning symbols which are displayed on the labels.
2. Take care to avoid spillage - if this occurs, neutralize any hazard and clean up immediately, including the outside of the container.
3. Some chemicals have a delayed or cumulative effect. Inform the instructor if any feeling of being unwell occurs when using chemicals.
4. Chemicals must not be disposed of by indiscriminate washing down the sink. Carefully read the appropriate material safety data sheet and follow the instructions.

CHEMICAL HAZARD SYMBOLS

Explosive

Mutagenic, carcinogenic, causing respiratory sensitization

Oxidizing

Corrosive

Extremely/Highly flammable

Dangerous for the environment

(Very) Toxic

Pressurized gases

Harmful

PIPETTING TECHNIQUE

Pipetting is one of the most frequent tasks in the laboratory and it directly affects the success and repeatability of the experiments. It is critical to follow good pipetting practice techniques.

ASEPTIC TECHNIQUE

Aseptic technique is a combination of procedures designed to reduce the probability of infection. In spite of the introduction of antibiotics, contamination with microorganisms remains a problem in tissue culture. Bacteria, mycoplasma, yeasts and fungal spores may be introduced by operator, atmosphere, work surfaces, solutions and many other sources. In order to avoid contamination aseptic technique should be used while handling cell cultures.

Correct aseptic technique provides a barrier between microorganisms in the environment and the culture within its flask or dish. Hence, all materials that will come into direct contact with the culture must be sterile and manipulations designed in such manner that exclude direct link between the culture and its nonsterile surroundings.

The elements of aseptic technique are a sterile work area, good personal hygiene, sterile reagents and media, and sterile handling.

Rules for sterile work:

1. Start with completely clear work area and wipe the surface with 70% alcohol and a sterile gauze.
2. Spray and wipe your hands with 70% ethanol.
3. Clean the outside of the containers and other objects with 70% ethanol before placing them in the microbiological safety cabinet.
4. The work surface should be uncluttered and contain only items required for a particular procedure; it should not be used as a storage area.
5. Remove everything that is no longer required and clean with 70% alcohol before the next procedure.
6. Arrange items to have easy access to all of them without having to reach over one item to get to another.
7. Work within your range of vision, e.g., insert a pipette in the pipetting device with the tip of the pipette in your line of sight continuously and not hidden by your arm.
8. Clean up any spillage immediately with absorbent tissues and wipe with 70% alcohol.
9. Remove everything when you finish and wipe the work surface with 70% ethanol.
10. Use ultraviolet light to sterilize the air and exposed work surfaces in the microbiological safety cabinet between uses.

GMO
GMO is an abbreviation for genetically modified organism. GMO is an organism that is created when a recipient (host) organism, with the help of a vector, successfully incorporates the insert in its genetic material and can transfer it to its descendants.
Closed system is a laboratory or some other closed room for GMO work.

Recipient (host) organism = cell/organism which accepts genetic material from the original organism or the environment, replicates and expresses it and can transfer it to its descendants.
Parent organism = recipient organism before the genetic change
Original organism = organism from which the genetic material for transfer in the host is acquired
Vector = DNA tool used in genetic engineering to harbour genes of interest and transfer them to the host
Insert = genetic material that is integrated into a vector

Example: In cell and molecular biology, the GFP **(**green fluorescent protein) gene **[insert]** is frequently used as a reporter of expression. GFP is a protein that exhibits bright green fluorescence when exposed to light in the blue to ultraviolet range. It was first isolated from the jellyfish *Aequorea victoria* **[original organism]**, although many marine organisms have similar green fluorescent proteins. It is carried on plasmids **[vector]** to the target cells **[parent organism].** The cells that manage to express the protein are called **host organisms** (GMO).

When working with GMO, traceability is essential. For that it is necessary to keep a good operating and autoclave log book. Operating log is used for writing down essential GMO information, work procedure, solid and liquid waste management and potential work related accidents. Autoclave log is a record of all waste that has been autoclaved.

GMO waste can be deactivated in two different ways – thermic or chemical treatment. Deactivation prevents the GMO`s to migrate out of the closed system. Sterilized liquids can be washed down the sink, dry sterilized solid waste can be thrown in municipal waste.

In case of a GMO accident the biosafety commissioner needs to be informed and his/her directions should be followed. If a spillage occurs there has to be enough absorbent material to absorb all the liquid. Work surfaces should be decontaminated with a disinfectant.

FURTHER READING:
Freshney R. I. Culture of animal cells: a manual of basic technique.3rd ed. Wiley-Liss, Inc. New York, 1994.

http://www.biotechnology-gmo.gov.si/eng/genetically_modified_organisms/index.html

NOTES

Electroporation hardware safety S2

Eva Pirc
University of Ljubljana, Faculty of Electrical Engineering

ELECTRIC SHOCK

Possible consequences of the current flow through the human body are ventricular fibrillation, cardiac asystole, respiratory arrest and burns. Voltages greater than 50 V applied across dry unbroken human skin or pulse energies above 50 J can cause ventricular fibrillation, if they produce electric currents above 30 mA in body tissues through the chest area. Frequently, the individual cannot let go of the power source due to involuntary muscle contraction. Side effect are conditioned by path of electric current, its magnitude, tissue characteristics and exposure time. The most sensitive organs to electric properties in human body are the heart and the brain. Human body is much more sensitive to mains-frequency alternating current (50/60 Hz) then to either direct current or high-frequency currents. Pain perception and muscle contraction at a given current level depend strongly on body weight and frequency. For example, 10 mA current at frequency of 50/60 Hz can result in strong muscle contraction, in a person that weights approximately 50 kg, but sensitivity decreases with the frequency increase. The amount of voltage needed to produce same effects depends on the contact resistance between the human and the power source. When dealing with high voltages we always have to keep in mind that air breakdown voltage is about 30 kV/cm, so also a non-direct contact can be dangerous.

GENERAL SAFETY PRECAUTIONS FOR WORKING WITH HIGH VOLTAGES

The following basic safety rules should be observed at all times in the laboratory:

10. Never work alone when dealing with high voltages. Consider having a co-worker with knowledge about equipment and risks.
11. Never leave electrical circuits/devices under high voltages when you are not present.
12. Before working with high voltage devices consider the potential risks. Do not have any contacts with conductive parts of device and keep distance from conductors under high voltage. Keep in mind that air breakdown can occur when dealing with voltages above 30 kV/cm.
13. Before high voltage circuit manipulation, switch OFF the power supply and discharge all high voltage capacitors (preferably through high voltage resistor).
14. Check if all high voltage capacitors are discharge using voltmeter.
15. Use only your right hand to manipulate high voltage electronic circuits, avoid simultaneous touching of two elements and make sure you are not grounded. Wear rubber bottom shoes or sneakers. Set up your work area away from possible grounds that you may accidentally contact.
16. When using electrolytic capacitors:
    a. DO NOT put excessive voltage across them,
    b. DO NOT put alternating current (AC) across them,
    c. DO NOT connect them in reverse polarity.
17. Make sure all high voltage connections, tools and instruments are adequately insulated and rated for the voltage and current used.
18. If someone comes in a contact with a high voltage, immediately shut off the power. Do not attempt to move injured person in contact with a high voltage.
19. In the event of an electrical fire do not use water but special fire extinguishers used for fires caused by electric current.
20. Do not wear any jewellery or other objects that could accidentally come in contact with the conductive parts of electrical circuit.
1. Protect your ears and eyes due to possible discharge sounds and element explosions.

NOTES

LABORATORY EXERCISES

The influence of Mg^{2+} ions on gene electrotransfer efficiency L1

Saša Haberl Meglič, Mojca Pavlin
University of Ljubljana, Faculty of Electrical Engineering

Duration of the experiment: day 1: 60 min; day 2: 60 min
Max. number of participants: 4
Location: Cell Culture Laboratory 3
Level: Basic

PREREQUISITES

Participants should be familiar with the Safety rules and Rules for sterile work in cell culture laboratory. No other specific knowledge is required for this laboratory practice.

THEORETICAL BACKGROUND

Gene electrotransfer is a non-viral method used to transfer genes into living cells by means of high-voltage electric pulses. An exposure of a cell to an adequate amplitude and duration of electric pulses leads to transient increase of cell membrane permeability for molecules which are otherwise deprived of membrane transport mechanisms. This allows various nonpermeant molecules, including DNA, to be transported across the membrane and enter the cell. Although mechanisms of the process are not yet fully elucidated, it was shown that several steps are crucial for gene electrotransfer: interaction of plasmid DNA (pDNA) with the cell membrane, translocation of pDNA across the membrane, migration of pDNA towards the nucleus, transfer of pDNA across the nuclear envelope and gene expression (Figure 1).

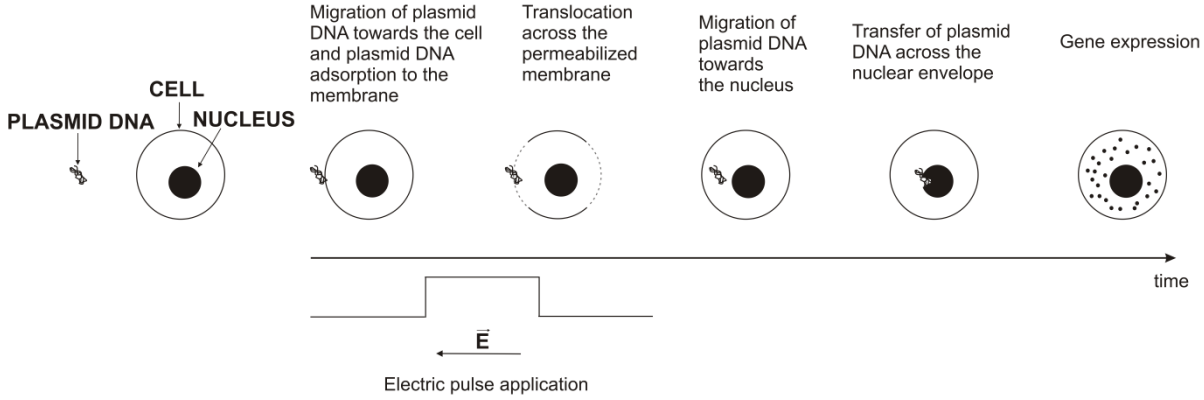

Figure 1. Steps involved in gene electrotransfer.

Many parameters have been described, which can influence the efficiency of gene electrotransfer. A few published reports have shown that the concentration of Mg^{2+} ions in electroporation medium has important impact on forming a complex between DNA and the cell membrane during application of electrical pulses. Namely, DNA is negatively charged polyelectrolyte and Mg^{2+} ions can bridge the DNA with negatively charged cell membrane. But it was shown that Mg^{2+} ions at higher concentrations may bind DNA to the cell membrane strong by enough to prevent translocation of DNA across the membrane and into the cell during electroporation consequently gene electrotransfer efficiency is decreased.

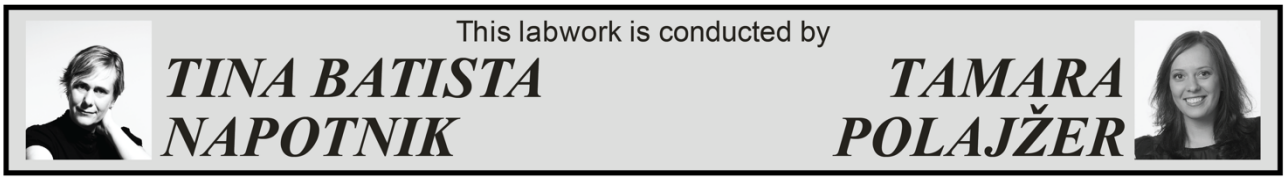

The aim of this laboratory practice is to demonstrate how different Mg^{2+} concentrations in electroporation medium affect the efficiency of gene electrotransfer and cell viability.

EXPERIMENT

We will transfect Chinese hamster ovary cells (CHO-K1) with plasmid DNA (pEGFP-N_1) that codes for GFP (green fluorescent protein) using two different electroporation media (see Protocol section). To generate electric pulses Jouan GHT 1287 electroporator (Jouan, St. Herblain, France) will be used. Pulses will be monitored on osciloscope (LeCroy 9310C).

We will determine gene electrotransfer efficiency and cell viability for both electroporation media.

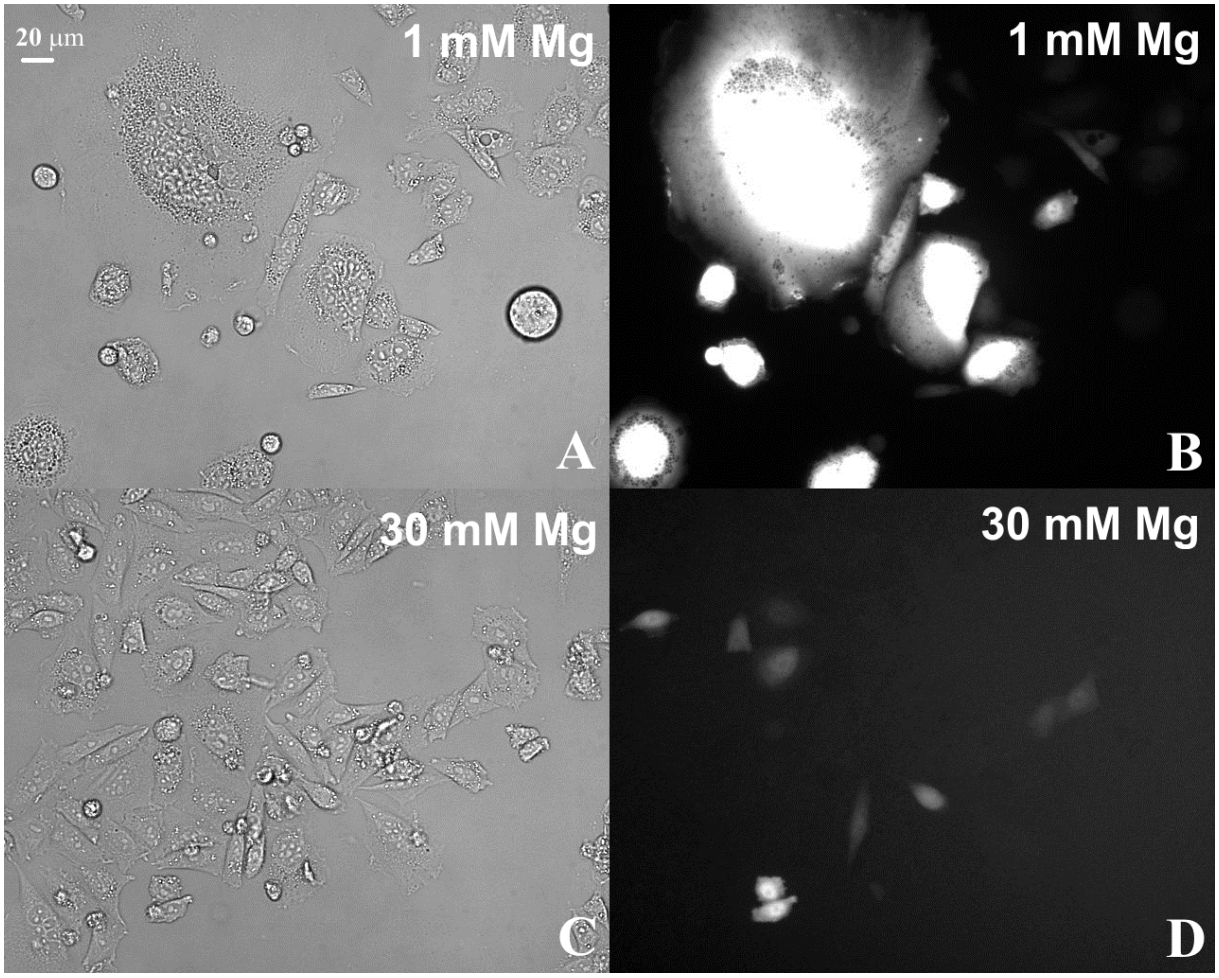

Figure 2. Gene electrotransfer of plated CHO cell 24 h after pulse application in 1 mM Mg or 30 mM Mg media. 8 x 1 ms (stainless steel wire electrodes with inter-electrode distance d = 2 mm; applied voltage U = 140 V resulting in electric field strength E = 0.7 kV/cm) pulses were applied with repetition frequency of 1 Hz to deliver pEGFP-N_1 (concentration of DNA in electroporation media was 10 μg/ml) into the cells. Phase contrast images of treated cells for (A) 1 mM Mg and (C) 30 mM Mg media and fluorescence images of treated cells for (B) 1 mM Mg and (D) 30 mM Mg media are presented. To visualize transfection 20x objective magnification was used.

Protocol 1/2 (Gene electrotransfer with different electroporation media): CHO cells will be grown in multiwells as a monolayer culture in Ham's tissue culture medium for mammalian cells with 10% fetal bovine serum (Sigma-Aldrich Chemie GmbH, Deisenhofen, Germany) at 37º C. Cells will be plated 24 h before the experiment in concentration 5 x 10^4 cells per well.

Just before the experiment remove culture media and replace it with 150 µl of electroporation media containing plasmid DNA with concentration 10 µg/ml. Use 1 mM or 30 mM electroporation media. Sucrose molarity has also been changed in order to attain the molarity of the media:

a) **1 mM Mg media** (10 mM phosphate buffer Na_2HPO_4/NaH_2PO_4, 1 mM $MgCl_2$, 250 mM sucrose; pH = 7.2)
b) **30 mM Mg media** (10 mM phosphate buffer Na_2HPO_4/NaH_2PO_4, 30 mM $MgCl_2$, 160 mM sucrose; pH = 7.2)

Incubate cells with plasmid DNA for 2-3 minutes at room temperature. Then apply a train of eight rectangular pulses with duration of 1 ms, U = 140 V resulting in electric field strength E = 0.7 kV/cm and repetition frequency 1 Hz to deliver plasmid DNA into the cells. Use stainless steel wire electrodes with inter-electrode distance d = 2 mm.
Cells in the control are not exposed to electric pulses.
Immediately after exposure of cells to electric pulses add 37.5 µl of fetal calf serum (FCS-Sigma, USA). Incubate treated cells for 5 minutes at 37ºC and then add 1 ml of culture media.

Protocol 2/2 (Determining gene electrotransfer efficiency and cell viability): After 24 h incubation at 37ºC determine the difference in gene electrotransfer efficiency and cell viability for both electroporation media by fluorescent microscopy (Leica, Wetzlar, Germany) at 20x magnification using GFP filter with excitation at 488 nm.

You will determine gene electrotransfer efficiency from the ratio between the number of green fluorescent cells (successfully transfected) and the total number of viable cells counted under the phase contrast. You will obtain cell survival from phase contrast images as the ratio between the number of viable cells in the treated sample and the number of viable cells in the control sample.

FURTHER READING:

Haberl S., Pavlin M., Miklavčič D. Effect of Mg ions on efficiency of gene electrotransfer and on cell electropermeabilization. *Bioelectrochemistry* 79: 265-271, 2010
Haberl S., Kandušer M., Flisar K., Bregar V.B., Miklavčič D., Escoffre J.M., Rols M.P., Pavlin M. Effect of different parameters used for in vitro gene electrotransfer on gene expression efficiency, cell viability and visualization of plasmid DNA at the membrane level. *J Gene Med* 15: 169-181, 2013
Rosazza C., Haberl Meglič S., Zumbusch A., Rols M.P., Miklavčič D. Gene electrotransfer: a mechanistic perspective. *Curr Gene Ther* 16: 98-129, 2016

NOTES & RESULTS

Electroporation media	Treated viable cells	Viable cells in control	Green fluorescent cells	Gene electrotransfer efficiency [%]	Viability [%]
1 mM Mg media					
30 mM Mg media					

NOTES & RESULTS

Monitoring cell membrane electroporation with ratiometric fluorescent dye Fura-2AM

L2

Gorazd Pucihar
University of Ljubljana, Faculty of Electrical Engineering

Duration of the experiments: 60 min
Max. number of participants: 4
Location: Cell Culture Laboratory 1
Level: Advanced

PREREQUISITES

Participants should be familiar with Laboratory safety (S1). The basic knowledge of handling with cells is required for this laboratory practice.

THEORETICAL BACKGROUND

Exposure of a biological cell to a sufficiently strong external electric field leads to a detectable increase of membrane permeability, a phenomenon termed electropermeabilization. Because it is assumed that an increased permeability is related to the occurrence of hydrophilic pores in the membrane, the phenomenon is often termed electroporation. Provided that the parameters of the electric field (amplitude, duration, number of pulses, frequency) are moderate, the increased permeability is reversible, and cells recover within a few minutes after the exposure. During the state of high permeability the molecules for which the membrane is otherwise impermeable (e.g. drugs, DNA) can be transported across the membrane. Electroporation is nowadays used in food processing, biotechnology, molecular biology, and different fields of medicine. It has already become an established method in oncology for electrochemotherapy of tumors, and holds great promises in gene therapy.

The efficiency of electroporation is influenced by the parameters of the electric field, cell size and geometry, and physiological characteristics of the medium surrounding the cell. Different fluorescent dyes (e.g. Propidium Iodide, Lucifer Yellow, Fura-2, Fura-3,…) can be employed to investigate the influence of these parameters on electroporation and the same dyes can be used to monitor electroporation.

The aim of this laboratory practice is to monitor electroporation with fluorescent dye and to determine the effect of cell size, shape and orientation on the efficiency of electroporation.

EXPERIMENT

We will monitor cell membrane electroporation using a fluorescent calcium sensitive indicator Fura-2AM. Calcium ions, present in the extracellular medium, do not readily cross an intact (nonporated) cell membrane and the intracellular Ca^{2+} concentration is low. Once the membrane becomes permeable due to electroporation, Ca^{2+} ions enter the cells, where they bind to the dye and change its excitation and emission spectrum (Figure 1).

This labwork is conducted by

TINA BATISTA NAPOTNIK

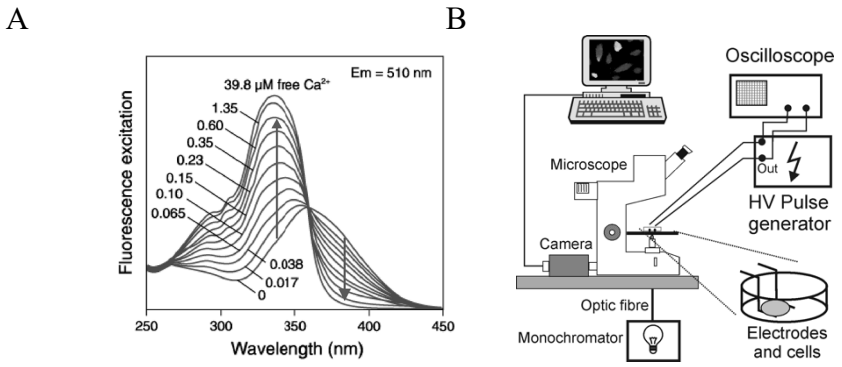

Figure 1: (A) Fluorescence excitation spectra of Fura-2 for different concentrations of Ca^{2+} (image from *http://probes.invitrogen.com/handbook/figures/0554.html*). (B) Schematic of the experiment.

Protocol: The experiments will be performed on Chinese hamster ovary cells (CHO) grown in Lab-Tek chambers (Nunc, Germany) in culture medium HAM-F12 supplemented with 10% fetal bovine serum, L-glutamine (all three from Sigma-Aldrich) and antibiotics. Plate 1.5×10^5 cells on cover glass of Lab-Tek chamber and keep them for 12-16 hours in the incubator. Before experiments, replace the culture medium with fresh medium containing 2 µM Fura-2 AM (Life Technologies). After 25-30 minutes of incubation at 37°C wash the excess dye and leave 1.5 ml of culture medium in the chamber.

Place the chamber under a fluorescence microscope (Zeiss AxioVert 200) and use ×63LD objective. Insert two parallel Pt/Ir wire electrodes with a 4 mm distance between them to the bottom of the chamber. Acquire the images using a cooled CCD camera (VisiCam 1280) and MetaFluor 7.7.5 software (Molecular Devices).

Using a ELECTRO cell B10 (BetaTech, France) device, deliver one electric pulse of 100 µs with voltages varying from 150 to 300 V. Immediately after the pulse, acquire two fluorescence images of cells at 540 nm, one after excitation with 340 nm and the other after excitation with 380 nm. Divide these two images in MetaFluor to obtain the ratio image ($R = F_{340}/F_{380}$). Wait for 5 minutes and apply pulse with a higher amplitude. After each pulse, determine which cells are being electroporated (Figure 2). Observe, which cells become electroporated at lower and which at higher pulse amplitudes.

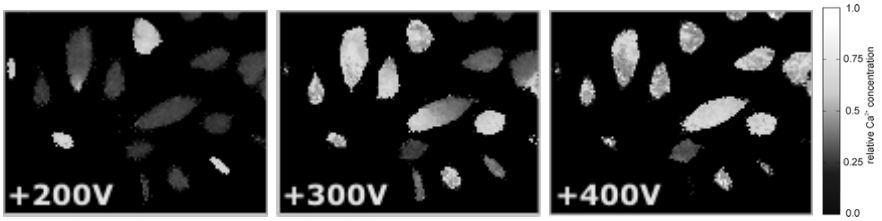

Figure 2: Cells stained with Fura-2AM and exposed to electric pulse with increasing amplitude.

FURTHER READING:

Neumann, E., S. Kakorin, and K. Toensing. Fundamentals of electroporative delivery of drugs and genes. *Bioelectrochem. Bioenerg.* 48:3-16, 1999.

Teissié, J., and M. P. Rols. An experimental evaluation of the critical potential difference inducing cell membrane electropermeabilization. *Biophys. J.* 65:409-413, 1993.

Grynkiewicz, G., M. Poenie, and R.Y. Tsien. A new generation of Ca^{2+} indicators with greatly improved fluorescence properties. *J. Biol. Chem.* 260:3440-3450, 1985.

Teruel M.N., and T. Meyer. Electroporation-induced formation of individual calcium entry sites in the cell body and processes of adherent cells. *Biophys. J.* 73:1785-1796, 1997.

Valič B., Golzio M., Pavlin M., Schatz A., Faurie C., Gabriel B., Teissié J., Rols M.P., and Miklavčič D. Effect of electric field induced transmembrane potential on spheroidal cells: theory and experiment. *Eur. Biophys. J.* 32: 519-528, 2003.

Towhidi L., Kotnik T., Pucihar G., Firoozabadi S.M.P., Mozdarani H., Miklavčič D. Variability of the minimal transmembrane voltage resulting in detectable membrane electroporation. *Electromagn. Biol. Med.* 27: 372-385, 2008.

Pucihar G., Krmelj J., Reberšek M., Batista Napotnik T., Miklavčič D. Equivalent pulse parameters for electroporation. *IEEE T. Biomed. Eng.* 58: 3279-3288, 2011.

NOTES & RESULTS

NOTES & RESULTS

Visualization of local ablation zone distribution between two needle electrodes L3

Tjaša Potočnik, Alenka Maček Lebar
University of Ljubljana, Faculty of Electrical Engineering

Duration of the experiments: 60 min
Max. number of participants: 4
Location: Cell Culture Laboratory 2 or Cell Culture Laboratory 3
Level: basic

PREREQUISITES

Participants should be familiar with Laboratory safety (S1) and Electroporation hardware safety (S2). No other specific knowledge is required for this laboratory practice.

THEORETICAL BACKGROUND

Electroporation is the method in which by applying external electric field of sufficient amplitude and duration membrane of exposed cells becomes permeabilized for molecules that otherwise cannot pass cell membrane. After reversible electroporation cell membrane reseals. With increasing amplitude of electric field the level of cell membrane permeabilization and the number of cells that are permeabilized increases. When pulses with sufficient magnitude and duration are applied, cell death is achieved and the process is defined as irreversible electroporation (IRE). IRE is an emerging ablation technique inducing apoptosis in successfully treated cells or tissues. Usually there is a sharp border between treated and untreated tissue regions because only the cells that are exposed to high enough electric field are ablated. Effective prediction of electric field can be obtained by numerical modeling, which includes the shape and position of the electrodes and parameters of electric pulses (amplitude, duration, number, frequency) used as well as electrical properties of the tissue. Using treatment planning, IRE offers benefits over other cancer therapies because it can be performed near large blood vessels, nerves, and ducts without causing damage to these structures, sparing extracellular matrix.

Electroporation can be detected by measuring increased transport of molecules across the membrane. Cell uptake of dyes, either fluorescent molecules (lucifer yellow, yo-pro-1, propidium iodide) or colour stains (such as trypan blue), is most often used for *in vitro* electroporation detection. Trypan blue can be used as an indicator of plasma membrane integrity and of cell viability. Trypan blue is normally impermeant to healthy cells. When cell membrane integrity is compromised, the dye is able to enter the cell and stains cellular structures blue, especially nuclei, making the cell appear blue. Cells that take up this dye several hours after exposure to electrical pulses are usually considered dead or dying.

The aim of this laboratory practice is to visualize local ablation zone distribution between two needle electrodes with increasing pulse amplitude using trypan blue.

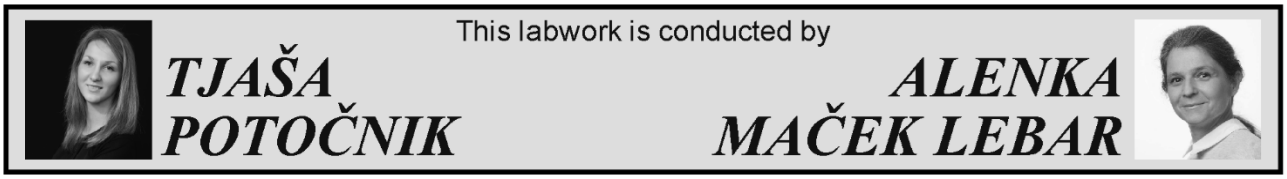

EXPERIMENT

We will visualize local ablation zone distribution between two needle electrodes using trypan blue. The effect of the pulse amplitude on the local ablation zone distribution between two needle electrodes will be determined for a train of eight 100 µs rectangular pulses delivered with the repetition frequency 1 Hz. The area of blue cells that is a consequence of efficient ablation increases with increasing pulse amplitude is presented in Figure 1.

Protocol: You will use Chinese hamster ovary cells (CHO), plated 48 h before experiment in concentration 2.5 x 10^5 cells per tissue culture dish. Cells are attached to the culture dish surface. Immediately before electric pulses are applied replace the growth medium with electroporation buffer. As electroporation buffer you will use isotonic 10 mM K_2HPO_4/KH_2PO_4 containing 1 mM $MgCl_2$ and 250 mM sucrose with pH 7.4. You will use needle electrodes 1 mm apart. For pulse delivery Gemini X2 electroporator (Hardvard apparatus BTX, USA) will be used. It can produce square and exponential pulses. During the experiment current will be monitored with an oscilloscope and a current probe. Electric field in the needle surrounding can be calculated numerically.

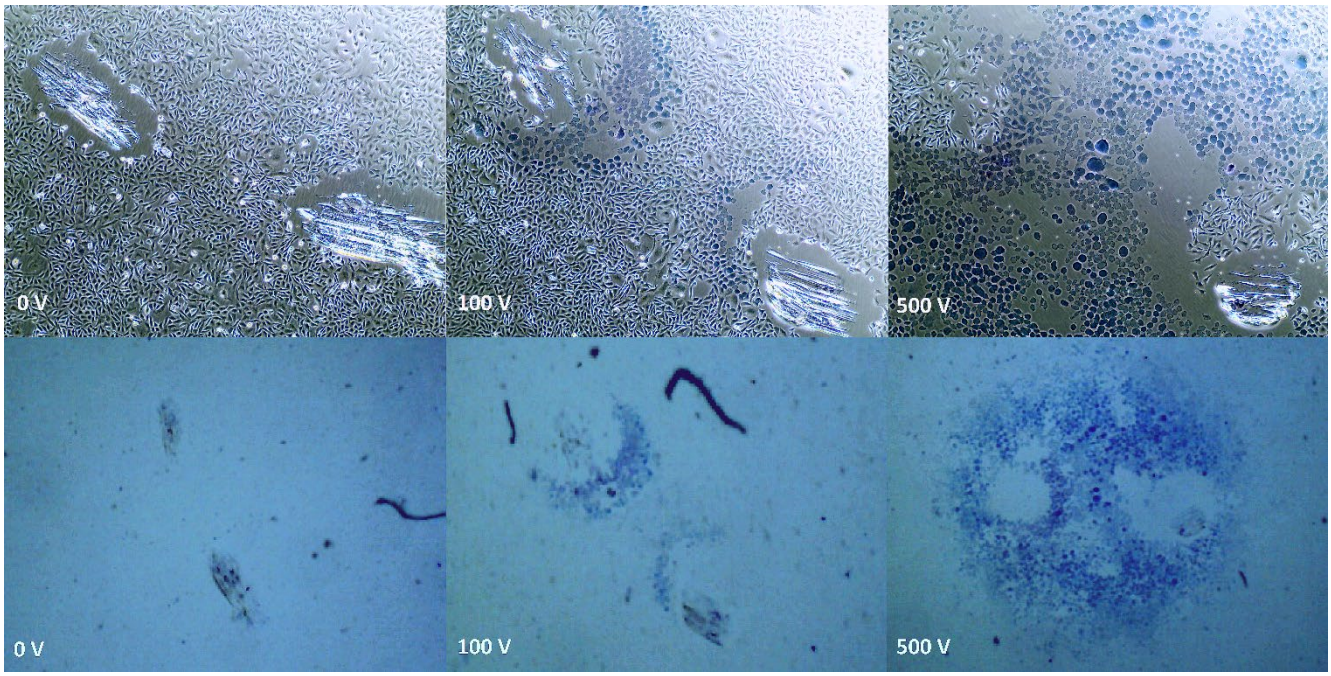

Figure 1: The sequence of the images of local ablation zone after cells were exposed to electric pulses with increasing pulse amplitude. The images were obtained by light microscopy under 10 × objective magnifications (top row) and under 5 × objective magnifications (bottom row).

Remove the tissue culture dish from the incubator and replace the growth medium with 500 µl of electroporation buffer. Carefully place needle electrodes on edge of tissue culture dish and apply electric pulses. Electric pulse parameters used are: 8 pulses, 100 µs duration and pulse repetition frequency 1 Hz, while pulse amplitude increases gradually. Increase the pulse amplitude from 0 V to 100 V, 300 V, 500 V and 700 V. After electroporation leave cells for 10 minutes at room temperature. Remove electroporation buffer and add 500 µl of trypan blue to tissue culture dish. Leave the cells for 5 minutes at room temperature then replace the trypan blue with 500 µl of fresh electroporation buffer. For visualization of local ablation zone, EVOS XL Core Imaging System (Invitrogen™) will be used.

FURTHER READING:

Batista Napotnik T, Miklavčič D. In vitro electroporation detection methods – An overview. Bioelectrochemistry 120: 166-182, 2018.
Čemažar, M, Jarm T., Miklavčič D, Maček Lebar A., Ihan A., Kopitar N.A., Serša G. Effect of electric field intensity on electropermeabilization and electrosensitivity of various tumor cell lines in vitro. *Electro and Magnetobiology* 17: 263-272, 1998.
Čorović S, Pavlin M, Miklavčič D. Analytical and numerical quantification and comparison of the local electric field in the tissue for different electrode configurations. Biomed. Eng. Online 6: 37, 2007.
Davalos RV, Mir IL, Rubinsky B. Tissue ablation with irreversible electroporation. Ann Biomed Eng 33(2):223-31, 2005.
Dermol J, Miklavčič D. Predicting electroporation of cells in an inhomogeneous electric field based on mathematical modeling and experimental CHO-cell permeabilization to propidium iodide determination. Bioelectrochemistry 100: 52-61, 2014.
Puc M., Kotnik T., Mir L.M., Miklavčič D. Quantitative model of small molecules uptake after in vitro cell electropermeabilization. Bioelectrochemistry 60: 1 – 10, 2003.
Rols M.P. Electropermeabilization, a physical method for the delivery of therapeutic molecules into cells. Biochim. Biophys Acta 1758: 423-428, 2006

NOTES & RESULTS

NOTES & RESULTS

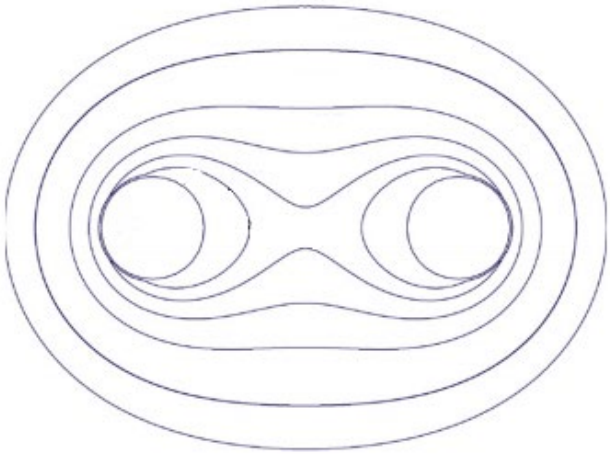

100 V

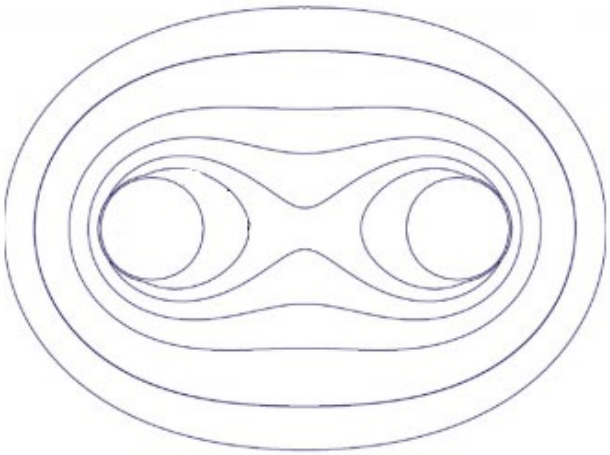

500 V

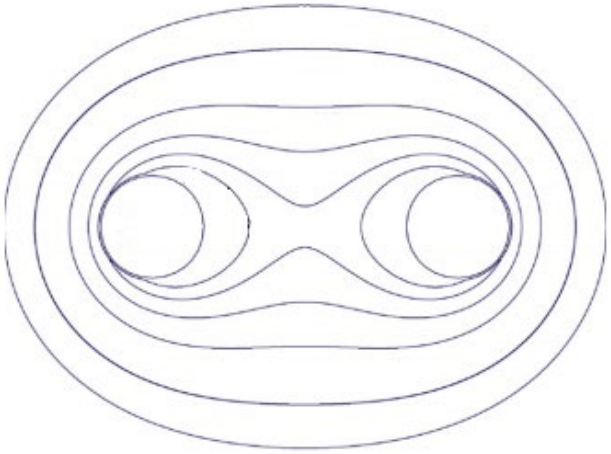

700 V

Effect of short high-frequency bipolar pulses on plasma membrane permeabilization L4

Janja Dermol-Černe, Lea Vukanović
University of Ljubljana, Faculty of Electrical Engineering

Duration of the experiments: 60 min
Max. number of participants: 4
Location: Cell Culture Laboratory 2
Level: basic

PREREQUISITES

Participants should be familiar with Laboratory safety (S1) and Electroporation Hardware Safety (S2). No other specific knowledge is required for this laboratory practice.

THEORETICAL BACKGROUND

In electrochemotherapy and irreversible electroporation as ablation technique, square 50-100 µs long monopolar pulses are usually applied at repetition frequency 1 Hz. The main drawbacks to the treatment of tissues with these monopolar pulses are discomfort and pain, the need to administer muscle relaxants and anesthesia, need for synchronization of the pulse delivery with the electrocardiogram and inhomogeneous tissue impedance. One of the possibilities to overcome these obstacles is high-frequency irreversible electroporation (HF-IRE). In HF-IRE, long monopolar pulses are replaced with bursts of a few µs long bipolar pulses, which mitigate muscle contractions, however at the expense of delivering higher energy.

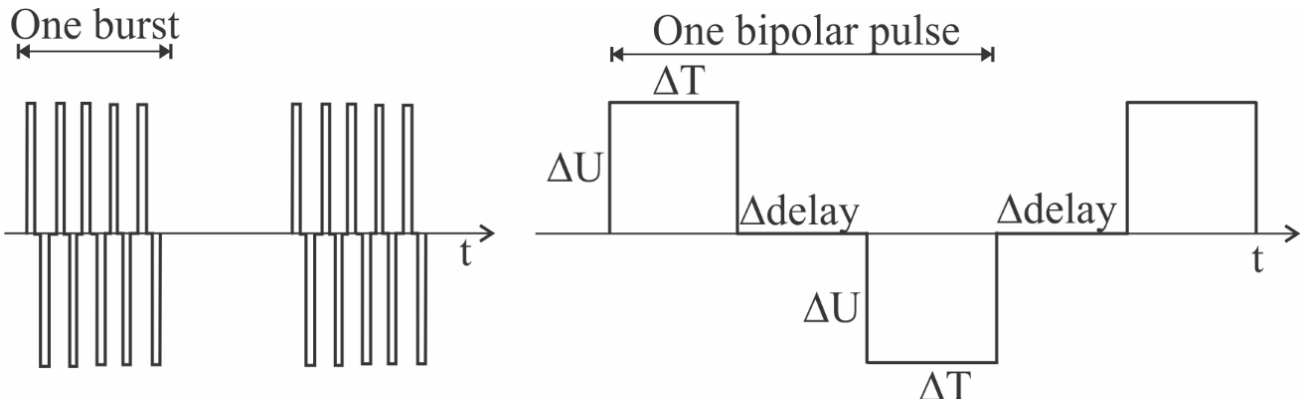

Figure 1: A typical waveform of pulses in the H-FIRE treatment. Pulses are usually delivered in several bursts delivered at repetition frequency 1 Hz. One pulse consists of a positive and a negative pulse and the delay between them.

The aim of this laboratory practice is the comparison of the effect of HF-IRE pulses and longer monopolar pulses on permeabilization of the plasma membrane as determined by spectrofluorometric measurements.

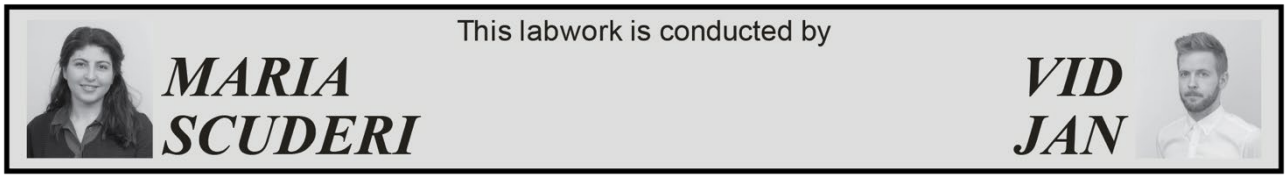

EXPERIMENT

We will detect electropermeabilization on spectrofluorometer using propidium iodide. Propidium iodide (PI) is a red-fluorescent dye. It is not permeant to live cells and is commonly used to detect dead cells in a population. After plasma membrane permeabilization, however, PI can diffuse into cells. It binds to DNA with little sequence preference. After binding, its fluorescence is increased 20- to 30-fold, with excitation maximum at 535 nm and emission maximum at 617 nm.

We will determine the effect of the pulse amplitude of HF-IRE pulses on the degree of cell membrane permeabilization. We will deliver 50 bipolar pulses consisting of 1 µs long positive 1 µs long negative pulse with 1 µs delay between them, delivered in 8 bursts at repetition frequency 1 Hz. We will compare the effect of the HF-IRE pulses on plasma membrane permeabilization with the monopolar pulses of parameters traditionally used in electrochemotherapy (8x100 µs pulses, 1 Hz repetition frequency). Thus, the duration of all pulses of HF-IRE pulses as well as of monopolar pulses is 800 µs.

We will use attached Chinese hamster ovary cells, $2.5x10^5$ cells per well plated 24 hours in advance in 24 well plate. As the electroporation buffer, we will use 10 mM K_2HPO_4/KH_2PO_4, 1 mM $MgCl_2$, 250 mM sucrose with 1.78 mS/cm, 292 mOsm/kg, and pH 7.4. We will use Pt/Ir wire electrodes with 0.8 mm diameter and 4 mm inter-electrode distance positioned at the bottom of the well. Between the electrodes, the electric field is approximately homogeneous and can be calculated as the ratio of the applied voltage and the inter-electrode distance.

For the application of pulses, we will use a laboratory prototype pulse HF-IRE pulse generator (University of Ljubljana) based on H-bridge digital amplifier with 1 kV MOSFETs (DE275-102N06A, IXYS, USA). We will monitor the delivered voltage and current by an oscilloscope, a differential probe and a current probe.

Protocol:

Remove the 24 well plate from the incubator and replace the growth medium with 300 µl per well of electroporation buffer containing 0.15 mM PI. Apply electric pulses and leave the cells for 3 minutes at room temperature to allow PI to diffuse into cells then replace the buffer with 1 ml of fresh electroporation buffer to stop PI influx. Increase the pulse amplitude of the bipolar pulses from 400 V to 1000 V. For the comparison with monopolar pulses, deliver 8x100 µs pulses with a repetition frequency of 1 Hz at 1000 V. As a negative control, apply no pulses to one well.

We will determine the fluorescence intensity spectrofluorometrically (Tecan, Infinite 200). Set the appropriate excitation and emission wavelengths for PI (535/617 nm). Plot a figure of fluorescence as a function of the electric field. Compare the fluorescence, obtained with the bipolar pulses, to the fluorescence, obtained with monopolar pulses of the same voltage.

FURTHER READING:

D. C. Sweeney, M. Reberšek, J. Dermol, L. Rems, D. Miklavčič, and R. V. Davalos, "Quantification of cell membrane permeability induced by monopolar and high-frequency bipolar bursts of electrical pulses," *Biochim. Biophys. Acta BBA - Biomembr.*, vol. 1858, no. 11, pp. 2689–2698, Nov. 2016.

C. B. Arena, M. B. Sano, M. N. Rylander, and R. V. Davalos, "Theoretical Considerations of Tissue Electroporation With High-Frequency Bipolar Pulses," *IEEE Trans. Biomed. Eng.*, vol. 58, no. 5, pp. 1474–1482, May 2011.

C. Yao *et al.*, "Bipolar Microsecond Pulses and Insulated Needle Electrodes for Reducing Muscle Contractions During Irreversible Electroporation," *IEEE Trans. Biomed. Eng.*, vol. 64, no. 12, pp. 2924–2937, Dec. 2017.

S. P. Bhonsle, C. B. Arena, D. C. Sweeney, and R. V. Davalos, "Mitigation of impedance changes due to electroporation therapy using bursts of high-frequency bipolar pulses," *Biomed. Eng. OnLine*, vol. 14, no. Suppl 3, p. S3, 2015.

NOTES & RESULTS

Bipolar/Monopolar	Bipolar	Bipolar	Bipolar	Bipolar	Bipolar	Monopolar
Voltage (V)	0	400	600	800	1000	1000
Pulse duration ΔT (μs)	0	1	1	1	1	100
Raw data (a.u.)						

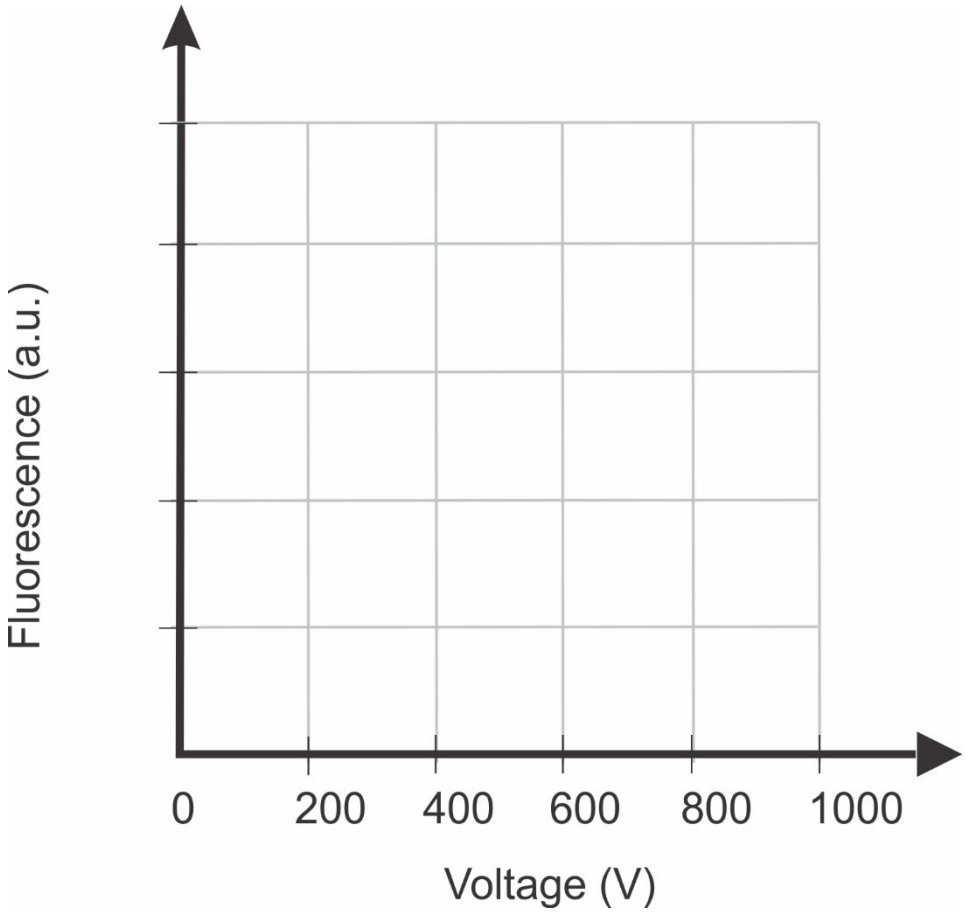

NOTES & RESULTS

Electrotransformation of *Escherichia coli* with plasmid DNA L5

Duša Hodžić, Saša Haberl Meglič
University of Ljubljana, Faculty of Electrical Engineering

Duration of the experiments: day 1: 90 min; day 2: 30 min
Max. number of participants: 4
Location: Microbiological laboratory 1
Level: Basic

PREREQUISITES

Participants should be familiar with Laboratory Safety (S1). No other specific knowledge is required for this laboratory practice.

THEORETICAL BACKGROUND

The ability to introduce plasmid DNA into bacterial cells is of great practical importance in molecular biology, genetic engineering, biotechnology etc. For example, bacteria with introduced plasmid DNA can have new pathways for production of proteins or are able to degrade organic pollutants (bioremediation). Since majority of bacterial species does not show a naturally occurring ability to take up DNA (competence) it is convenient to have methods that allow us such genetic manipulation of bacteria. The well-known methods are: chemical transformation, electrotransformation, biolistic transformation and sonoporation. Main advantages of electroporation compared to other methods are shorter time needed, easy application and no need of toxic chemicals. Nevertheless, optimization of electric pulses and other parameters is necessary for high yields of transformants.

Electrotransformation is transformation of bacteria by means of electroporation, a phenomenon that occurs when the cell is exposed to the external electric field of sufficient amplitude and duration which leads to permeabilization of the membrane. Increasing electric field amplitude or duration of pulses increases the level of cell membrane permeabilization and thus transformation effectiveness. When electric field parameters used are below the critical value, cell membrane can reseal and treated bacteria survive. This is also known as reversible electroporation.

The aim of this laboratory practice is to demonstrate transformation of *Escherichia coli* with plasmid DNA using reversible electroporation.

EXPERIMENT

Our experimental organism will be competent bacteria *E.coli* DH5α and the plasmid pSEUDO-GFP. We will detect transformed and surviving bacteria by counting colony forming units (CFU count) on LB agar plates with antibiotic erythromycin for selection.

Protocol 1/2 (Electroporation of bacteria): On the first day of experiment 200 µl of competent bacterial cells in 10% glycerol and water will be mixed with plasmid DNA (pSEUDO-GFP), incubated for 2 minutes on ice and exposed to electric field. Electric pulses will be applied with electric pulse generator Vitae HVP-VG (Igea, Italy). Samples for treatment are placed in electroporation cuvettes with integrated aluminium electrodes 2 mm apart (VWR, Belgium). Immediately after electroporation the recovery medium SOC will be added to bacterial suspension. After 60 minutes' incubation at 37 °C, bacteria will be plated on LB agar with selective antibiotic for transformants. Control sample will be the

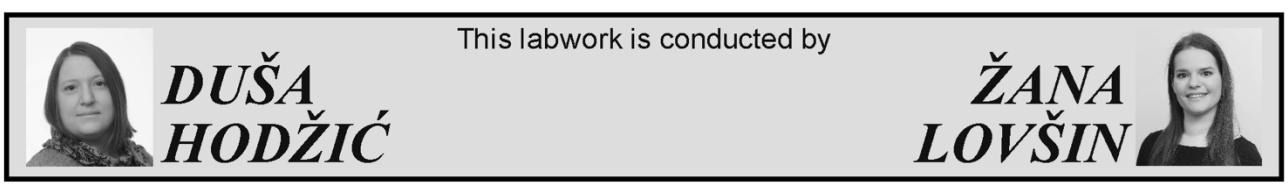

untreated suspension of bacteria. To determine the number of bacterial cells you will need to prepare serial dilutions of resuspended bacteria ranging from 10^{-1} to 10^{-6}. Dilute 100 µl of bacterial suspension in tubes containing 900 µl of sterile 0,9 % NaCl. Pipette 100 µl of suspension per LB agar plate and spread them evenly with a sterile Drigalski spatula. All agar plates will be incubated overnight at 37 °C.

Protocol 2/2 (Counting bacterial colonies): Determine electrotransformation efficiency and total cell count. The efficiency of reversible electroporation is expressed as number of transformants per microgram of DNA and can be monitored by plating the treated sample on nutrient agar with selective antibiotic and counting the number of CFU. Each colony may arise from one or a group of bacterial cells and they represent the cells that have successfully undergone the transformation.

FURTHER READING:

Calvin N.M., Hanavalt P.C. High-efficiency transformation of bacterial cells by electroporation. *Journal of Bacteriology* 170: 2796-2801, 1988.

Yoshida N., Sato M. Plasmid uptake by bacteria: a comparison of methods and efficiencies. *Applied Microbiology and Biotechnology* 83:791-798, 2009.

Kotnik T., Frey W., Sack M., Haberl Meglič S., Peterka M., Miklavčič D. Electroporation-based applications in biotechnology. *Trends in Biotechnology. Review* 33:480-488, 2015.

Munazza Gull and Sondos El-Baz (November 5th 2018). Introductory Chapter: Preface to Plasmids, Plasmid, Munazza Gull, IntechOpen, DOI: 10.5772/intechopen.78673. Available from: https://www.intechopen.com/books/plasmid/introductory-chapter-preface-to-plasmids

NOTES & RESULTS

Electric pulse parameters *n* x *t* (µs) *E* [kV/cm], *f* [Hz]	1 x 100 µs 7.5 kV/cm 1 Hz	1 x 100 µs 12.5 kV/cm 1 Hz	8 x 100 µs 12.5 kV/cm 1 Hz	1 x 1000 µs 12.5 kV/cm 1 Hz
Total cell count [*number of viable cells / ml*]				
Transformation efficiency [*number of transformants / µg pDNA*]				

NOTES & RESULTS

NOTES & RESULTS

Electroporation of planar lipid bilayers L6

Peter Kramar, Aljaž Velikonja, Alenka Maček Lebar
University of Ljubljana, Faculty of Electrical Engineering, Slovenia

Duration of the experiments: 120 min
Max. number of participants: 4
Location: Laboratory for skin and planar lipid bilayers
Level: Basic

PREREQUISITES

Participants should be familiar with Laboratory safety (S1). No other specific knowledge is required for this laboratory practice.

THEORETICAL BACKGROUND

A planar lipid bilayer can be considered as a small fraction of total cell membrane. As such it has often been used to investigate basic aspects of electroporation; especially because of its geometric advantage allowing chemical and electrical access to both sides of the lipid bilayer. Usually a thin bi-molecular film composed of specific phospholipids and organic solvent is formed on a small aperture separating two aqueous compartments. Electrodes immersed in these two aqueous compartments allow to measure current and voltage across the lipid bilayer (Figure 1).

Two different measurement principles of planar lipid bilayer's properties can be used: voltage or current clamp method. Planar lipid bilayer from an electrical point of view can be considered as imperfect capacitor, therefore two electrical properties, capacitance and resistance, mostly determine its behaviour.

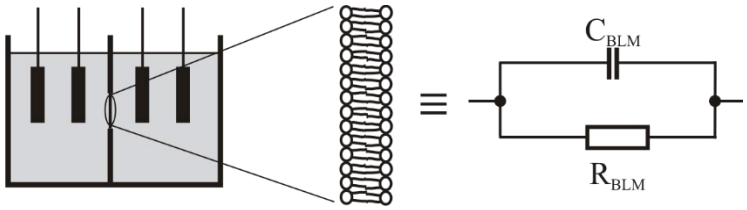

Figure 1: Equivalent circuit of a planar lipid bilayer.

The aim of this laboratory practice is to build a planar lipid bilayer by painting method (Muller - Rudin method) or/and foldig method (Montal – Mueller) and to determine capacitance and resistance of the planar lipid bilayer using LCR meter. Basic aspects of planar lipid bilayer electroporation will be given by observing formation of the pores and determining its breakdown voltage.

This labwork is conducted by

KATJA BALANTIČ

EXPERIMENT

Protocol:

Muller-Rudin method

Form a planar lipid bilayer by covering the surface of the aperture in a barrier separating two compartments of a measuring vessel with a lecithin solution (20 mg/ml of hexane). After evaporation of hexane, fill compartments with solution consisting of 0.1 mol KCl, 0.01 mol of HEPES, at pH=7.4. Connect the electrodes and apply a drop of lecithin dissolved in decane (20 mg/ml) to the aperture by the micropipette or paint it by a teflon brush. Measure capacitance and determine if the formation of planar lipid bilayer is appropriate.

Montal – Mueller method

Cover the surface of the aperture in a barrier separating two compartments of a measuring vessel with 1 µl lecithin solution (10 mg/ml of hexane and ethanol absolute in ratio 9:1). After evaporation of hexane and ethanol, add on the aperture 1,5 µl solution of pentan and hexadecane in ratio 7:3. Fill compartments with solution consisting of 0.1 mol NaCl, 0.01 mol of HEPES, at pH=7.4. On the solution surface apply 2 µl of lecithin solution in each compartment. Wait approximately 15 minutes that lipid molecules are equally spread on the solution surface. Then rise the solution surface above aperture synchronously in both compartments by pumps. Measure capacitance and determine if the formation of planar lipid bilayer is appropriate.

Measuring methods: When the planar lipid layer is formed, we apply the current or voltage to the planar lipid bilayer. In the current clamp method the current is applied to the planar lipid bilayer and we measure voltage across the bilayer. Apply a linearly increasing current and record a voltage across the bilayer. During the experiment you will obtain the time course of the voltage across the bilayer and the plot of the programmed current flowing between two current electrodes. In the voltage clamp method the voltage across the planar lipid bilayer is applied and current, which flows through planar lipid bilayer, is measured. To the planar lipid bilayer apply a linearly increasing voltage and record a flowing current. Like at the current clamp method you will obtain the time course of the flowing current and the plot of the programmed voltage across the planar lipid bilayer.

From collected data determine the breakdown voltage (U_{br}) and the lifetime (t_{br}) of planar lipid bilayer.

FURTHER READING:

Kalinowski S., Figaszewski Z., A new system for bilayer lipid membrane capacitance measurements: method, apparatus and applications, *Biochim. Biophys. Acta* 1112:57-66, 1992.

Pavlin M, Kotnik T, Miklavcic D, Kramar P, Macek-Lebar A. Electroporation of planar lipid bilayers and membranes. In Leitmanova Liu A (ed.), *Advances in Planar Lipid Bilayers and Liposomes*, *Volume 6*, Elsevier, Amsterdam, pp. 165-226, 2008.

Koronkiewicz S., Kalinowski S., Bryl K., Programmable chronopotentiometry as a tool for the study of electroporation and resealing of pores in bilayer lipid membranes. *Biochim. Biophys. Acta*, 1561:222–229, 2002.

Kotulska M., Natural fluctuationsof an electropore show fractional Lévy stable motion, *Biophys. J.*, 92:2412-21, 2007.

Montal M., Mueller, P., Formation Of Bimolecular Membranes From Lipid Monolayers And A Study of their Electrical Properties, *PNAS*, 69:3561-3566, 1972.

Kramar P, Miklavčič D, Maček-Lebar A. Determination of the lipid bilayer breakdown voltage by means of a linear rising signal. *Bioelectrochemistry* 70: 23-27, 2007.

NOTES & RESULTS

NOTES & RESULTS

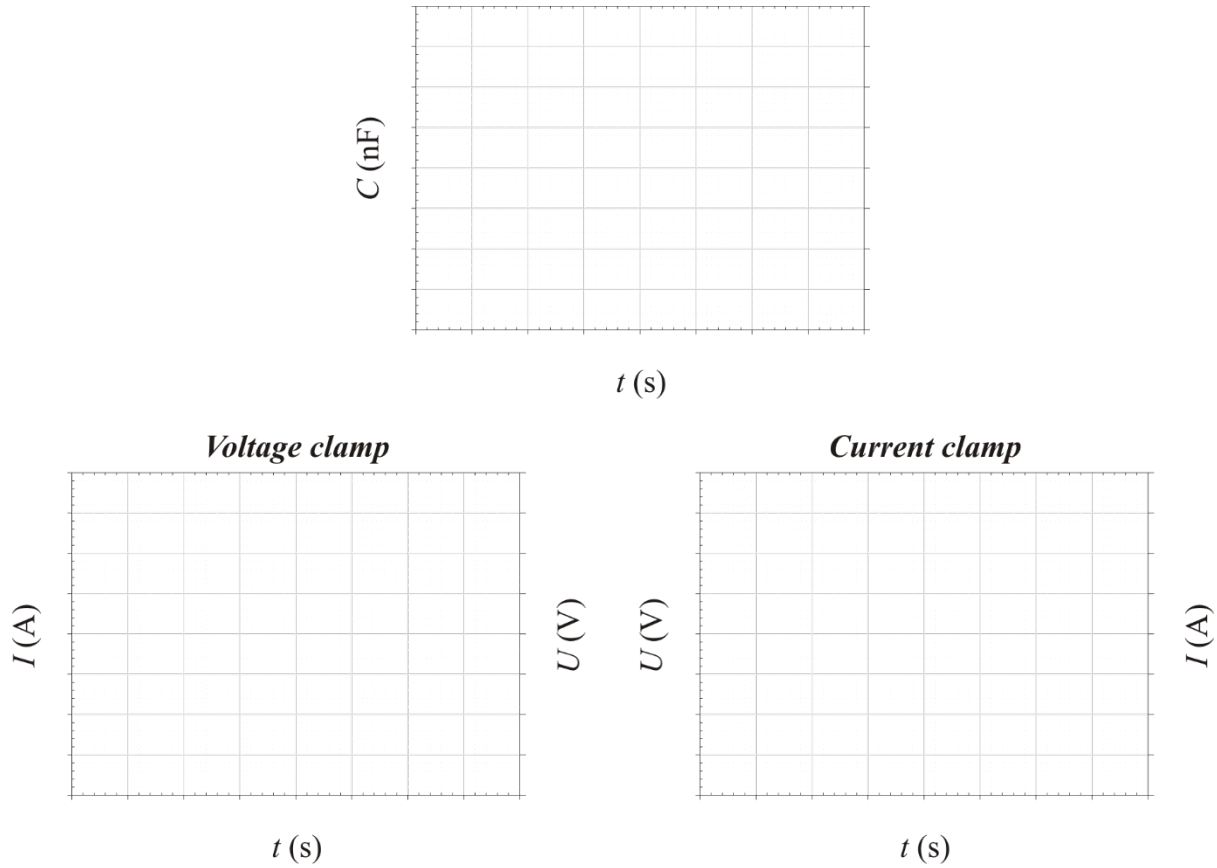

NOTES & RESULTS

E. coli inactivation by pulsed electric fields in a continuous flow system L7

Saša Haberl Meglič, Karel Flisar
University of Ljubljana, Faculty of Electrical Engineering

Duration of the experiment: day 1: 90 min; day 2: 60 min
Max. number of participants: 4
Location: Microbiological laboratory 2
Level: Basic

PREREQUISITES

Participants should be familiar with the Safety rules and Rules for sterile work in cell culture laboratory. No other specific knowledge is required for this laboratory practice.

THEORETICAL BACKGROUND

The first description of the profound effect of electrical pulses on the viability of a biological cell was given in 1958. If a cell is exposed to a sufficiently high electric field, its membrane becomes permanently permeable, resulting in leakage of cellular components, which leads to cell death. The method gained ground as a tool for microbial inactivation and the influence of different pulsed electric fields (PEF) on microbial viability was extensively studied on various microorganisms.

Since PEF microbial inactivation in controlled laboratory conditions showed promise, the idea arose of also removing pathogenic microorganisms from various water sources, hospital wastewaters and liquid food, without destroying vitamins or affecting the food's flavour, colour or texture. In order to facilitate PEF application on a large scale, the development of flow processes has been pursued. A standard PEF treatment system therefore consists of a pulse generator that enables continuous pulse treatment, flow chambers with electrodes and a fluid-handling system.

Several parameters have been described, which can influence inactivation of microbial cells. Specifically in a continuous flow system the flow rate of a liquid must be adjusted in order for each bacterial cell to be exposed to appropriate pulse conditions.

The aim of this laboratory practice is to demonstrate how different pulse parameters in a continuous flow system affect bacterial inactivation.

EXPERIMENT

We will inactivate *Escherichia coli* K12 TOP10 cells carrying plasmid pEGFP-N1, which encodes kanamycin resistance (Clontech Laboratories Inc., Mountain View, CA, USA) in a continuous flow system (see Figure 1) using different electric pulse parameters. To generate electric pulses square wave prototype pulse generator will be used. Pulses will be monitored on osciloscope (LeCroy 9310C). The inactivation level will be determined by plate count method.

Bacterial cells will be grown prior experiment for 17 hours at 37°C in Luria Broth (LB) medium (Sigma-Aldrich Chemie GmbH, Deisenhofen, Germany) with shaking.

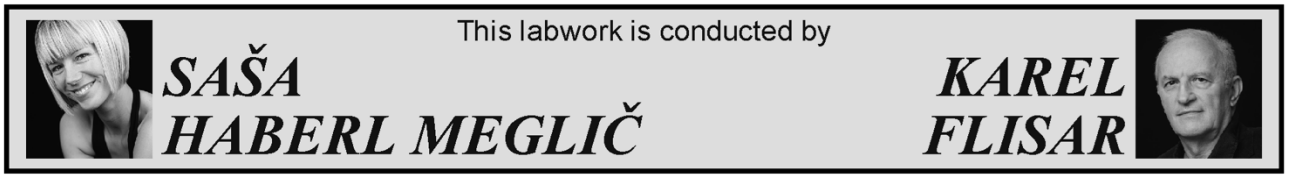

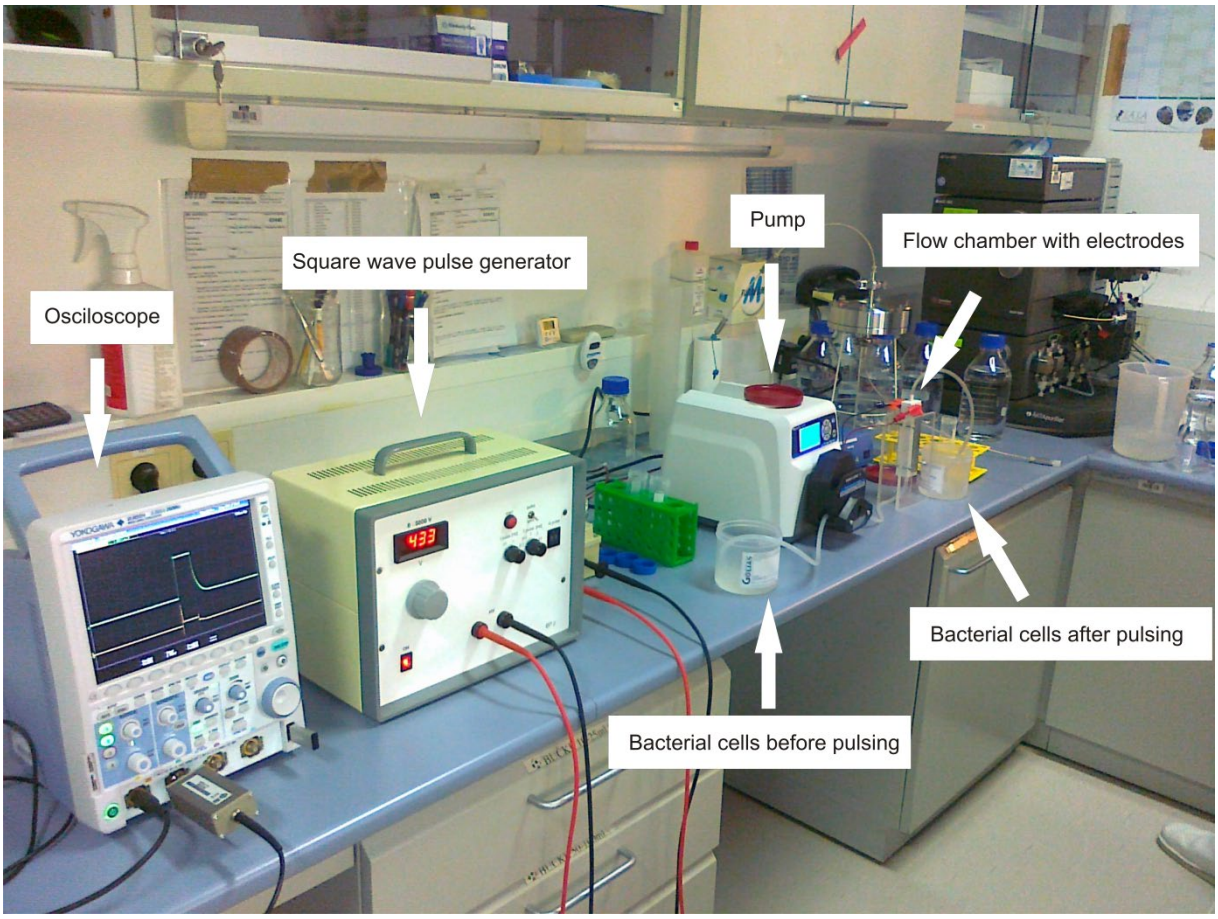

Figure 1. Continuous flow electroporation system. The circuit system includes a flow chamber with electrodes and a prototype square wave pulse generator. Voltage and current are both monitored throughout the experiment.

Protocol 1/2 (Electroporation of bacteria in a continuous flow system): On the first day of experiment *E. coli* cells will be centrifuged (4248 g, 30 min, 4°C) and the pellet will be re-suspended in 10 ml of distilled water and 100x diluted. The total volume of prepared bacterial cells for the treatment will be 0.3 L.

In order to determine the number of bacterial cells in our sample, you will prepare serial dilutions of bacterial sample ranging from 10^{-1} to 10^{-6} (in 900 µl of sterile distilled water you will dilute 100 µl of bacterial sample). You will pipette 100 µl of dilutions 10^{-5} and 10^{-6} on LB agar containing kanamycin antibiotic and evenly spread the liquid with sterile plastic rod.

The exposure of cells to electric pulses in flow through chamber in a continuous flow system depends on the geometry of the chamber, the frequency of pulses at which electroporator operates. The number of pulses is given by equation 1. At that flow, the desired number of pulses are applied to the liquid and thus to the cells in the flow-through chamber. Because the volume of our cross-field chamber between the electrodes (Q = 0.0005 L) and the frequency (10 Hz in our case) are constant, the flow through the chamber can be determined:

$$q = \frac{f}{n} \cdot Q \qquad (1)$$

where q (L/min) is the flow rate, Q (L) the volume between the two electrodes and n is the number of pulses received by the fluid in the chamber in residence time. For a frequency of 10 Hz, you will calculate

the flow rate (q) at which the whole liquid will be subjected to at least one pulse. For PEF flow through treatment you will use 0.3 L (10^{-2} dilution) of prepared bacterial cells. Bacterial cells will be pumped through the system at the calculated flow rate and pulses will be applied by prototype pulse generator.

After PEF treatment take 100 µl of treated sample and prepare dilutions ranging from 10^{-1} to 10^{-6}. You will pipette 100 µl of dilutions 10^{-4}, 10^{-5} and 10^{-6} on LB agar with kanamycin antibiotic and evenly spread the liquid with sterile plastic rod.

Protocol 2/2 (Determining bacterial viability): After 24 h incubation at 37ºC count colony forming units. Express the viability as log (N/N_0), where N represents the number of colony forming units per ml in a treated sample (bacterial cells exposed to electric pulses) and N_0 the number of colony forming units per ml in an untreated sample (bacterial cells not exposed to electric pulses).

Example of determining bacterial viability:
You counted 70 CFU in a control sample (dilution 10^{-7}) and 30 CFU in a treated sample (dilution 10^{-5}).

Number of bacterial cells per ml (control sample) = 70 x 10^7 (dilution factor of sample) x 10 (dilution factor of plating) = 7 x 10^9 bacterial cells/ml

Number of bacterial cells per ml (treated sample) = 30 x 10^5 (dilution factor of sample) x 10 (dilution factor of plating) = 3 x 10^7 bacterial cells/ml

log N/N_0 = log (3 x 10^7/ 7 x 10^9) = ***-2.368***

FURTHER READING:

Flisar K., Haberl Meglic S., Morelj J., Golob J., Miklavčič D. Testing a prototype pulse generator for a continuous flow system and its use for E. coli inactivation and microalgae lipid extraction. *Bioelectrochemistry* doi: 10.1016/j.bioelechem.2014.03.008, 2014
Gerlach D., Alleborn N., Baars A., Delgado A., Moritz J., Knorr D. Numerical simulations of pulsed electric fields for food preservation: A review. *Innov Food Sci Emerg Technol* 9: 408-417, 2008
Gusbeth C., Frey W., Volkmann H., Schwartz T., Bluhm H. Pulsed electric field treatment for bacteria reduction and its impact on hospital wastewater. *Chemosphere* 75: 228-233, 2009
Pataro G., Senatore B., Donsi G., Ferrari G. Effect of electric and flow parameters on PEF treatment efficiency. *J Food Eng* 105: 79-88, 2011

NOTES & RESULTS

NOTES & RESULTS

Analysis of electric field orientations on gene electrotransfer – visualization at the membrane level L8

Saša Haberl Meglič, Matej Reberšek
University of Ljubljana, Faculty of Electrical Engineering

Duration of the experiment: 90 min
Max. number of participants: 4
Location: Cell Culture Laboratory 1
Level: Advanced

PREREQUISITES

Participants should be familiar with Laboratory safety (S1). The basic knowledge of handling with cells is required for this laboratory practice.

THEORETICAL BACKGROUND

Gene electrotransfer is a non-viral method used to transfer genes into living cells by means of high-voltage electric pulses. An exposure of a cell to an adequate amplitude and duration of electric pulses leads to transient increase of cell membrane permeability for molecules which are otherwise deprived of membrane transport mechanisms. This allows various nonpermeant molecules, including DNA, to be transported across the membrane and enter the cell. Although mechanisms of the process are not yet fully elucidated, it was shown that several steps are crucial for gene electrotransfer: interaction of plasmid DNA (pDNA) with the cell membrane, translocation of pDNA across the membrane, migration of pDNA towards the nucleus, transfer of pDNA across the nuclear envelope and gene expression.

Many parameters (such as electric pulse protocol) can influence the first step (interaction of DNA with the cell membrane) and by that gene electrotransfer efficiency. Therefore, different electric pulse protocols are used in order to achieve maximum gene transfection, one of them is changing the electric field orientation during the pulse delivery. Since DNA is a negatively charged molecule and it is dragged towards the cell with the electrophoretic force in the opposite direction of the electric field, changing electric field orientation increases the membrane area competent for DNA entry into the cell.

The aim of this laboratory practice is to demonstrate how different pulse polarity affects formation of DNA – membrane complex after electric pulse application.

EXPERIMENT

We will focus on the interaction of DNA with the cell membrane by using TOTO-1 dye. For the experiment, we will use Chinese hamster ovary cells (CHO-K1) and plasmid DNA (pEGFP-N_1) that codes for GFP (green fluorescent protein). To generate and deliver electric pulses a βtech electroporator (Electro cell B10, Betatech, France) and electrodes with 4 mm inter-electrode distance will be used. Pulses will be monitored on osciloscope (LeCroy 9310C).

This labwork is conducted by

TAMARA POLAJŽER

Pulse protocols (see also Figure 1):

a) SP (single polarity): the direction of electric field is the same for all pulses
b) BP (both polarities): the direction of the electric field is changed between the pulses

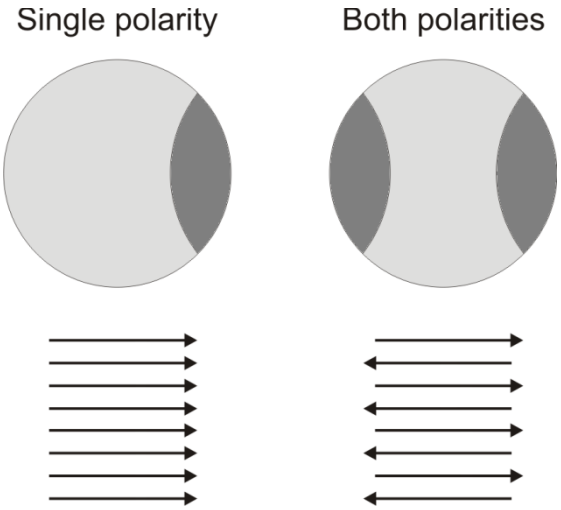

Figure 1: Two different pulse protocols will be used: single polarity (SP) and both polarities (BP).

Protocol:

Interaction of DNA with the cell membrane: CHO cells will be grown in Lab-Tek chambers as a monolayer culture in Ham's tissue culture medium for mammalian cells with 10% fetal bovine serum (Sigma-Aldrich Chemie GmbH, Deisenhofen, Germany) at 37º C. Cells will be plated 1 h before the experiment in concentration 1 x 10^5 cells per chamber.

To visualize DNA interaction with cell membrane TOTO-1 nucleic acid stain (Molecular Probes-Invitrogen, Carlsbad, California, USA) will be used. The plasmid pEGFP-N1 will be labelled on ice with 2.3 x 10^{-4} M TOTO-1 DNA intercalating dye 1 h before the experiment. Plasmid concentration will be 1 µg/µl, which yields an average base pair to dye ratio of 5.

Just before the experiment remove culture medium and rinse the cells with 1 ml of electroporation buffer (10 mM phosphate buffer K_2HPO_4/KH_2PO_4, 1 mM $MgCl_2$, 250 mM sucrose; pH = 7.4). Afterwards add 500 µl of electroporation buffer containing 5 µg of labelled plasmid DNA. Then apply a train of eight pulses with amplitude of 350 V, duration of 1 ms and repetition frequency 1 Hz using single polarity or both polarities (see Pulse protocols).

Immediately after exposure of cells to electric pulses rinse the cells three times with 1 ml of electroporation buffer. Add again 500 µl of electroporation buffer and observe the interaction of DNA with the cell membrane with fluorescent microscopy (Zeiss 200, Axiovert, Germany) using 100x oil immersion objective using TOTO filter with excitation at 514 nm.

FURTHER READING:

Faurie C., Reberšek M., Golzio M., Kandušer M., Escoffre J. M., Pavlin M., Teissie J., Miklavčič D., Rols M. P. Electro-mediated gene transfer and expression are controlled by the life-time of DNA/membrane complex formation. *J Gene Med* 12: 117-125, 2010

Golzio M., Teissié J., Rols M. P. Direct visualization at the single-cell level of electrically mediated gene delivery. *PNAS* 99: 1292-1297, 2002.

Reberšek M., Faurie C., Kandušer M., Čorović S., Teissié J., Rols M.P., Miklavčič D. Electroporator with automatic change of electric field direction improves gene electrotransfer *in vitro*. *Biomed Eng Online* 6: 25, 2007.

Reberšek M., Kandušer M., Miklavčič D. Pipette tip with integrated electrodes for gene electrotransfer of cells in suspension: a feasibility study in CHO cells. *Radiol Oncol* 45: 204-208, 2011.

Video Article:

Pavlin M., Haberl S., Reberšek M., Miklavčič D., Kandušer M. Changing the direction and orientation of electric field during electric pulses application improves plasmid gene transfer in vitro. *J Vis Exp*, 55: 1-3, 2011.

NOTES & RESULTS

NOTES & RESULTS

Comparison of flow cytometry and spectrofluorometric measurements in cell permeabilization experiments L9

Janja Dermol, Lea Vukanović
University of Ljubljana, Faculty of Electrical Engineering

Duration of the experiments: 90 min
Max. number of participants: 4
Location: Cell Culture Laboratory 2
Level: advanced

PREREQUISITES

Participants should be familiar with Laboratory safety (S1). The basic knowledge of handling with cells is required for this laboratory practice.

THEORETICAL BACKGROUND

When cells are exposed to high electric fields, otherwise non-permeant molecules can cross the cell membrane. A commonly used way of detecting cell membrane permeabilization is by using fluorescent dyes such as propidium iodide. When the cell is permeabilized, the propidium ion enters the cell, binds to nucleic acids in the cytosol and nucleus, and upon excitation starts to emit 20-times higher fluorescence than in the unbound state. Cell membrane permeabilization can be determined using different methods, e.g. fluorescent microscopy, spectrofluorometric measurements, flow cytometry, or clonogenic test after electroporation with chemotherapeutics. In this lab work, we will compare spectrofluorometric measurements and flow cytometry.

Spectrofluorometric measurements allow for the analysis of a large number of cells at different wavelengths, but the exact number of permeabilized cells cannot be extracted. Namely, as a result, we obtain the sum of the fluorescence intensities of all cells which can conceal subpopulations of differently permeabilized or even non-permeabilized cells.

Flow cytometry, on the other hand, gives information on the shape, size, internal structure, and fluorescence of each separate cell, and thus offers possibility to detect subpopulations which differ in any of the measured parameters. Cells (or any other particle) move through a laser beam and refract or scatter light in all directions. Forward scatter (FSC) is the light that is scattered in the forward direction as laser strikes the cell while side scatter (SSC) is the light that is scattered at larger angles. The magnitude of FSC is roughly proportional to the size of the particle and SSC is indicative of the granularity and the internal structural complexity. Fluorescence can be measured at different wavelengths, and the measured signal is proportional to the amount of the emitted fluorescence. After measurements, the analysis is done by gating to separate different cell subpopulations (Figure 1).

The aim of this laboratory practice is the comparison of two different methods of permeabilization detection using fluorescent dye propidium iodide.

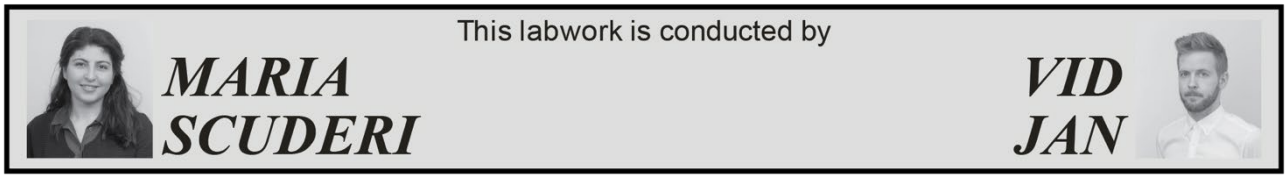

EXPERIMENT

We compare the fluorescence detected by flow cytometry (Life Technologies, Attune NxT, USA) and by the spectrofluorometer (Tecan Infinite 200, Tecan, Austria) after standard electroporation protocol (8, 100 µs pulses of different voltage applied at 1 Hz). To apply the pulses, we use the Gemini X2 electroporator (Harvard apparatus BTX, USA), and we monitor the pulses by an oscilloscope and current probe (both LeCroy, USA).

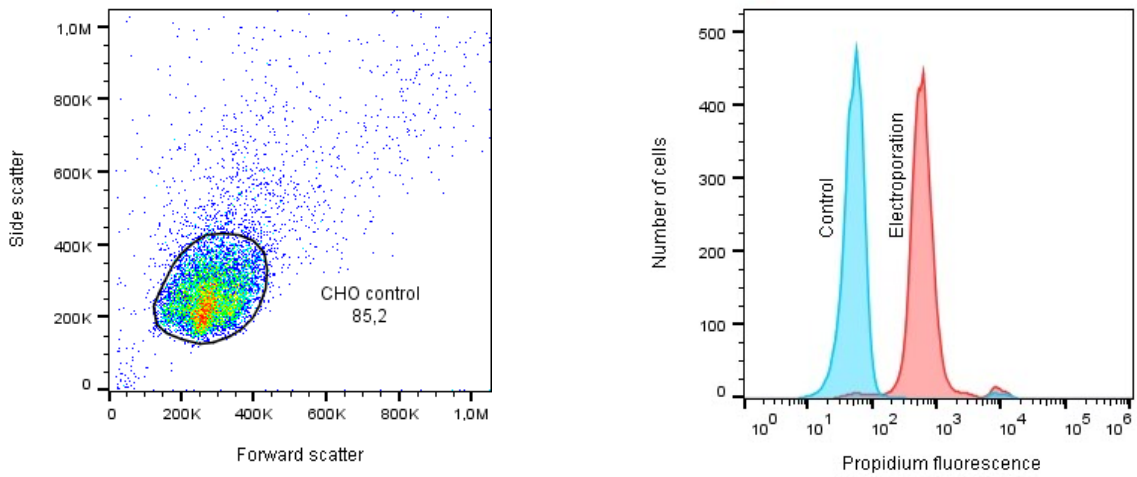

Figure 1: The analysis of the permeabilization data obtained by flow cytometry measurements in the software FlowJo (TreeStar, USA). Left: the viable cells are determined from the FSC-A and SSC-A dot diagram by gating. Right: histogram of measured fluorescence for control and pulsed cells. After electroporation, the cell fluorescence shifts for two decades which allows the discrimination between permeabilized and non-permeabilized cells. The peak at 10^4 are the dead and/or irreversibly permeabilized cells.

Protocol:

The experiments are performed on Chinese Hamster Ovary (CHO) cells. First, cells are detached by 10x trypsin-EDTA (Sigma-Aldrich, Germany), diluted 1:9 in Hank's basal salt solution (Sigma-Aldrich, Germany). Then, they are centrifuged (180g, 21°C, 5 min), the supernatant is removed and replaced with the low-conductivity KPB buffer (10 mM KH_2PO_4/K_2HPO_4, 1 mM $MgCl_2$, 250 mM sucrose) in concentration 10^7 cells/ml. 100 µl of cell suspension is dispensed in 1.5 ml microcentrifuge tubes (Isolab, Germany). Immediately before pulse application, 10 µl of 1.5 mM propidium iodide (Life Technologies, USA) is added to the tube. Then, 100 µl of cell suspension with propidium iodide is pipetted between 2 mm stainless-steel electrodes. Using Gemini X2 electroporator, 8, 100 µs pulses of different voltage at 1 Hz are applied. After the pulse application, 80 µl of cell suspension is transferred from between the electrodes to a new 1.5 ml tube. Two minutes after pulse application, the sample is centrifuged (1 min, 2000g, room temperature), the supernatant is removed and replaced by 500 µl of KPB buffer. The change of the buffer stops propidium influx in the cells and allows us to compare different parameters at the same time point. From each tube, 100 µl of the cell suspension is transferred to a 96-well plate in triplicates. 100 µl of the cell suspension is transferred to a 5 ml tube. Then, the protocol is repeated for the next sample. When all samples are prepared, we start with the measurements.

First, the fluorescence intensity is determined spectrofluorimetrically. We set the appropriate excitation (535 nm) and emission (617 nm) wavelengths. We measure at an optimal gain which prevents from signal saturation. The optimal gain is automatically determined by the software based on sensor sensitivity and the maximum signal intensity we are measuring. The average fluorescence intensity is calculated for each voltage from the triplicates. We plot the fluorescence intensity in dependence on the applied voltage.

Second, we determine the number of fluorescent cells by flow cytometry. On the control cells, we set up the optimal measuring parameters at the lowest flow rate (12.5 µl/min). When optimal parameters are determined, we measure 10,000 events for each voltage with higher flow rate (200 µl/min). By gating, living cells and the percentage of permeabilized cells are determined for each voltage. We plot the cell permeabilization in dependence on the applied voltage for both measurements (spectrofluorometric and flow cytometry) and compare the results.

FURTHER READING:

Kotnik T, Maček Lebar A, Miklavčič D, Mir, LM. Evaluation of cell membrane electropermeabilization by means of nonpermeant cytotoxic agent. Biotechniques. 2000;28**:** 921–926.

Marjanovič I, Kandušer M, Miklavčič D, Keber MM, Pavlin M. Comparison of Flow Cytometry, Fluorescence Microscopy and Spectrofluorometry for Analysis of Gene Electrotransfer Efficiency. J Membr Biol. 2014;247: 1259–1267. doi:10.1007/s00232-014-9714-4

Michie, J., Janssens, D., Cilliers, J., Smit, B. J., Böhm, L. Assessment of electroporation by flow cytometry. Cytometry 2000:41: 96–101.

Rols MP, Teissié J. Flow cytometry quantification of electropermeabilization. Methods Mol Biol Clifton NJ. 1998;91: 141–147.

Shapiro, H. M. *Practical flow cytometry*. (Wiley-Liss, 2003).

NOTES & RESULTS

Voltage (V)	0	100	150	200	250	0 and 250
Fluorescence intensity as measured with spectrofluorometer (a.u.)						
Percentage of fluorescent cells as determined by the flow cytometry (%)						

NOTES & RESULTS

Monitoring of electric field distribution in biological tissue by means of magnetic resonance electrical impedance tomography L10

Matej Kranjc[1], Igor Serša[2]
[1]University of Ljubljana, Faculty of Electrical Engineering
[2]Institut "Jožef Stefan"

Duration of the experiment: day 1: 90 min
Max. number of participants: 4
Location: MRI Laboratory (Jožef Stefan Institute)
Level: Basic

PREREQUISITES

Participants should be familiar with Laboratory safety (S1). No other specific knowledge is required for this laboratory practice.

THEORETICAL BACKGROUND

A method capable of determining electric field distribution during the pulse delivery has a practical value as it can potentially enable monitoring of the outcome of electroporation which strongly depends on the local electric field. Measurement of electric field distribution enables detection of insufficient electric field coverage before the end of either reversible or irreversible electroporation treatment, thus enabling corrections of field coverage during the treatment and consequently increasing and assuring its effectiveness. As there are no available approaches for measurement of electric field distribution *in situ*, an indirect approach using magnetic resonance techniques was suggested. Magnetic resonance electrical impedance tomography (MREIT) enables reconstruction of electric field distribution by measurement of electric current density distribution, first, and calculation of electrical conductivity of the treated subject during application of electric pulses using MRI data as an input to numerical algorithms, second. This method enables determination of electric field distribution *in situ* also accounting for changes that occur in the tissue due to electroporation.
MREIT is a relatively new medical imaging modality based on numerical reconstruction of electrical conductivity inside a tissue by means of current density distribution measured by current density imaging (CDI) sequence. The MREIT algorithm applied for reconstruction of electrical conductivity of the tissue is based on solving Laplace's equation through iterative calculation. Electrical conductivity is updated after each iteration (k+1):

$$\sigma^{k+1} = \frac{|\mathbf{J}_{\mathrm{CDI}}|}{|\nabla u^k|}.$$

where $\mathbf{J}_{\mathrm{CDI}}$ is current density obtained by CDI and u^k is electric potential obtained as a solution of Laplace's equation. When difference between two successive conductivities falls below certain value electric field distribution can be calculated using:

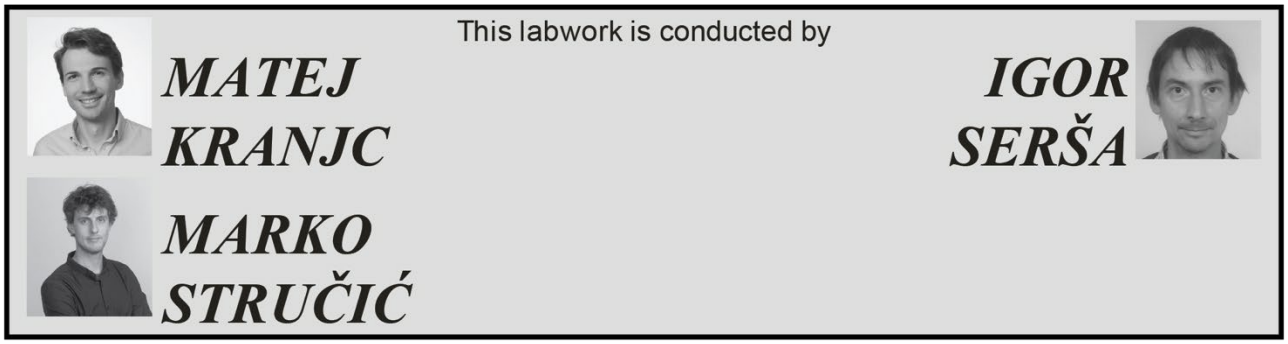

$$\mathbf{E} = \frac{\mathbf{J}_{\mathrm{CDI}}}{\sigma}.$$

The aim of this laboratory practice is to demonstrate monitoring of electric field distribution in a biological tissue using MREIT.

EXPERIMENT

We will monitor current density distribution and electric field distribution in biological tissue exposed to electric pulses by means of MREIT. We will then compare measured current density distribution and reconstructed electric field distribution with simulation results obtained by a numerical model of the tissue.

Protocol

The experiment will be performed on biological tissue (chicken liver) sliced in a disc-like sample measuring 21 mm in diameter and 2 mm in height (Fig. 1a). Electric pulses will be delivered via two cylindrically shaped electrodes inserted into the sample. After the insertion, the electrodes will be connected to an electric pulse generator connected to an MRI spectrometer. The sample will be placed in a 25 mm MR microscopy RF probe (Fig. 1b) inside a horizontal-bore superconducting MRI magnet (Fig. 1c). Electroporation treatment of the sample will be performed by applying two sequences of four high voltage electric pulses with a duration of 100 μs, a pulse repetition frequency of 5 kHz and with an amplitude of 500 V and 1000 V.

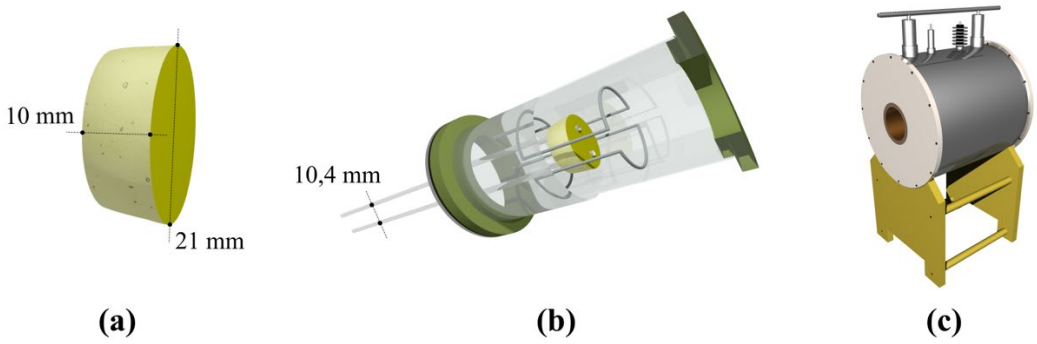

Figure 1: Biological sample (a) placed in a MR microscopy probe (b) inside a horizontal MRI magnet (c).

MR imaging will be performed on a MRI scanner consisting of a 2.35 T (100 MHz proton frequency) horizontal bore superconducting magnet (Oxford Instruments, Abingdon, United Kingdom) equipped with a Bruker micro-imaging system (Bruker, Ettlingen, Germany) for MR microscopy with a maximum imaging gradient of 300 mT/m and a Tecmag Apollo spectrometer (Tecmag, Houston TX, USA). Monitoring of electric field is enabled by CDI, which is an MRI method that enables imaging of current density distribution inside conductive sample. We will apply two-shot RARE version of the CDI sequence (Fig. 2).

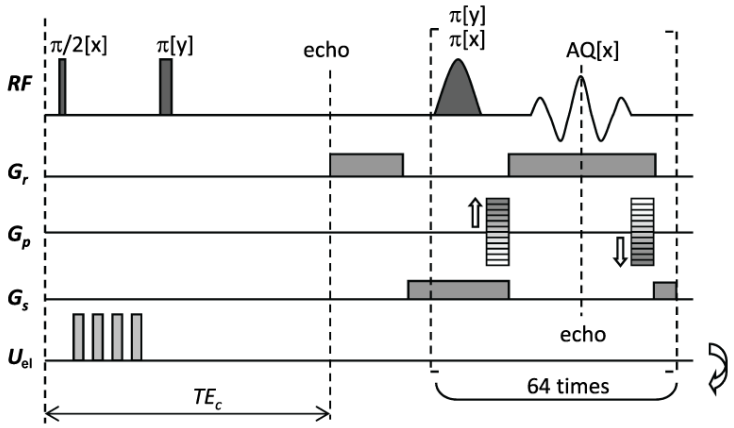

Figure 2: Two-shot RARE pulse sequence used for acquisition of current density distribution. The sequence consists of a current encoding part with a short (100 μs long) high-voltage electroporation pulse (U_{el}) delivered immediately after the nonselective 90° radiofrequency (RF) excitation pulse. In the second part of the sequence signal acquisition is performed using the single-shot RARE signal acquisition scheme that includes standard execution of readout (G_r), phase-encoding (G_p) and slice-selection (G_s) magnetic field gradients. Due to auxiliary phase encoding induced by the electric pulse, the RARE sequence is repeated twice, each time with a different phase of the refocusing pulses (0°and 90°), and the corresponding signals are co-added.

Electric field distribution in the sample will be reconstructed by iteratively solving Laplace's equation using J-substitution mathematical algorithm and finite element method with the numerical computational environment MATLAB on a desktop PC. We will compare measured current density distribution obtained by means of CDI and reconstructed electric field distribution obtained by means of MREIT in the sample with simulation results obtained by a numerical model of the sample.

FURTHER READING

Kranjc M., Bajd F, Sersa I., Miklavcic D., Magnetic resonance electrical impedance tomography for monitoring electric field distribution during tissue electroporation. *IEEE Trans Med Imaging* 30:1771–1778, 2011.

Kranjc M., Bajd F., Serša I., Miklavčič D., Magnetic resonance electrical impedance tomography for measuring electrical conductivity during electroporation. *Physiol Meas* 35:985–96, 2014.

Kranjc M, Markelc B, Bajd F, Čemažar M, Serša I, Blagus T, Miklavčič D. In situ monitoring of electric field distribution in mouse tumor during electroporation. Radiology 274: 115-123, 2015.

Kranjc M., Bajd F., Serša I. de Boevere M., Miklavcic D., Electric field distribution in relation to cell membrane electroporation in potato tuber tissue studied by magnetic resonance techniques. *Innov Food Sci Emerg Technol*, 2016.

Woo E. J. and Kranjc M. Principles and use of magnetic resonance electrical impedance tomography in tissue electroporation in *Handbook of Electroporation* (ed. Miklavcic, D.) 1–18 Springer, 2016.

Seo J.K., Woo E.J., Magnetic Resonance Electrical Impedance Tomography (MREIT). *SIAM Rev* 53:40–68, 2011.

Sersa I. Auxiliary phase encoding in multi spin-echo sequences: application to rapid current density imaging. *J Magn Reson*, 190(1):86–94, 2008

NOTES & RESULTS

NOTES & RESULTS

Measurements of the induced transmembrane voltage with fluorescent dye di-8-ANEPPS

L11

Gorazd Pucihar
University of Ljubljana, Faculty of Electrical Engineering

Duration of the experiments: 60 min
Max. number of participants: unlimited
Location: Online ONLY
Level: Advanced

PREREQUISITES

Participants should be familiar with Laboratory safety (S1). The basic knowledge of handling with cells is required for this laboratory practice.

THEORETICAL BACKGROUND

When a biological cell is placed into an external electric field the induced transmembrane voltage (ITV) forms on its membrane. The amplitude of the ITV is proportional to the amplitude of the applied electric field, and with a sufficiently strong field, this leads to an increase in membrane permeability - electroporation. Increased permeability is detected in the regions of the cell membrane where the ITV exceeds a sufficiently high value, in the range of 250 – 1000 mV, depending on the cell type. In order to obtain an efficient cell electroporation it is therefore important to determine the distribution of the ITV on the cell membrane. The ITV varies with the position on the cell membrane, is proportional to the electric field, and is influenced by cell geometry and physiological characteristics of the medium surrounding the cell. For simple geometric shapes the ITV can be calculated analytically (e.g. for a spherical cell, using Schwan's equation). For more complicated cell shapes experimental and numerical methods are the only feasible approach to determine the ITV.

The aim of this laboratory practice is to measure the ITV on a spherical cell by means of a fluorescent potentiometric dye di-8-ANEPPS.

EXPERIMENT

Potentiometric fluorescent dyes allow observing the variations of the ITV on the membrane and measuring its value. Di-8-ANEPPS is a fast potentiometric fluorescent dye, which becomes fluorescent when it binds to the cell membrane, with its fluorescence intensity varying proportionally to the change of the ITV. The dye reacts to the variations in the ITV by changing the intramolecular charge distribution that produce corresponding changes in the spectral profile or intensity of the dye's fluorescence.

Protocol: The experiments are performed on Chinese hamster ovary cells (CHO) grown in Lab-Tek chambers (Nunc, Germany) in culture medium HAM-F12 supplemented with 10% fetal bovine serum, L-glutamine (all three from Sigma-Aldrich) and antibiotics. When cells attach to the cover glass of a Lab-Tek chamber (usually after 2 to 3 hours to obtain attached cells of spherical shape), carefully replace the culture medium with 1 ml of SMEM medium (Spinner's modification of the MEM, Sigma-Aldrich) containing 30 μM of di-8-ANEPPS and 0.05% of Pluronic (both Life Technologies). After staining for 12 min at 4°C, wash the cells thoroughly with pure SMEM to remove the excess dye. After washing leave 1.5 ml of SMEM in the chamber. Place the chamber under a fluorescence microscope (Zeiss

This labwork is conducted by

LEA REMS

AxioVert 200, Germany) and use ×63 oil immersion objective. Position two parallel Pt/Ir wire electrodes, with a 4 mm distance between them, to the bottom of the chamber. Set a single 40 V, 50 ms pulse on the programmable square wave electroporator TSS20 (Intracel). This will result in a voltage-to-distance ratio of ~100 V/cm. The pulse must be synchronized with the image acquisition. Set the excitation wavelength to 490 nm and use ANEPPS filter to detect fluorescence (emission 605 nm).
Find the cells of interest. Acquire the control fluorescence image and subsequently the image with a pulse, using a cooled CCD camera (VisiCam 1280, Visitron) and MetaFluor 7.7.5 (Molecular Devices). Apply four pulses with a delay of 4 s between two consecutive pulses. For each pulse, acquire a pair of images, one immediately before (control image) and one during the pulse (pulse image) (Figures 1A and B).
Open the images in MetaMorph 7.7.5 (Molecular Devices). To *qualitatively* display the ITV on the cell membrane, convert the acquired 12-bit images to 8-bit images. For each pulse, obtain the difference image by subtracting (on a pixel-by-pixel basis) the control image from the pulse image. Add 127, so that 127, i.e. mid-gray level, corresponds to 0 V, brighter levels to negative voltages, and darker levels to positive ones (Figure 1C). Average the three difference images to increase the signal-to-noise ratio.
To *quantitatively* determine the ITV, open the acquired, unprocessed fluorescence images. Determine the region of interest at the site of the membrane and measure the fluorescence intensities along this region for the control and pulse image. Transform the values to the spreadsheet. Measure the background fluorescence in both images and subtract this value from the measured fluorescence. Calculate the relative changes in fluorescence ($\Delta F/F_C$) by subtracting the fluorescence in the control image F_C from the fluorescence in the pulse image F_P and dividing the subtracted value by the fluorescence in the control F_C; $\Delta F/F_C = (F_P - F_C) / F_C$. Average the relative changes calculated for all four acquired pairs of images. Transform the fluorescence changes to the values of the ITV (ΔF/F = -6% / 100 mV), and plot them on a graph as a function of the arc length (Figure 1D).

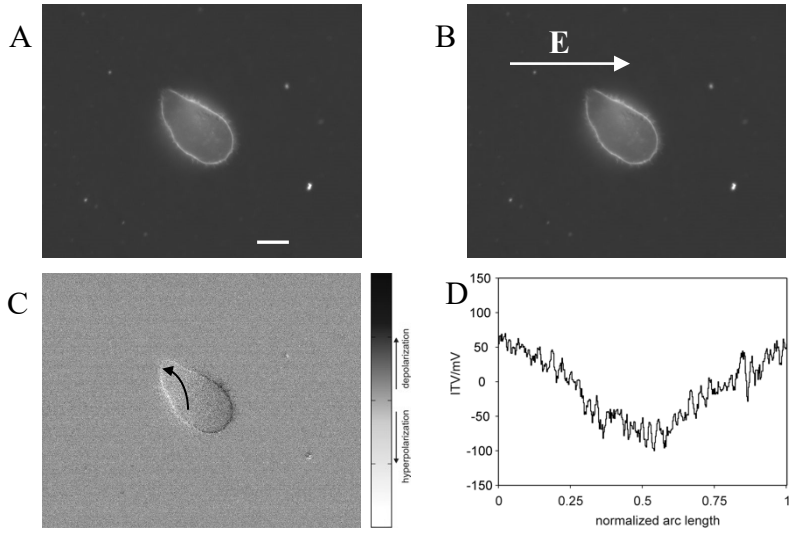

Figure 1: Measurements of the induced transmembrane voltage (ITV) on an irregularly shaped CHO cell. (A) A control fluorescence image of a cell stained with di-8-ANEPPS. Bar represents 10 μm. (B) Fluorescence image acquired during the exposure to a 35 V (~88 V/cm), 50 ms rectangular pulse. (C) Changes in fluorescence of a cell obtained by subtracting the control image A from the image with pulse B and shifting the grayscale range by 50%. The brightness of the image was automatically enhanced. (D) ITV measured along the path shown in C.

FURTHER READING:

Teissié J., and Rols M. P. An experimental evaluation of the critical potential difference inducing cell membrane electropermeabilization. *Biophys. J.* 65:409-413, 1993.

Gross D., Loew L. M, and Webb W. Optical imaging of cell membrane potential changes induced by applied electric fields *Biophys. J.* 50:339-348, 1986.

Montana V., Farkas D. L., and Loew L. M. Dual-wavelength ratiometric fluorescence measurements of membrane-potential. *Biochemistry* 28:4536-4539, 1989.

Loew L. M. Voltage sensitive dyes: Measurement of membrane potentials induced by DC and AC electric fields. *Bioelectromagnetics* Suppl. 1:179-189, 1992.

Hibino M., Itoh H., and Kinosita K. Time courses of cell electroporation as revealed by submicrosecond imaging of transmembrane potential. *Biophys. J.* 64:1789-1800, 1993.

Kotnik T., Bobanović F., and Miklavčič D. Sensitivity of transmembrane voltage induced by applied electric fields – a theoretical analysis. *Bioelectrochem. Bioenerg.* 43:285-291, 1997.

Pucihar G., Kotnik T., Valič B., Miklavčič D. Numerical determination of transmembrane voltage induced on irregularly shaped cells. *Annals Biomed. Eng.* 34: 642-652, 2006.

Video Article:

Pucihar G., Kotnik T., Miklavčič D. Measuring the induced membrane voltage with di-8-ANEPPS (Video Article). *J. Visual Exp.* 33: 1659, 2009.

NOTES & RESULTS

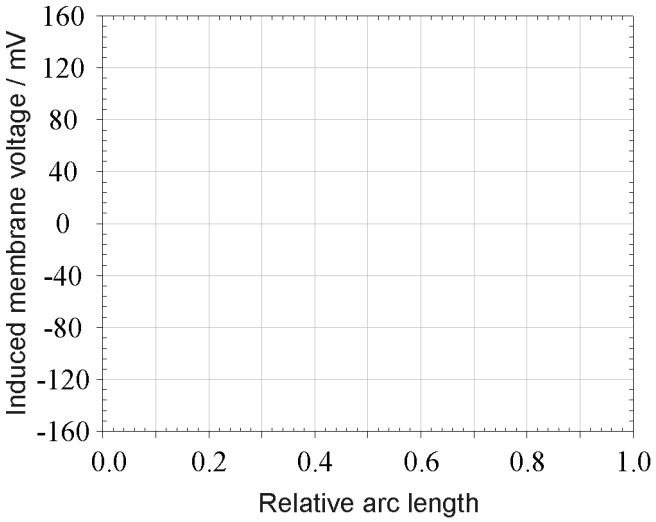

NOTES & RESULTS

Analysis of electric field orientations on gene electrotransfer efficiency L12

Saša Haberl Meglič, Matej Reberšek
University of Ljubljana, Faculty of Electrical Engineering

Duration of the experiment: 60 min
Max. number of participants: Unlimited
Location: Online ONLY
Level: Advanced

PREREQUISITES

Participants should be familiar with the Safety rules and Rules for sterile work in cell culture laboratory. The basic knowledge of handling with cells is required for this laboratory practice.

THEORETICAL BACKGROUND

Gene electrotransfer is a non-viral method used to transfer genes into living cells by means of high-voltage electric pulses. An exposure of a cell to an adequate amplitude and duration of electric pulses leads to transient increase of cell membrane permeability for molecules which are otherwise deprived of membrane transport mechanisms. This allows various nonpermeant molecules, including DNA, to be transported across the membrane and enter the cell. Although mechanisms of the process are not yet fully elucidated, it was shown that several steps are crucial for gene electrotransfer: interaction of plasmid DNA (pDNA) with the cell membrane, translocation of pDNA across the membrane, migration of pDNA towards the nucleus, transfer of pDNA across the nuclear envelope and gene expression.

Many parameters (such as electric pulse protocol) can influence the first step (interaction of DNA with the cell membrane) and by that gene electrotransfer efficiency. Therefore different electric pulse protocols are used in order to achieve maximum gene transfection, one of them is changing the electric field orientation during the pulse delivery. Since DNA is a negatively charged molecule and it is dragged towards the cell with the electrophoretic force in the opposite direction of the electric field, changing electric field orientation increases the membrane area competent for DNA entry into the cell.

The aim of this laboratory practice is to demonstrate how different pulse polarity affects the efficiency of gene electrotransfer and cell viability.

EXPERIMENT

For the experiment we will use Chinese hamster ovary cells (CHO-K1) and plasmid DNA (pEGFP-N_1) that codes for GFP (green fluorescent protein). To generate and deliver electric pulses a high-voltage prototype generator and electrodes with four cylindrical rods, which were developed at a Laboratory of Biocybernetics will be used. Pulses will be monitored on osciloscope (LeCroy 9310C).

Pulse protocols (see also Figure 1):

a) SP (single polarity): the direction of electric field is the same for all pulses

This labwork is conducted by

SAŠA HABERL MEGLIČ

b) OBP (orthogonal both polarities): the direction of the electric field is changed between the pulses

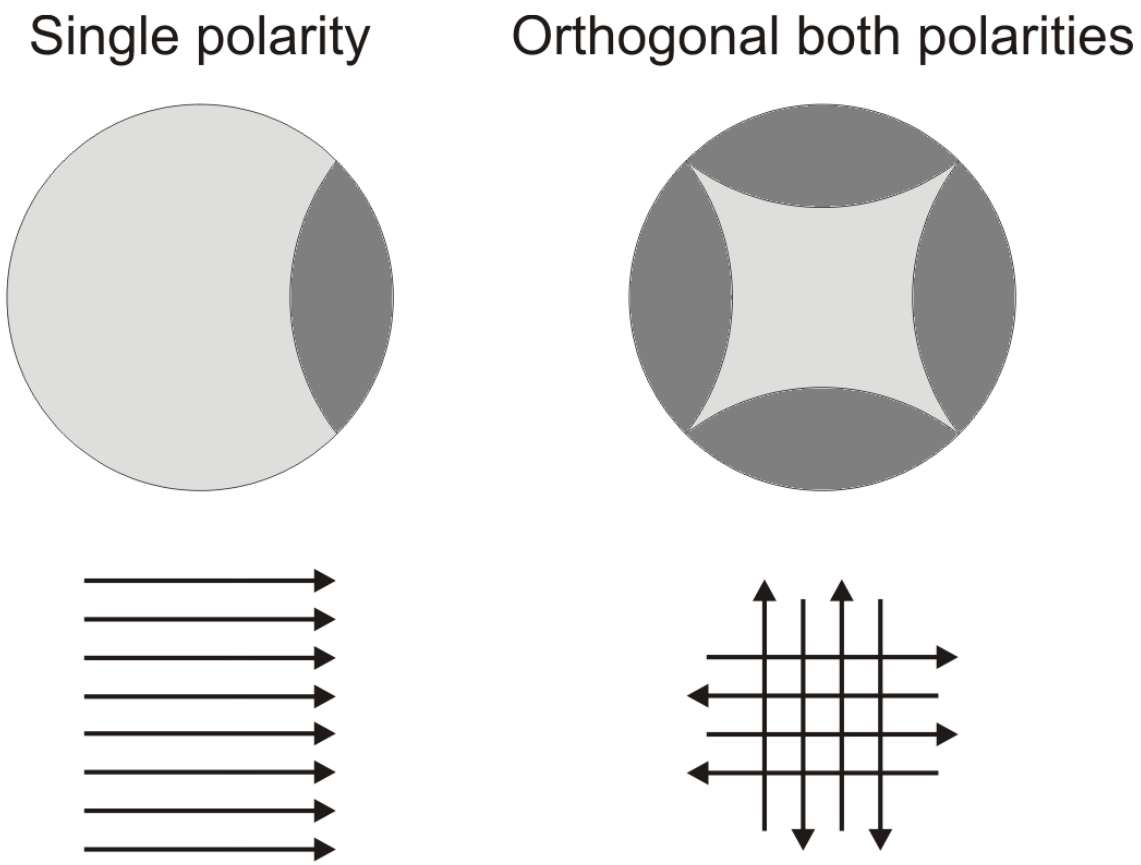

Figure 1: Two different pulse protocols will be used: single polarity (SP) and orthogonal both polarities (OBP)

Protocol 1/2 (Gene electrotransfer with different pulse parameters): CHO cells will be grown in multiwells as a monolayer culture in Ham's tissue culture medium for mammalian cells with 10% fetal bovine serum at 37º C. Cells will be plated 24h before the experiment in concentration 5 x 10^5 cells per well.
Just before the experiment remove culture medium and replace it with 150 µl of electroporation buffer containing plasmid DNA with concentration 10 µg/ml. Incubate cells with plasmid for 2-3 minutes at room temperature. Then apply a train of eight pulses with amplitude of 225 V, duration of 1 ms and repetition frequency 1 Hz using single polarity and orthogonal both polarities (see Pulse protocols) to deliver plasmid DNA into the cells.
Cells in the control are not exposed to electric pulses.
Immediately after exposure of cells to electric pulses add 37 µl of fetal calf serum (FCS-Sigma, USA). Incubate treated cells for 5 minutes at 37º C and then add 1 ml of culture medium.

Protocol 2/2 (Determining gene electrotransfer efficiency and cell viability): After 24 h incubation at 37º C determine the difference in gene electrotransfer efficiency and cell viability for both pulse protocols by fluorescent microscopy (Leica, Wetzlar, Germany) at 20x magnification using GFP filter with excitation at 488 nm.

You will determine gene electrotransfer efficiency from the ratio between the number of green fluorescent cells (successfully transfected) and the total number of cells counted under the phase

contrast. You will obtain cell survival from phase contrast images as the ratio between the number of viable cells in the treated sample and the number of viable cells in the control sample.

FURTHER READING:

Faurie C., Reberšek M., Golzio M., Kandušer M., Escoffre J. M., Pavlin M., Teissie J., Miklavčič D., Rols M. P. Electro-mediated gene transfer and expression are controlled by the life-time of DNA/membrane complex formation. *J Gene Med* 12: 117-125, 2010

Golzio M., Teissié J., Rols M. P. Direct visualization at the single-cell level of electrically mediated gene delivery. *PNAS* 99: 1292-1297, 2002

Pavlin M., Haberl S., Reberšek M., Miklavčič D., Kandušer M. Changing the direction and orientation of electric field during electric pulses application improves plasmid gene transfer in vitro. *J Vis Exp*, 55: 1-3, 2011

Reberšek M., Faurie C., Kandušer M., Čorović S., Teissié J., Rols M.P., Miklavčič D. Electroporator with automatic change of electric field direction improves gene electrotransfer *in vitro*. *Biomed Eng Online* 6: 25, 2007

Reberšek M., Kandušer M., Miklavčič D. Pipette tip with integrated electrodes for gene electrotransfer of cells in suspension: a feasibility study in CHO cells. *Radiol Oncol* 45: 204-208, 2011

NOTES & RESULTS

Pulse parameters	Gene electrotransfer efficiency [%]	Cell viability [%]
Single polarity		
Orthogonal both polarities		

Monitoring cell membrane depolarization due to electroporation using fluorescent plasma membrane potential indicator

L13

Anja Blažič and Lea Rems
University of Ljubljana, Faculty of Electrical Engineering

Duration of the experiments: 90 min
Max. number of participants: 4
Location: Cell Culture Laboratory 3
Level: Advanced

PREREQUISITES

Participants should be familiar with Laboratory safety (S1). The basic knowledge of handling with cells is required for this laboratory practice.

BACKGROUND

All cells maintain an electric potential difference across their plasma membranes, which results from the differences in membrane permeabilities for potassium, sodium, calcium, and chloride ions. This potential difference is called the resting transmembrane voltage or resting potential and is maintained by a system of ion channels and pumps. By convention the resting transmembrane voltage is negative, meaning that the cell interior is electrically more negative compared to its exterior, and the membrane is considered hyperpolarized. The value of the resting transmembrane voltage changes dynamically with the cell cycle and has an important biological function by controlling the activity of various membrane proteins. When cells are electroporated, their transmembrane voltage changes and the membrane remains depolarized for several minutes after pulse exposure. As membrane depolarization acts as a biological signal, factors that influence prolonged depolarization upon electroporation can have an important influence on the biological outcome of electroporation.

The aim of this laboratory practice is to monitor the time course of transmembrane voltage changes after exposure to conventional electroporation pulses, and to determine the influence of pulse amplitude and ambient temperature on the extent and longevity of membrane depolarization.

EXPERIMENT

We will monitor the time course of membrane potential changes using the plasma membrane potential indicator (PMPI) fluorescent dye of the FLIPR Membrane Potential Assays Kit (Molecular Devices). PMPI consists of a two-part system which includes a fluorescent anionic voltage-sensor and a quencher. When the interior of the cell has a relatively negative charge the anion dye remains on the extracellular side, where the quencher prevents fluorescence excitation. During depolarization the voltage sensor translocates to the intracellular side, which increases the fluorescence intensity inside the cells. This translocation is reversible, which makes it possible to monitor membrane depolarization and repolarization as the cells recover and return to their baseline level. The fluorescence intensity is linearly proportional to the change in the membrane potential difference, making this method comparable to patch-clamp measurements upon dye calibration.

This labwork is conducted by

ANJA BLAŽIČ

Protocol: U87-MG human glioblastoma cells will be plated in Nunc Lab-Tek II chambered coverglass three to four days before the experiments. On the day of the experiments, the cells will be stained for 30 min at 37°C with the Component A of the FLIPR Membrane Potential Assay Red (Molecular Devices, #R7291), diluted in Live Cell Imaging Solution (Invitrogen, #A14291DJ). Afterwards, the cells will be placed on the microscope stage. The cells will be exposed to a single 100 μs pulse of selected amplitude, delivered by BTX Gemini pulse generator through a pair of Pt-Ir wire electrodes. Time lapse images of the cells will be acquired before and after pulse application. We will compare the response of the cells at room temperature and at 37°C, to observe how cell recovery depends on the temperature. The cells will be imaged on inverted microscope Leica DMi8 with LED8 illumination source controlled by the LasX software (all Leica Microsystems). The membrane potential dye will be excited with green LED (555/28 nm) and its florescence will be passed through DFT51010 filter and detected with the Leica DFC9000 Gt camera.

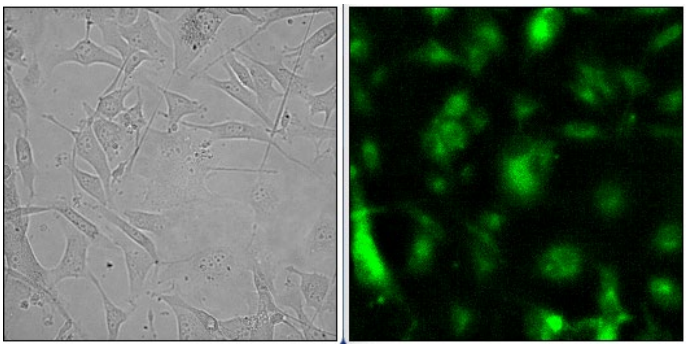

Figure 1: Brightfield image (*left*) and fluorescence (*right*) of U87-MG cells stained with FLIPR membrane potential assay.

FURTHER READING:

Wegner, L.H., W. Frey, and A. Silve. Electroporation of DC-3F cells is a dual process. *Biophys. J.* 108:1660–71, 2015.
Baxter, D.F., M. Kirk, A.F. Garcia, A. Raimondi, M.H. Holmqvist, K.K. Flint, D. Bojanic, P.S. Distefano, R. Curtis, and Y. Xie. A novel membrane potential-sensitive fluorescent dye improves cell-based assays for ion channels. *J. Biomol. Screening* 7:79–85, 2002.
Klapperstück, T., D. Glanz, S. Hanitsch, M. Klapperstück, F. Markwardt, and J. Wohlrab. Calibration procedures for the quantitative determination of membrane potential in human cells using anionic dyes. *Cytometry Part A* 83A:612–26, 2013.
Burke, R.C., S.M. Bardet, L. Carr, S. Romanenko, D. Arnaud-Cormos, P. Leveque, and R.P. O'Connor. Nanosecond pulsed electric fields depolarize transmembrane potential via voltage-gated K^+, Ca^{2+} and TRPM8 channels in U87 glioblastoma cells. *Biochim. Biophys. Acta (BBA) - Biomembranes* 1859: 2040–50, 2017.
Dermol-Černe, J., D. Miklavčič, M. Reberšek, P. Mekuč, S.M. Bardet, R. Burke, D. Arnaud-Cormos, P. Leveque, and R.P. O'Connor. Plasma membrane depolarization and permeabilization due to electric pulses in cell lines of different excitability. *Bioelectrochemistry* 122:103–14, 2018.
Blackiston, D.J., McLaughlin, K.A., M. Levin. Bioelectric controls of cell proliferation: ion channels, membrane voltage and the cell cycle. *Cell Cycle* 8(21): 3527-36, 2009.
L. Vodovnik, D. Miklavčič, G. Serša. Modified cell proliferation due to electrical currents. *Med Biol Eng Comput* 30(4): CE21-8, 1992.

NOTES & RESULS

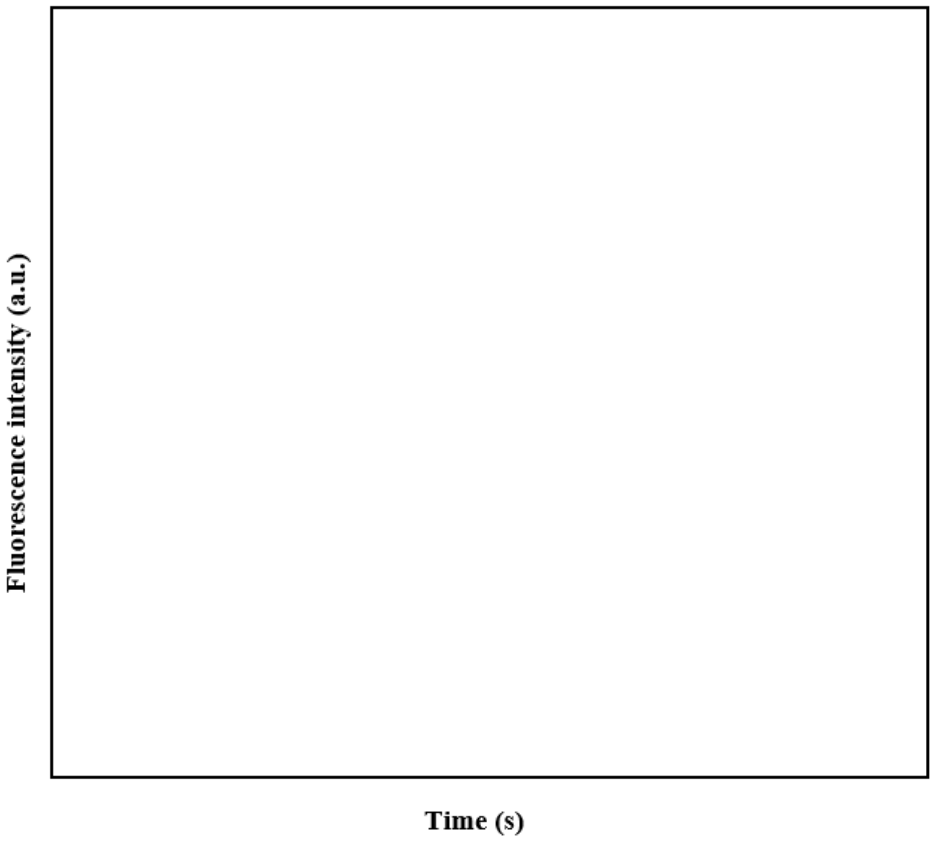

Impedance and texture analysis techniques for detecting and characterising electroporation in plant tissues L14

Samo Mahnič-Kalamiza, Rok Šmerc
University of Ljubljana, Faculty of Electrical Engineering

Duration of the experiments: 120 min
Max. number of participants: 4
Location: Tissue Laboratory
Level: Basic

PREREQUISITES

Participants should be familiar with Laboratory safety (S1). No prior knowledge of laboratory work is required. Basic skills of handling electronic instruments such as an oscilloscope and impedance analyser are an advantage, but not prerequisite.

THEORETICAL BACKGROUND

The application of PEF treatment in food processing is gaining momentum and seeing intensive research and development. New electroporation-based treatments are continuously put to the test and are optimized both at the laboratory and industrial scale processes. PEF treatment offers increasing benefits in terms of low energy requirements and minimization of food quality deterioration. For successful treatment, an appropriate choice of methods assessing changes due to electroporation occurring in biological matrices of alimentary interest is crucial. Despite a considerable body of literature in the field, detailed information regarding the detection and quantification of the effects of electroporation in complex and highly inhomogeneous multicellular systems, such as real food systems (e.g., plant tissues), is still limited. Moreover, due to the unique characteristics and properties of the biological tissue processed, a case-by-case PEF treatment optimization protocol is often required.

In food-related PEF applications, measurements of the dielectric properties of the tissue are often used for the determination of the degree of cell membrane disruption by electroporation. Electrical impedance spectroscopy (EIS) has been suggested as a reliable method to estimate the extent of tissue damage due to PEF treatment. EIS relies on the theory that, from an electrical point of view, an individual cell can be represented as an insulating membrane exhibiting relatively high resistance to electric current and considerable capacitance, and intra- and extra-cellular media (electrolytes) that behave as a resistive (ohmic) load up to hundreds of MHz. As electroporation affects the permeability (i.e., conductivity) of the cell membrane, multifrequency impedance measurements can be used to assess the degree of membrane permeabilization due to PEF treatment.

Another possibility of assessing changes in electroporated plant tissues is offered by texture analysis (texture in the sense of the response of a material to mechanical forces). Plant tissues in structures such as roots, fruits, and tubers, often exhibit considerable turgidity (high turgor pressure) when fresh and not dehydrated. Disrupting the selectively permeable membrane of the cells by electroporation can result in release of the intracellular water that is filtered out through the extracellular matrix. From the analysis of tissue's response to external force at the exact moment of electroporation and within minutes after, it is possible to evaluate the extent to which the electroporated plant tissue has been affected by the

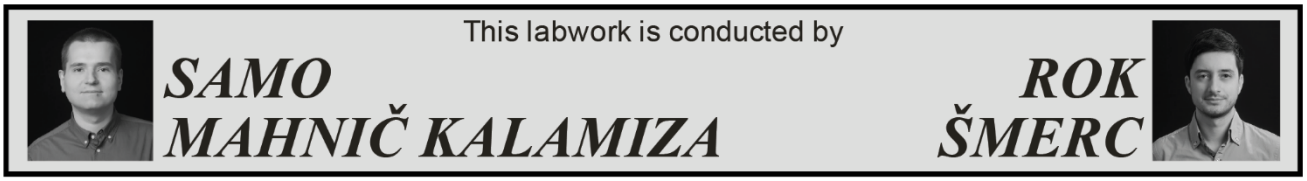

treatment. Texture analysis offers an alternative method to evaluating the degree of cell membrane disruption in treatment protocol optimisation where impedance measurements are either unavailable or impractical.

The aim of this laboratory practice is to detect (and quantify) electroporation effects in plant tissues of disparate origin, structure, and water content & solute composition, by employing electrical impedance measurements and texture analysis (i.e., tissue's response to mechanic forces). Students will learn of the importance of plant tissue composition and structure, and how these properties impact detection and quantification of electroporation effects in fresh plant matrices.

EXPERIMENT

We will perform concurrent sample deformation analysis (at constant loading force) and impedance measurements (pre- and post-pulse delivery) on two plant tissues: an apple fruit sample, and a potato tuber sample. To vary the treatment efficacy, and thus the extent of changes in tissue caused by electroporation, we will perform a voltage escalation study at three different voltages (and thus three different voltage-to-distance ratios), and repeat every experiment twice to ensure we have a stable set of data to work with (we would opt for a higher number of repetitions in a non-learning environment, the limit to two is due to time constraints). Altogether, we will perform 12 sets of impedance and texture measurements. In addition to recording the impedance and piston displacement, we will also be monitoring the pulse voltage and current with an oscilloscope (Teledyne LeCroy HDO6104A-MS).

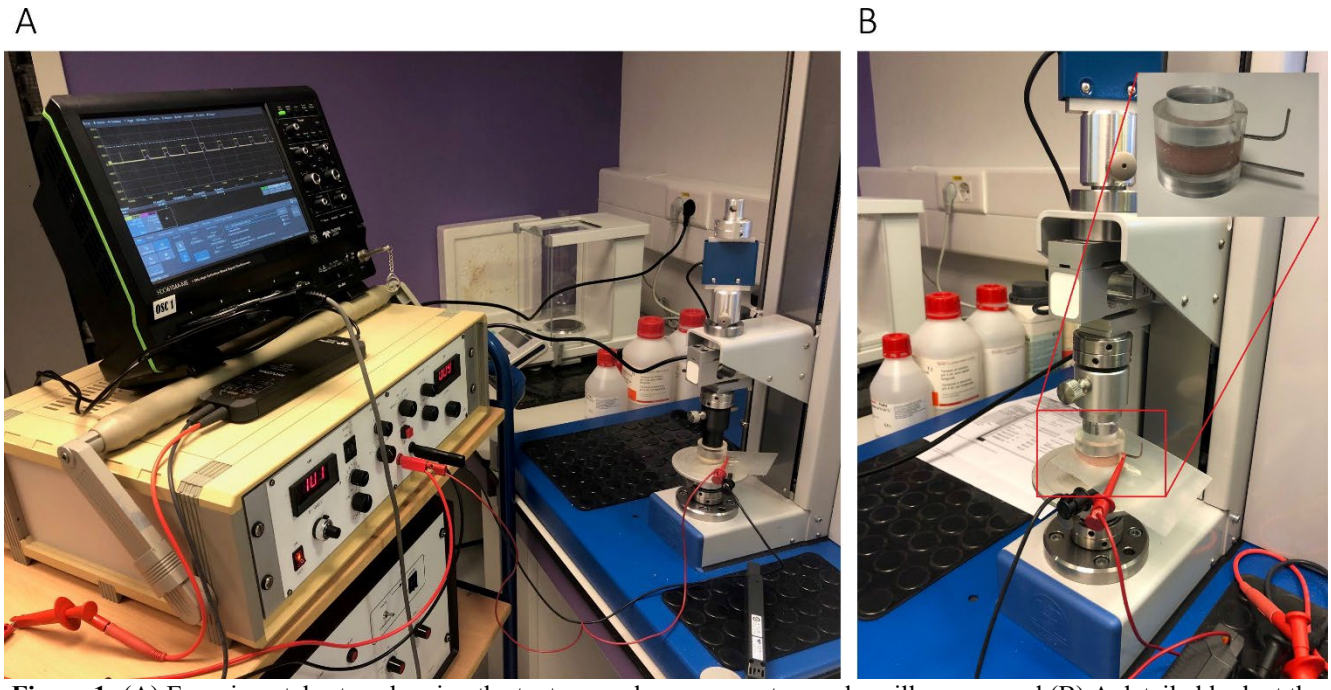

Figure 1: (A) Experimental setup showing the texture analyser, generator, and oscilloscope; and (B) A detailed look at the treatment chamber as set up under the texture analyser piston and of the treatment chamber setup on its own.

Protocol:

We will prepare six samples of apple fruit (cultivar depending on availability) cut into 6 mm thick cylinders of 25 mm in diameter. We will also prepare six samples of a potato tuber (cultivar depending on availability) cut into cylinders of identical dimensions as for the apple fruit.
Samples will be placed into a cylindrical treatment chamber with plate electrodes at the top and bottom of the sample (see Figure 1), the entire setup will then be placed under the piston of a texture analyser

(Hegewald & Peschke Inspect solo 1 kN-M) and subjected to a constant force of 5 N and 10 N for apple fruit and potato tuber, respectively. Electrodes will be connected both to a pulse generator (prototype device), as well as an impedance analyser (in short – an LCR meter, Keysight E4980A), and a switching circuit that will switch between the pulse generator and the impedance analyser to protect the LCR instrument from high-voltage pulses (prototype device).
The force will be applied for a total of 2 minutes. After 30 seconds under load, you will measure the pre-pulse impedance, and then immediately deliver 8 pulses of 100 us at 1 Hz repetition frequency, then immediately measure the post-pulse impedance. The loading of the sample will then continue for another minute or so (until 2 minutes total loading time is reached).
Deformation curves obtained from the texture analyser and impedance measurements will then be imported into MATLAB using scripts prepared in advance for further analysis, during which you will:

- Calculate the ratio of post- to pre-pulse electrical impedance of the sample at 5 kHz frequency and plot it versus the applied voltage.
- Calculate the total deformation of the sample from the moment of pulse delivery and up to the end of the constant force application and plot this deformation versus the applied voltage.

We will then compare the two functions/plots for both plant tissues and we will discuss the interpretation. The lab work concludes with a printout of graphs that you will paste into your workbooks (under NOTES & RESULTS to the right).

FURTHER READING:

Lebovka, N., & Vorobiev, E. (2017). Techniques to detect electroporation in food tissues. In Handbook of electroporation. https://doi.org/10.1007/978-3-319-32886-7_150.
Angersbach, A., Heinz, V., & Knorr, D. (1999). Electrophysiological model of intact and processed plant tissues: Cell disintegration criteria. Biotechnology Progress 15/4, 753-762. https://doi.org/10.1021/bp990079f.
Grimi, N., Lebovka, N., Vorobiev, E., Vaxelaire, J. (2009). Compressing Behavior and Texture Evaluation for Potatoes Pretreated by Pulsed Electric Field. Journal of Texture Studies 40, 208–224. https://doi.org/10.1111/j.1745-4603.2009.00177.x.
Mahnič-Kalamiza, S., Vorobiev, E. (2014). Dual-porosity model of liquid extraction by pressing from biological tissue modified by electroporation. Journal of Food Engineering 137, 76–87. https://doi.org/10.1016/j.jfoodeng.2014.03.035.

NOTES & RESULS

COMPUTER MODELING

Treatment planning for electrochemotherapy and irreversible electroporation: optimization of voltage and electrode position C1

Anže Županič[1], Bor Kos[2]
[1]Eawag - Swiss federal institute of aquatic science and technology, Switzerland
[2]University of Ljubljana, Faculty of Electrical Engineering

Duration of the experiments: 60 min
Max. number of participants: 6
Location: Laboratory of Biocybernetics
Level: Basic

PREREQUISITES

No specific knowledge is required for this laboratory exercise.

THEORETICAL BACKGROUND

Electrochemotherapy (ECT) is an efficient local treatment of cutaneous and subcutaneous tumors, which combines the delivery of nonpermeant, cytotoxic chemotherapeutics (e.g. bleomycin, cisplatin) and short high-voltage electric pulses. The pulses induce electric fields inside the tissue, thereby increasing cell membrane permeability in tissue (electropermeabilization) to otherwise nonpermeant chemotherapeutics. ECT requires the electric field inside the tumor to be higher than the threshold value needed for reversible electroporation (E_{rev}) while irreversible electroporation (E_{irrev}) in nearby critical structures should be limited. For IRE, the electric field in the entire tumor volume needs to be above the irreversible electroporation threshold. It is not necessary that the whole tumor is electropermeabilized by one pulse or pulse sequence - sometimes a combination of several pulse sequences or a combination of different electrodes is required.

The aim of this laboratory practice is to learn how to use optimization techniques to achieve suitable electric field distribution for electrochemotherapy experimental planning and treatment planning.

EXPERIMENT

A finite element based numerical modeling program package COMSOL Multiphysics version 5.4 (COMSOL AB, Stockholm, Sweden) will be used to optimize voltage between the electrodes and position of the electrodes on a simple 3D model of a spherical subcutaneous tumor and surrounding tissue (Figure 1a). Electrode positions and the applied voltage should be chosen, so that the following objectives are fulfilled:

- For electrochemotherapy: the tumor is permeabilized ($E_{tumor} > E_{rev} = 400\ V/cm$),
- For irreversible electroporation: the tumor is permeabilized above the irreversible threshold ($E_{tumor} > E_{irrev} = 600\ V/cm$),
- the damage to healthy tissue is kept to a minimum.

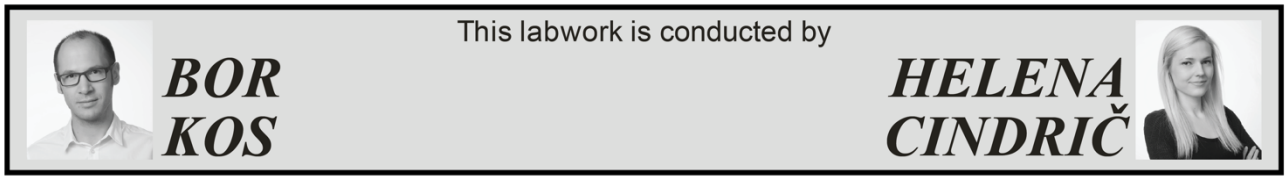

We will calculate the electric field distribution in the model after each change of the electrode placement or voltage. The final goal of this exercise is to achieve 100 % $E_{tumor} > E_{rev}$ (or 100 % $E_{tumor} > E_{irr}$ when planning for IRE) and minimize E_{irr} in healthy tissue.

Protocol: Build the 3-d model by following the lecturer's instructions and take into account your tissue-specific electric properties. Solve the model and evaluate the initial solution. In case, the initial solution is inappropriate (see e.g., Figure 1b), try to improve on the solution by changing electrode positions and voltage between the electrodes. Calculate the electric field distribution in the model after changing the electrode positions or voltage and then determine the coverage of tumor tissue with $E_{tumor} > (E_{rev}$ or $E_{irrev})$ and determine damage to healthy tissue due to irreversible electroporation. Repeat the process, until the quality of your solution reaches the set goals. Compare the results with others, who have used different tissue properties. Use a parametric study to find the lowest voltage which achieves the objective for the selected electrode geometry.

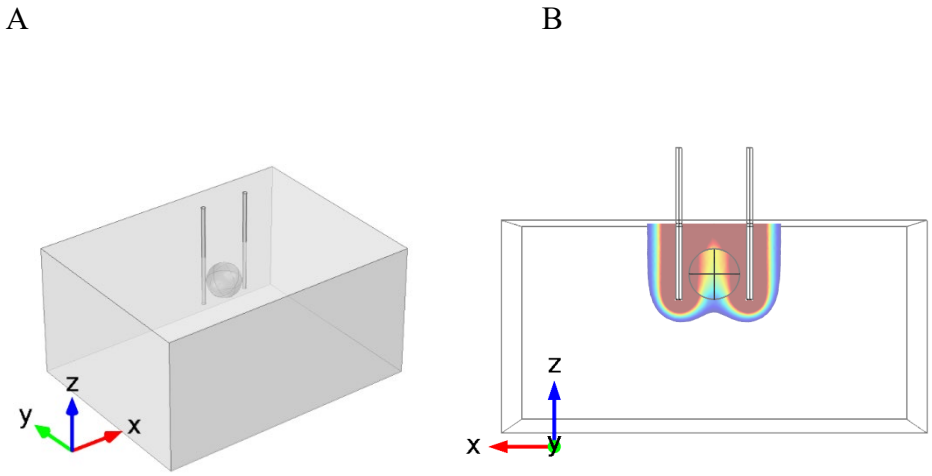

Figure 1: (A) Simple 3D model of tumor and needle electrodes in healthy tissue; (B) electric field over reversible threshold inside the healthy tissue and the tumor.

FURTHER READING:

Miklavčič D, Čorović S, Pucihar G, Pavšelj N. Importance of tumor coverage by sufficiently high local electric field for effective electrochemotherapy. *EJC Supplements*, 4: 45-51, 2006.

Čorović S, Županič A, Miklavčič D. Numerical modeling and optimization of electric field distribution in subcutaneous tumor treated with electrochemotherapy using needle electrodes. *IEEE Trans. Plasma Sci.,* 36: 1665-1672, 2008.

Županič A, Čorović S, Miklavčič D. Optimization of electrode position and electric pulse amplitude in electrochemotherapy. *Radiol. Oncol.,* 42: 93-101, 2008.

Edd JF, Davalos RV. Mathematical modeling of irreversible electroporation for treatment planning, *Technol. Cancer Res. Treat.,* 6: 275-286, 2007.

Kos B, Zupanic A, Kotnik T, Snoj M, Sersa G, Miklavcic D. Robustness of Treatment Planning for Electrochemotherapy of Deep-Seated Tumors, Journal of Membrane Biology 236: 147-153, 2010.

Cukjati, D, Batiuskaite D, Andre F, Miklavcic D, Mir L. Real Time Electroporation Control for Accurate and Safe in Vivo Non-viral Gene Therapy. *Bioelectrochemistry* 70: 501–507, 2007.

NOTES & RESULTS

NOTES & RESULTS

Numerical Modeling of Thermal Effects during Irreversible Electroporation Treatments

C2

Paulo A. Garcia[1] and Bor Kos[2]
[1]Virginia Tech – Wake Forest University
[2]University of Ljubljana, Faculty of Electrical Engineering

Duration of the experiment: 90 min
Max. number of participants: 6
Location: Laboratory of Biocybernetics
Level: Advanced

PREREQUISITES

Basic to advanced knowledge of finite element modeling

THEORETICAL BACKGROUND

Irreversible electroporation (IRE) is a new, safe, and effective minimally invasive ablation modality with the potential to treat many currently unresectable and/or untreatable tumors. The non-thermal mode of cell death in IRE is unique in that it does not rely on thermal changes from Joule heating to kill tumor cells thus allowing for successful treatment even in close proximity to critical structures and without being affected by the heat sink effect. Accurate modeling of the electrical and thermal responses in tissue is important to achieve complete coverage of the tumor and ensure that the thermal changes during a procedure do not generate thermal damage, especially in critical structures (e.g. bile ducts, nerves and sensitive blood vessels).

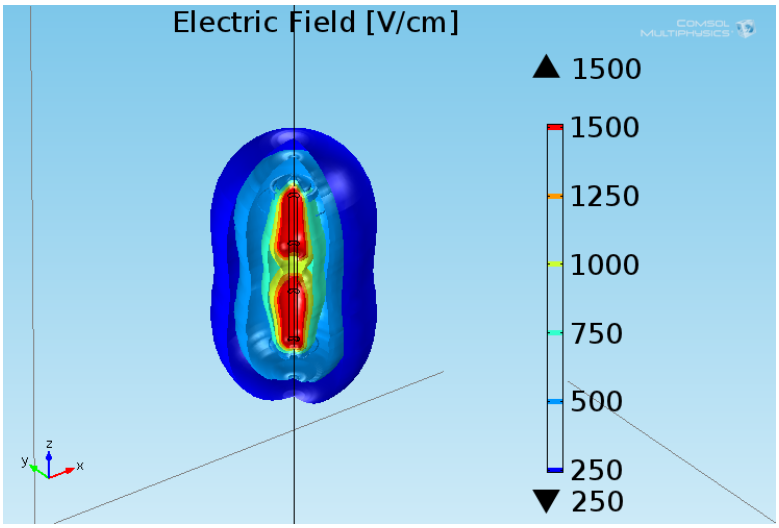

Figure 4: Electric Field distribution resulting from a bipolar electrode with an applied voltage of 1250 V.

The temperature distribution (T) within the tissue will be obtained by transiently solving a modified heat conduction equation with the inclusion of the Joule heating source term $Q = \sigma|\nabla\varphi|^2$

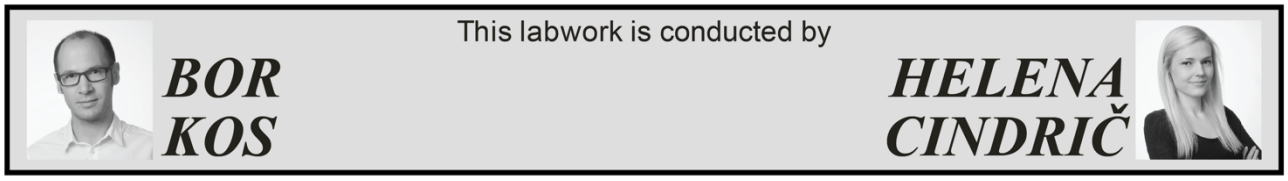

$$\rho C \frac{\partial T}{\partial t} = \nabla \cdot (k \nabla T) + Q \qquad (1)$$

where σ is the electrical conductivity, φ the electric potential, k is the thermal conductivity, C is the specific heat capacity, and ρ is the density of the tissue. At each time step, the current density and electric field distribution are determined and updated in the Joule heating term to capture the electrical conductivity changes in liver tissue from electroporation and temperature.

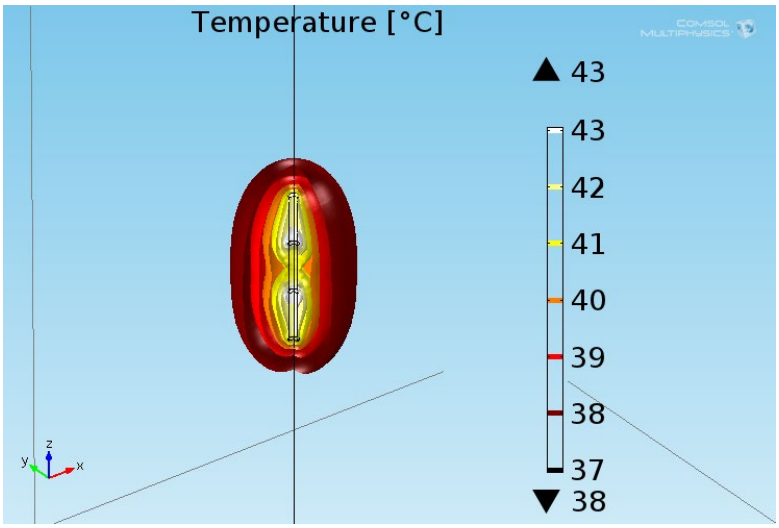

Figure 5: Temperature distribution after a ninety 100-µs pulse IRE treatment in liver tissue at 1 pulse per second.

Thermal damage is a process that depends on temperature and time. If the exposure is long, damage can occur at temperatures as low as 42°C, while 50°C is generally chosen as the target temperature for instantaneous damage. The damage can be calculated based on the temperatures to assess whether a particular set of pulse parameters and electrode configuration will induce thermal damage in superposition with IRE. The thermal damage will be quantified using the Arrhenius rate equation given by:

$$\Omega(t) = \int_{t=0}^{t=\tau} \zeta \cdot e^{\frac{-E_a}{R \cdot T(t)}} dt \qquad (2)$$

where R is the universal gas constant, 8.314 J/(mol·K); ζ is the pre-exponential factor, 7.39×10^{39} s^{-1}, a measure of the effective collision frequency between reacting molecules in bimolecular reactions; E_a the activation energy barrier that molecules overcome to transform from their "native state" to the "damaged state", 2.577×10^5 J/mol for liver tissue. It is important to note that the pre-exponential factor and activation energy are tissue specific parameters that describe different modes of thermal damage such as microvascular blood flow stasis, cell death, and protein coagulation. In terms of finite element modeling of thermal damage, an integral value $\Omega(t) = 1$ corresponds to a 63% probability of cell death and an integral value $\Omega(t) = 4.6$ corresponds to 99% probability of cell death due to thermal effects. In order to convert the damage integral to a probability of cell death, $P(\%)$, we will use:

$$P(\%) = 100 \cdot \left(1 - e^{-\Omega(t)}\right)$$

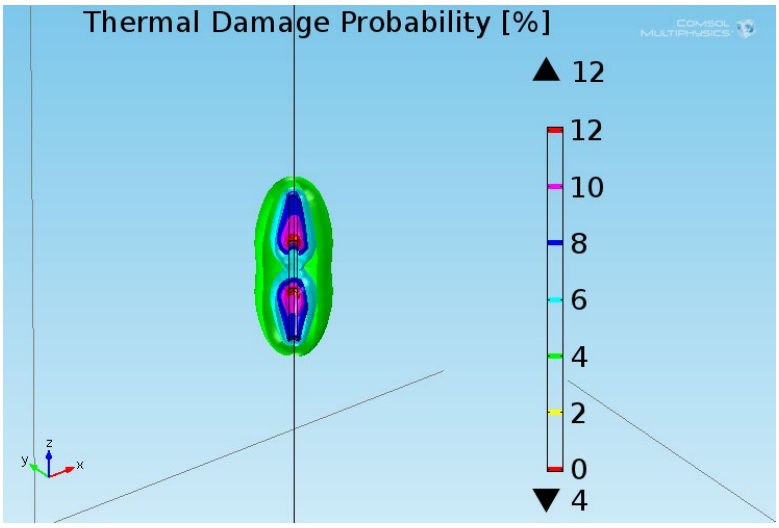

Figure 6: Thermal damage probability of cell death due to excessive thermal effects as a result of Joule heating.

The aim of this laboratory practice is to get familiar with the numerical simulation tools needed for capturing the electrical and thermal responses during a ninety 100-µs pulse IRE. We will accomplish this by coupling the Laplace, Heat Conduction, and Arrhenius equations using COMSOL Multiphysics 5.4 (Comsol AB, Stockholm, Sweden) to determine the IRE zones of ablation and evaluate if the increase in temperature due to Joule heating due to the pulses generates any potential thermal damage.

EXPERIMENT

In this exercise we will compare the effect of a static, σ_0, and dynamic, $\sigma(E)$, electrical conductivity functions in the resulting electrical and thermal effects during an entire IRE protocol in liver tissue. Initially we will determine the volume of tissue affected by IRE from the electric field distributions. We will then evaluate the temperature increase in liver tissue as a result of the Joule heating and determine if there was a probability of cell death due to thermal damage with the given IRE protocols employed. This exercise will provide the participants with accurate predictions of all treatment associated effects which is a necessity toward the development and implementation of optimized treatment protocols.

Specifically:
1) Simulate the electric field distribution using a static conductivity and 1000 V, 1500 V, and 2000 V.
2) Simulate the electric field distribution using a dynamic conductivity and 1000 V and 1500 V.
3) Include the Heat Conduction Equation by coupling with the Laplace Equation via Joule Heating.
4) Explore the resulting temperature distributions as a function of pulse number and frequency.
5) Incorporate the Arrhenius equation to assess potential thermal damage from the Joule Heating.
6) Investigate the effect of pulse frequency (1 Hz, 10 Hz, and 100 Hz) for ninety 100-µs pulses.

FURTHER READING:

Davalos RV, Rubinsky B, Mir LM. Theoretical analysis of the thermal effects during in vivo tissue electroporation. *Bioelectrochemistry* 61(1-2): 99-107, 2003

Chang, IA and Nguyen, UD., Thermal modeling of lesion growth with radiofrequency ablation devices. *Biomed Eng Online*, 3(1): 27, 2004

Davalos, R.V. and B. Rubinsky, Temperature considerations during irreversible electroporation. *International Journal of Heat and Mass Transfer*, 51(23-24): 5617-5622, 2008

Pavšelj N and Miklavčič D, Numerical modeling in electroporation-based biomedical applications. *Radiology and Oncology*, 42(3): 159-168, 2008

Lacković I, Magjarević R, Miklavčič D. Three-dimensional finite-element analysis of joule heating in electrochemotherapy and in vivo gene electrotransfer. *IEEE T. Diel. El. Insul.* 15: 1338-1347, 2009

Garcia, PA, et al., A Parametric Study Delineating Irreversible Electroporation from Thermal Damage Based on a Minimally Invasive Intracranial Procedure. *Biomed Eng Online*, 10(1): 34, 2010

Pavšelj N, Miklavčič D. Resistive heating and electropermeabilization of skin tissue during in vivo electroporation: A coupled nonlinear finite element model. *International Journal of Heat and Mass Transfer* 54: 2294-2302, 2011

Garcia PA, Davalos RV, Miklavčič D. A numerical investigation of the electric and thermal cell kill distributions in electroporation-based therapies in tissue. *PLOS One* 9(8): e103083, 2014.

NOTES & RESULTS

Molecular dynamics simulations of membrane electroporation C3

Mounir Tarek
CNRS- Université de Lorrains, Nancy France
Europeen Laboratory EBAM

Duration of the experiments: 90 min
Max. number of participants: 18
Location: Computer room (P18-A2)
Level: Basic

PREREQUISITES

No specific knowledge is required for this laboratory practice.

THEORETICAL BACKGROUND

The application of high electric fields to cells or tissues permeabilizes the cell membrane and is thought to produce aqueous-filled pores in the lipid bilayer. Electroporation is witnessed when the lipid membrane is subject to transmembrane voltages (TMV) of the order of few hundred millivolts, which results from the application of electrical pulses on a microsecond to millisecond time scale

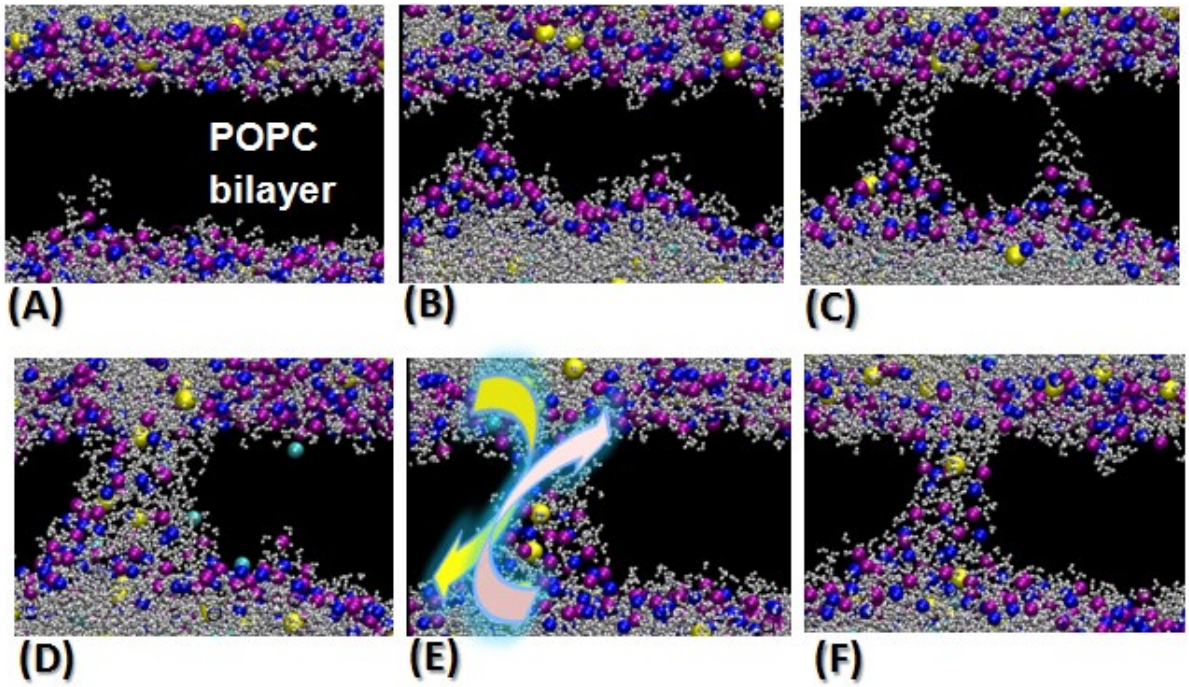

Figure 1: Configurations from the MD simulation for a large POPC subject to a transverse electric field (A) Bilayer at equilibrium. (B-C) Formation of water wires at the initial stage of the electroporation process (D-F) Formation at a later stage of large water pores that conduct ions across the membrane and that are stabilized by lipid head-group (yellow cyan). (Delemotte and Tarek. *J. Membr. Biol.* 2012).

This labwork is conducted by

MOUNIR TAREK

which are sufficient to produce a transient trans-membrane potential and an electrical field across the membrane of the order of ~ 10^8 V/m. This process is believed to involve (1) charging of the membrane due to ion flow, (2) rearrangement of the molecular structure of the membrane, (3) formation of pores, which perforate the membrane and are filled by water molecules (so-called aqueous, or hydrophilic, pores), (4) an increase in ionic and molecular transport through these pores, and, under appropriate conditions, membrane integrity recovery when the external field stress is removed.

Molecular Dynamics (**MD**) simulations belong to a set of computational methods in which the dynamical behaviour of an ensemble of atoms or molecules, interacting via approximations of physical pair potentials, is determined from the resolution of the equation of motions. MD simulations enable ones to investigate the molecular processes affecting the atomic level organization of membranes when these are submitted to voltage gradient of magnitude similar to those applied during electropulsation. The aim of this practical exercise is to characterize from MD simulations trajectories the electrostatic properties of membranes subject to a transmembrane potential (0 to 2 V).

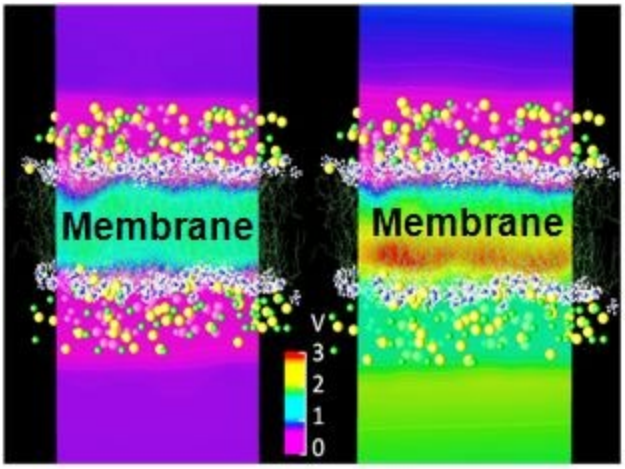

Figure 2: Electrostatic potential maps generated from the MD simulations of a POPC lipid bilayer (acyl chains, green; head groups, white) surrounded by electrolyte baths at 1 M NaCl (Na+ yellow, Cl- green, water not shown) terminated by an air/water interface. Left: net charge imbalance Q = 0 e (TMV=0 mV). Right: Q = 6 e (TMV=2 V).

The aim of this laboratory practice is to get familiar with the tools for molecular dynamics, possibilities to set on models and graphical presentation of atomistic models.

EXPERIMENT

Due to the limited time and large resources needed to generate MD trajectories of membranes, the latter will be provided to the students. The simulations concern pure planar phospholipid bilayers (membrane constituents) and water described at the atomic level. A set of long trajectories spanning few nanoseconds generated with or without a transmembrane voltage induced by unbalanced ionic concentrations in the extracellular and intracellular will be provided. The students will (1) determine the distribution of potential and electric field in model membrane bilayers (2) measure the membrane capacitance, (3) visualize at the molecular level the formation of membrane pores under the influence of a transmembrane voltage, and measure the intrinsic conductance of such pores.

FURTHER READING:

Tarek, M. Membrane Electroporation: A Molecular Dynamics Study *Biophys. J.* 88: 4045-4053, 2005.
Dehez, F.; Tarek, M.; and Chipot, C. Energetics of Ion Transport in a Peptide Nanotube *J. Phys. Chem. B* 111: 10633-10635, 2007
Andrey A. Gurtovenko, Jamshed Anwar, and Ilpo Vattulainen, Defect-Mediated Trafficking across Cell Membranes: Insights from in Silico Modeling, *Chem. Rev.* 110: 6077-6103, 2010.
Delemotte, L. and Tarek, M. Molecular Dynamics Simulations of Membrane Electroporation *J. Membr. Biol.* 245/9:531-543, 2012.
Polak A, Tarek M, Tomšič M, Valant J, Poklar Ulrih N, Jamnik A, Kramar P, Miklavčič D. Electroporation of archaeal lipid membranes using MD simulations. *Bioelectrochemistry* 100: 18-26, 2014.

NOTES & RESULTS

NOTES & RESULTS

HARDWARE
DEVELOPMENT AND MEASUREMENT

Measurement of electroporation pulses with oscilloscope, and voltage and current probes

H1

Matej Reberšek
University of Ljubljana, Faculty of Electrical Engineering

Duration of the experiment: 60 min
Max. number of participants: 10
Location: Laboratory of Biocybernetics
Level: Basic

PREREQUISITES

No specific knowledge is required for this laboratory exercise.

THEORETICAL BACKGROUND

Electroporation is initiated by the delivery of electrical pulses to biological cells. Electrical pulses may vary in pulse parameters such as pulse shape, amplitude, duration and polarity. We may deliver different number of pulses, use combination of different pulses or vary pulse repetition rates. We also may deliver pulses in bursts or in different directions relative to the cell. The process of the electroporation is strongly dependent on the pulse parameters of the delivered electrical pulses. In order to control the process of the electroporation and to exactly specify the experimental method, and thus enable the reproduction of experiments under the same conditions, we should exactly determine and describe these electrical parameters. When reporting electroporation methods we should: 1) describe exactly how the electric pulses were measured; 2) provide time-domain waveforms of the electric pulse at the electrodes; and 3) calculate or otherwise determine to what electric field the cells were exposed to.

The aim of this laboratory practice is to learn how to use standard measurement equipment to measure or monitor the delivery of electroporation pulses. During the laboratory practice we will also learn what are the electrical parameters of electroporation pulses, what should we report in our studies concerning the measurement and what are some possible complications during the pulse delivery or measurement.

EXPERIMENT

Oscilloscope, and voltage and current probes will be used to monitor the delivery of the electroporation pulses to the load. We will first learn how to set the three main controls (vertical, horizontal and trigger) for adequate data acquisition. We will learn how to use measuring tool to automatically measure the pulse parameters, how to use sequencing to measure several pulses with low pulse repetition rate and how to set acquire to measure bursts of pulses.

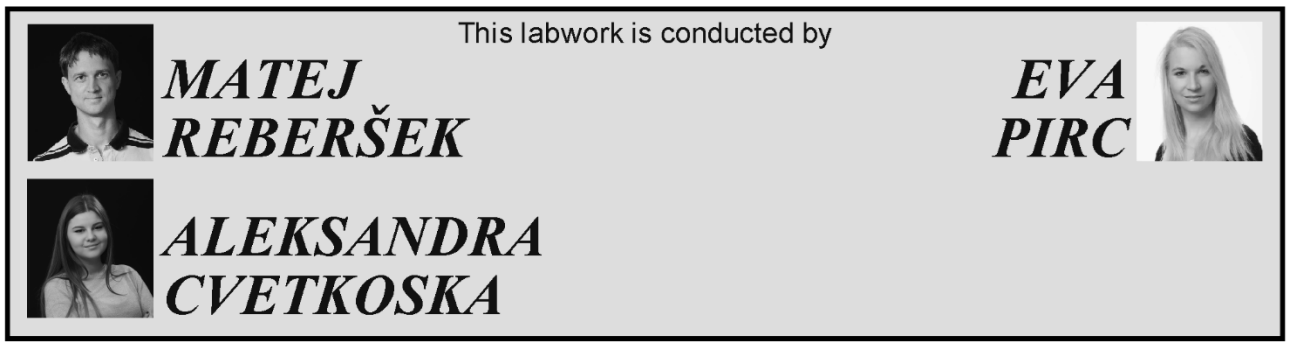

We will monitor the delivery of microsecond and nanosecond pulses to the load. Learn how to detect disconnection and improper impedance matching of the load, and how a point of measuring and improper wiring may affect the measuring and the delivery of the pulse.

Eight different commercial available electroporators: BTX (GEMINI X^2), IGEA (Cliniporator Vitae, GeneDrive), Invitrogen (Neon), Intracel (TSS20), Leroy(Beta-tech B10), Pulse Biosciences (CellFX), Societe Jouan (JOUAN) will be presented during the exercise and available for demonstrations at the end of the exercise. Additionally, also custom made prototype electroporaotrs designed and developed in our laboratory will be on display.

FURTHER READING:

Batista Napotnik T, Reberšek M, Vernier PT, Mali B, Miklavčič D. Effects of high voltage nanosecond electric pulses on eukaryotic cells (in vitro): A systematic review. *Bioelectrochemistry*, 110: 1-12, 2016.

Reberšek M, Miklavčič D, Bertacchini C, Sack M. Cell membrane electroporation –Part 3: The equipment. *IEEE Electr. Insul. M.,* 30(3): 8-18, 2014.

Silve A, Vézinet R, Mir LM. Nanosecond-Duration Electric Pulse Delivery *In Vitro* and *In Vivo*: Experimental Considerations. IEEE Trans. Instrum. Meas., 61(7): 1945-1954, 2012.

Kenaan M, El Amari S, Silve A, Merla C, Mir LM, Couderc V, Arnaud-Cormos D, Leveque P. Characterization of a 50-Ω Exposure Setup for High-Voltage Nanosecond Pulsed Electric Field Bioexperiments. *IEEE T. Biomed. Eng.* 58(1): 207-214, 2011.

Reberšek M, Miklavčič D. Concepts of Electroporation Pulse Generation and Overview of Electric Pulse Generators for Cell and Tissue Electroporation. In *Advanced Electroporation Techniques in Biology and Medicine*, *CRC Press*, 17:341-352, 2010.

Silve A, Villemejane J, Joubert V, Ivorra A, Mir LM. Nanosecond Pulsed Electric Field Delivery to Biological Samples: Difficulties and Potential Solutions. In *Advanced Electroporation Techniques in Biology and Medicine*, Pakhomov AG, Miklavcic D, Markov MS, *CRC Press*, 18: 353–368, 2010.

NOTES & RESULTS

NOTES & RESULTS

Development of pulsed power generators for electroporation H2

Matej Reberšek and Eva Pirc
University of Ljubljana, Faculty of Electrical Engineering

Duration of the experiment: 60 min
Max. number of participants: 4
Location: Laboratory for Physiological Measurements
Level: Advanced (Electrical Engineer)

PREREQUISITES

Basic to advanced knowledge of electrical engineering.

THEORETICAL BACKGROUND

Electroporation is initiated by the delivery of electrical pulses to biological cells. To generate electrical pulses for electroporation applications a pulsed power generator is required. Pulsed power generators operate in two phases: a charge and a discharge phase. During the charge phase, energy is accumulated over a long period of time in an energy storage element such as capacitor. In the discharge phase, stored energy is quickly released into the load. Several different concepts are used to generate electroporation pulses. The most common method of generating micro- and millisecond electroporation pulses is a square wave pulse generator, in which an on/off switch is used to connect and disconnect capacitor to the load. To generate nanosecond square wave electroporation pulses pulse forming networks or lines are used because high-voltage power switches cannot turn off in nanoseconds.

The aim of this laboratory practice is to learn how to develop milli-, micro- and nanosecond square wave pulse generators. During the laboratory practice we will learn how to choose or calculate the values of the electrical components for a given load and pulse duration.

EXPERIMENT

We will design and assemble two pulse generators: a square wave pulse generator and a Blumlein generator. The square wave pulse generator will enable generation of up to 1 kV micro- and millisecond electroporation pulses. And the Blumlein generator will enable generation of up to 1 kV nanosecond pulses. The output signals of the generators will be measured by oscilloscope, and voltage and current probes.

Square wave pulse generator: We will assemble this generator (Figure 1) by using: a high voltage power supply (V), high voltage capacitor (C), MOSFET switch (S), MOSFET driver (MD) and function generator (FG).

This labwork is conducted by

MATEJ REBERŠEK

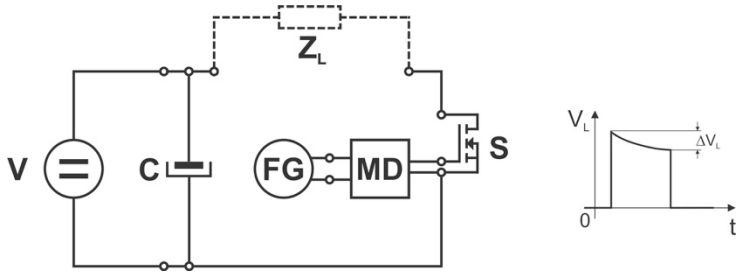

Figure 1. Schematics of the square wave pulse generator and its typical output waveform on load (Z_L).

To power the generator, we will use high voltage DC power supply MCP 350-1250 (FUG, Germany). To store enough energy in the capacitor for the pulse generation, we will calculate its minimal capacitance (equation 1). MOSFET switch will be chosen from the datasheets considering the pulse maximal output voltage and current, and rise, fall and turn off delay time. We will use 4422 (Microchip, USA) MOSFET driver circuit to drive the MOSFET switch and a function generator (HP, USA) to generate a control signal.

$$i_C = C\frac{dV_C}{dt};\ \ i_L = \frac{V_L}{Z_L} \xrightarrow{i_C=i_L;\ V=V_C=V_L;\ dV=\Delta V;\ dt=N\cdot t_P} C = \frac{N\cdot t_P}{\frac{\Delta V}{V}Z_L} \tag{1}$$

We will assemble the square wave pulse generator in four steps, by gradually increasing the requirements for pulse parameters and load (Table 1). We will vary pulse number (N), pulse duration (t_P), relative voltage drop ($\Delta V/V$) and resistance of the load (Z_L). In the first step, we will assemble the generator for one short (10 µs) fully square (1%) pulse on high resistive (1 kΩ) load. In the second step, we will lower the resistance of the load and observe the operation of MOSFET switch and output pulse waveform. In the third step, we will improve the pulse waveform. And in the final step, we will improve the pulse waveform for prolonged pulse duration and number of pulses.

Table 1. Parameters of the pulses that will be generated and resistance of the loads that will be used in specific assembly step.

Step	N	t_P [µs]	$\Delta V/V$ [%]	Z_L [Ω]	C [µF]	S
1	1	10	1	1000		
2	1	10		50	1	
3	1	10	1	50		
4	8	100	5	50		

Blumlein generator: We will assemble this generator (Figure 2) by using: a high voltage power supply (V), resistor (R), transmission lines (T_1 and T_2), radiofrequency MOSFET switch (S), MOSFET driver (MD) and function generator (FG).

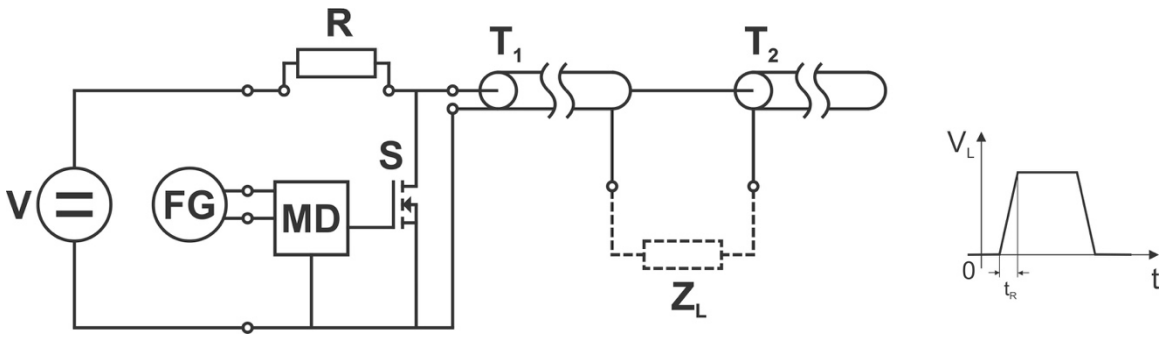

Figure 2. Schematics of the Blumlein generator and its typical output waveform on load (Z_L).

To power the generator, we will use high voltage DC power supply MCP 350-1250 (FUG, Germany). High-voltage and high-impedance resistor will be used to charge the transmission lines. The length of the transmission lines will be calculated (Equation 2) by propagation velocity (v_P) of the signal in transmission line. High-voltage, high- frequency and high-current MOSFET switch (IXYS, USA) will be used to quickly discharge the transmission lines. We will use 4422 (Microchip, USA) MOSFET driver circuit to drive the MOSFET switch and a function generator (HP, USA) to generate control signal.

$$v_P = \frac{1}{\sqrt{\varepsilon \cdot \mu}} \overset{\mu_r=1}{\Longrightarrow} \frac{c}{\sqrt{\varepsilon_r}} \overset{polyethylene}{\Longrightarrow} \frac{3 \cdot 10^8 \frac{m}{s}}{\sqrt{2.25}} = 0.2 \frac{m}{ns}; \quad l = \frac{v_P \cdot t_P}{2} \tag{2}$$

The Blumlein generator will be assembled to generate 1 kV, 20 ns square wave pulses on 100 Ω load.

FURTHER READING:

Reberšek M, Miklavčič D, Bertacchini C, Sack M. Cell membrane electroporation –Part 3: The equipment. *IEEE Electr. Insul. M.,* 30(3): 8-18, 2014.
Reberšek M, Miklavčič D. Advantages and disadvantages of different concepts of electroporation pulse generation. *Automatika (Zagreb)*, 52: 12-19, 2011.
Reberšek M, Miklavčič D. Concepts of Electroporation Pulse Generation and Overview of Electric Pulse Generators for Cell and Tissue Electroporation. In *Advanced Electroporation Techniques in Biology and Medicine*, *CRC Press*, 17:341-352, 2010.
Kolb JF. Generation of Ultrashort Pulse. In *Advanced Electroporation Techniques in Biology and Medicine*, *CRC Press*, 17:341-352, 2010.
Smith PW. Transient Electronics: Pulsed Circuit Technology. *Wiley*, 2002.

NOTES & RESULTS

NOTES & RESULTS

E-LEARNING

Electroporation of cells and tissues - interactive e-learning course E1

Selma Čorović and Samo Mahnič-Kalamiza
University of Ljubljana, Faculty of electrical engineering

Duration of the experiment: app. 90 min
Max. number of participants: 18
Location: Computer room (P9-B0)
Level: Basic

PREREQUISITES

No specific knowledge is required for this laboratory practice.

The aim of this laboratory practice is to provide the participants with basic knowledge on local electric field distribution in cells and tissues exposed to high voltage electric pulses (i.e. electroporation pulses) by means of interactive e-learning course content. The e-learning content is based on the available knowledge from the scientific literature.

PROTOCOL OF THE E-LEARNING COURSE

The participants will be gathered in a computer-computer classroom providing each participant with a computer. A short test will be given to establish the baseline knowledge before the e-learning course. Within the first part of the e-learning course we will bring together the educational material on basic mechanisms underlying electroporation process on the levels of cell membrane, cell and tissues as a composite of cells (Figure 1).

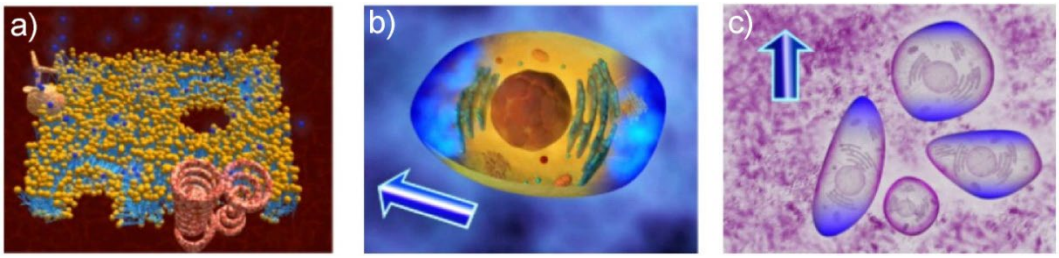

Figure 1: Introduction of small molecules (blue molecules) through a cell membrane (a) into an electroporated cell (b) and into the successfully electroporated cells within an exposed tissue (c) (Čorović et al., 2009).

Within the second part of the course we will provide basic knowledge on important parameters of local electric field needed for efficient cells and tissue electroporation, such as: electrode geometry (needle or plate electrodes as illustrated in Figure 2, electrode position with respect to the target tissue and its surrounding the tissues (Figure 3), the contact surface between the electrode and the tissue, the voltage applied to the electrodes and electroporation threshold values. This part of the e-learning course content will be provided by an interactive module we developed in order to visualize the local electric field distribution in 2D and 3D dimensional tissue models.

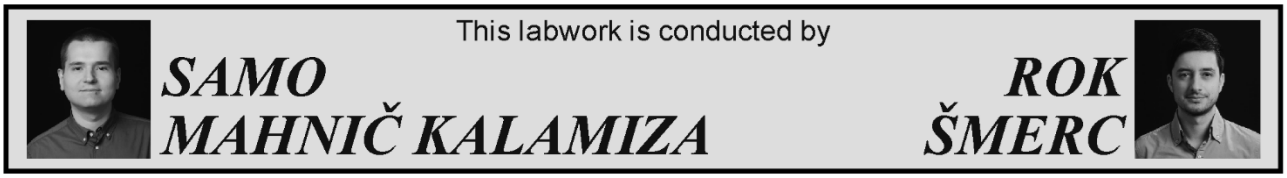

The objective of this module is to provide:
- local electric field visualization in cutaneous (protruding tumors) and subcutaneous tumors (tumors more deeply seeded in the tissue);
- guideline on how to overcome a highly resistive skin tissue in order to permeabilize more conductive underlying tissues and
- visualization and calculation of successfully electroporated volume of the target tissue and its surrounding tissue (i.e. the treated tissue volume exposed to the electric field between reversible and irreversible electroporation threshold value $E_{rev} \leq E < E_{irrev}$) with respect to the selected parameters such as: number and position of electrodes, applied voltage on the electrodes.

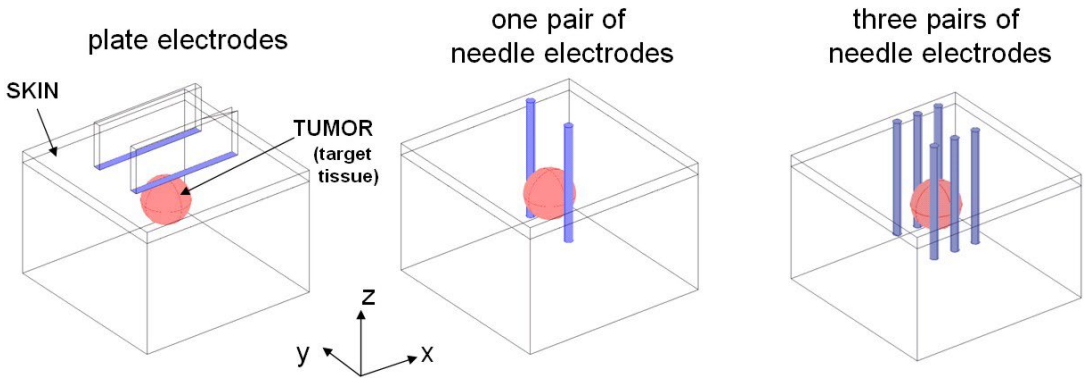

Figure 2: Plate electrodes vs. needle electrodes with respect to the target tissue (e.g. tumor tissue).

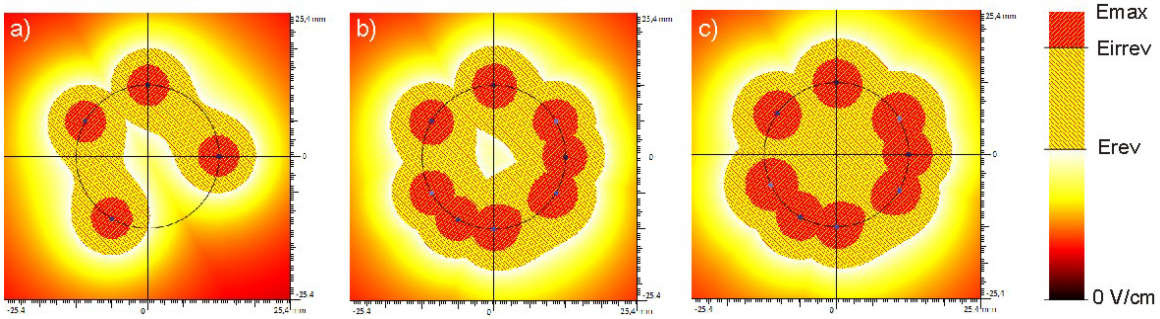

Figure 3: Electric field distribution within the tumor (inside the circle) and within its surrounding tissue (outside the circle) obtained with three different selection of parameters (number and position of electrodes and voltage applied): (a) 4 electrodes, (b) 8 electrodes and (c) 8 electrodes with increased voltage on electrodes so that the entire volume of tumor is exposed to the $E_{rev} \leq E < E_{irrev}$.

After the e-learning course the pedagogical efficiency of presented educational content and the e-learning application usability will be evaluated.

FURTHER READING:

Čorović S, Pavlin M, Miklavčič D. Analytical and numerical quantification and comparison of the local electric field in the tissue for different electrode configurations. *Biomed. Eng. Online* 6: 37, 2007.
Serša G, Miklavcic D: Electrochemotherapy of tumours (Video Article). *J. Visual Exp.* 22: 1038, 2008.
Čorović S, Županič A, Miklavčič D. Numerical modeling and optimization of electric field distribution in subcutaneous tumor treated with electrochemotherapy using needle electrodes. *IEEE T. Plasma Sci.* 36: 1665-1672, 2008.
Čorović S, Bešter J, Miklavčič D. An e-learning application on electrochemotherapy. *Biomed. Eng. Online* 8: 26, 2009.
Čorović S, Županič A, Kranjc S, Al Sakere B, Leroy-Willig A, Mir LM, Miklavčič D. The influence of skeletal muscle anisotropy on

electroporation: in vivo study and numerical modeling. *Med. Biol. Eng. Comput.* 48: 637-648, 2010.
Edhemovic I, Gadzijev EM, Brecelj E, Miklavcic D, Kos B, Zupanic A, Mali B, Jarm T, Pavliha D, Marcan M, Gasljevic G, Gorjup V, Music M, Pecnik Vavpotic T, Cemazar M, Snoj M, Sersa G. Electrochemotherapy: A new technological approach in treatment of metastases in the liver. *Technol Cancer Res Treat* 10:475-485, 2011.
Bergues Pupo AE, Reyes JB, Bergues Cabrales LE, Bergues Cabrales JM. Analitical and numerical quantification of the potential and electric field in the tumor tissue for different conic sections. *Biomed. Eng. Online* 10:85, 2011.
Neal RE II, Garcia PA, Robertson JL, Davalos RV. Experimental characterization and numerical modeling of tissue electrical conductivity during pulsed electric fields for irreversible electroporation treatment planning. *IEEE T. Biomed. Eng.* 59(4):1077-1085, 2012.
Čorović S, Mir LM, Miklavčič D. In vivo muscle electroporation threshold determination: realistic numerical models and in vivo experiments. *Journal of Membrane Biology* 245: 509-520, 2012.
Essone Mezeme M, Pucihar G, Pavlin M, Brosseau C, Miklavčič D. A numerical analysis of multicellular environment for modeling tissue electroporation. *Appl. Phys. Lett.* 100: 143701, 2012.
Mahnič-Kalamiza S, Kotnik T, Miklavčič D. Educational application for visualization and analysis of electric field strength in multiple electrode electroporation. BMC Med. Educ. 12: 102, 2012.
Čorović S, Lacković I, Šuštarič P, Šuštar T, Rodič T, Miklavčič D. Modeling of electric field distribution in tissues during electroporation. Biomed. Eng. Online 12: 16, 2013.

NOTES & RESULTS

NOTES & RESULTS

Faculty members

Damijan Miklavčič
University of Ljubljana, Faculty of Electrical Engineering,
Tržaška 25, SI-1000 Ljubljana, Slovenia
E-mail: damijan.miklavcic@fe.uni-lj.si

Lluis M. Mir
Université Paris-Saclay, CNRS, Institut Gustave Roussy, Metabolic and systemic aspects of oncogenesis (METSY),
114 rue Edouard Vaillant, F-94805 Villejuif Cédex, France
E-mail: Luis.MIR@gustaveroussy.fr

Marie-Pierre Rols
Institute of Pharmacology and Structural Biology, CNRS - University of Toulouse III,
IPBS UMR 5089, 205, route de Narbonne, 31077 Toulouse, France
E-mail: marie-pierre.rols@ipbs.fr

Gregor Serša
Institute of Oncology,
Zaloška 2, SI-1000 Ljubljana, Slovenia
E-mail: gsersa@onko-i.si

Mounir Tarek
Theoretical Physics and Chemistry Laboratory, Université de Lorraine,
CNRS, LPCT, F-54000 Nancy
E-mail: mounir.tarek@univ-lorraine.fr

P. Thomas Vernier
Frank Reidy Research Center for Bioelectrics, Old Dominion University,
4211 Monarch Way, Norfolk, VA 23508, USA
E-mail: pvernier@odu.edu

Julie Gehl
University of Copenhagen, Department of Clinical Medicine,
Blegdamsvej 3, 2200 København N Denmark
E-mail: julie.gehl@sund.ku.dk

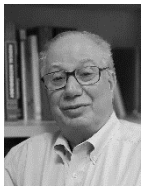

Richard Heller
Department of Medical Engineering, College of Engineering and Morsani College of Medicine
University of South Florida
12901 Bruce B. Downs Blvd., MDC 111, Tampa, FL 33612
E-Mail rheller@usf.edu